

**WIDE-BAND MICROSTRIP ANTENNA FOR
FUTURISTIC COMMUNICATION SYSTEMS**

A

Thesis

Submitted to



For the award of

DOCTOR OF PHILOSOPHY (Ph.D)

in

ELECTRONICS AND ELECTRICAL ENGINEERING

By

Deepinder Singh Wadhwa

(41400709)

Supervised by

Dr. Praveen Kumar Malik

Professor,

SEEE, LPU,

Phagwara

Co-Supervised by

Dr. Jaspal Singh Khinda

Electronics and Communication

Engineering

Patiala

LOVELY FACULTY OF SCIENCE AND TECHNOLOGY

LOVELY PROFESSIONAL UNIVERSITY

PUNJAB

2021

DECLARATION

I declare that the thesis entitled "Wide-Band Microstrip Antenna for Futuristic Communication Systems" has been prepared by me under the guidance of Dr. Praveen Kumar Malik, Professor, School of Electronics and Electrical Engineering Engineering, Lovely Professional University, and Co-Supervisor Dr. Jaspal Singh Khinda, Electronics and Communication Engineering, Patiala, Punjab, India. No component of this dissertation has created on the foundation used for the grant of any degree or fellowship formerly.

The translations set forth depend on my perusing and comprehension of the original texts and they are not distributed anyplace as books, monographs or articles. Different books, articles and sites, which I have utilized, are acknowledged at the particular spot in the content.

Further, I certify that:

- The research work enclosed in this dissertation is novel and has been finished by me under the direction of my supervisor (s).
- The research work has not been submitted to any other University / Institute for the award of any other degree or diploma.
- I have followed the guidelines provided by the University / Institute while preparing this dissertation.
- Wherever/at whatever point, the material(s) utilized, for example, (information, hypothetical investigation, figures and text) from the different assets, I have given due credit to them by referring to them in the content of the dissertation and giving their subtleties in the references.

Deepinder Singh Wadhwa
School of Electronics and Electrical Engineering
Lovely Professional University
Jalandhar, Delhi G.T.Road (NH-1)
Phagwara, Punjab-144411, India
Date: October 11, 2021

CERTIFICATE

This is to certify that the thesis entitled “**Wide-Band Microstrip Antenna for Futuristic Communication Systems**”, which is being submitted by **Deepinder Singh Wadhwa** for the award of the level of Doctor of Philosophy in Electronics and Electrical Engineering from the Faculty of Engineering and Technology, Lovely Professional University, Punjab, India, is completely founded on the work did by him under our supervision and direction. The work revealed, typifies the first work of the candidate and has not been submitted to some other college or organization for the award of any degree or confirmation, as per the best of our insight.

Supervisor

Dr. Praveen Kumar Malik

Professor
School of Electronics and Electrical Engineering
Lovely Professional University
Phagwara, Punjab-144411, India
Date: October 11, 2021
E-mail: pkmalikmeerut@gmail.com
Contact No: +91-9719437711

Co-Supervisor

Dr. Jaspal Singh Khinda

Electronics and Communication
Engineering
Patiala
Punjab-147001
Date: October 11, 2021
E-mail: jskhinda@gmail.com
Contact No: 9780032210

ABSTRACT

With the increasing and endless demand of high speed wireless communication systems, the millimeter wave (mm-wave) systems are likely to meet the challenges faced by the current 4G scenario in terms of required bandwidth, high gain and several other network related issues. Therefore, in order to solve these networks related issues researchers from the industry; academia has shown more interest for the development of appropriate solutions. Thus, it becomes necessary to introduce such low profile and portable devices that can easily handle and support the futuristic mm-wave networks. So, microstrip patch antennas with wide-band frequency range are the most promising candidates to solve the above said issues. As we know that in wireless communication system, antenna plays a vital role to convert electrical signals into electromagnetic waves and act as transducer at transmitter and receiver side. These well designed, optimized and tested antennas can provide wide impedance bandwidth with low profile and high stable gain. It is also necessary to reduce overall dimensions for RF components, antenna miniaturization therefore become an essential task to obtain optimized design for various portable and handheld devices. World radio communications (WRC-19) and Federal communication commission (FCC) has jointly proposed upper 5G cellular bands for specific applications for different countries such as satellite communications, radar services and earth observations whose application spectrum falls within the range of 24-42.5GHz. Conventional antenna usually operates on narrow band range of frequency but with for the fifth generation requirements there is need to such antennas which can support mm-wave range and omit the need of multiple antennas in one device. The designed mm-wave antennas are helpful for the upcoming 5G communication technology applications and therefore can reduce the problems of the current service providing networks.

So, Microstrip patch antenna is greatly regarded and it is the proved as the best candidate for the mm-wave wireless communication applications due to its low weight, low profile and cheap in cost as fabricated using PCB technology if the suitable substrate material is selected.

In literature, researchers have used different methodologies, state of art structures, diverse techniques have been adopted to develop the prototypes such as array, MIMO, Massive MIMO; defected ground structures (DGS) and beam forming to enhance gain in mm-wave or to satisfy the mm-wave applications though none of them covers the lower 5G band to mm-wave application range. In microstrip patch antenna, wide band mm-wave range can be achieved by modification to the patch structure which

act as main radiator by implementing and relying on three different strategies. The first one is by designing the feed shape and size to the radiating patch. The second one which plays major role in achieving the wide band mm-wave range characteristics is the selection of the partial ground plane. The third one is the etching the slots and slits of suitable shapes and sizes on the radiating patch for different frequencies thereby increasing electrical size of the antenna without effecting overall antenna dimensions to achieve wideband mm-wave range characteristics.

Major purpose of this thesis is to design wideband mm-wave microstrip patch antenna for futuristic communication systems with wide impedance bandwidth and high stable gain using partial ground plane technique. In one of the antenna, the corners of upper and lower patch are tapered in different shapes to enhance the impedance bandwidth. Further, to achieve mm-wave spectrum, two tilted irregular structures are etched on patch at have been proposed at the specific angle. The designed prototype is simulated, optimized using electromagnetic solver i.e. High Frequency Structured Simulator (HFSS) and fabricated using PCB fabrication technology. The designed prototype antenna's performance is analyzed for return loss (RL) and bandwidth using VNA. Proposed antenna shows wideband characteristics for n-260 and n-261 band wireless applications.

Second compact millimeter-wave (mm-wave) microstrip antenna for futuristic 5G wireless communication application is designed with wide impedance bandwidth of 17.33–40GHz and high stable gain. By triangularly clipping the lower corners of the radiating patch and embedding 2-AHSS (2- armed H shaped slot) and (Inverted T-shaped slot) ITSS of different shapes and sizes, multiple resonances of antenna are obtained. A prototype of size $37 \times 15 \text{ mm}^2$ is fabricated and tested to measure performance parameters using VNA Bench and established a high-quality accord with simulated results. Further, the design is extended for 1 x 4 MIMO array for indoor applications with high gain.

Third compact broadband millimeter wave (mm-wave) antenna is designed with (PGP) i.e. partial ground plane on $10 \times 10 \text{ mm}^2$ substrate and patch with 50Ω microstrip line feeding excited by source in XZ- plane. The mm-wave antenna covers wide impedance bandwidth and 3 dBi gain bandwidth of 30.77–45.91GHz, peak gain of 7.9 dBi and average radiation efficiency of 82.8%. Thus, the proposed antenna is well suited for futuristic K_a -band applications.

ACKNOWLEDGEMENTS

I express thanks all who somehow contributed in the culmination of this proposition. To start with, I express appreciation to God for security and capacity to tackle job.

I might want to recognize my profound and genuine respects to my supervisor, Prof.(Dr.) Praveen Kumar Malik, School of Electronics and Electrical Engineering, Lovely Professional University, Phagwara who made this work possible. His amicable direction and master counsel have been priceless all through all phases of the work. In addition, I also owe my sincerest gratitude towards my Co-Supervisor Dr. Jaspal Singh Khinda, Electronics and Communication Engineering, Patiala, Punjab, India for expanded conversations and important ideas which have contributed incredibly to the improvement of this dissertation. His healthy criticisms, valuable advice, energy and direction throughout my research work show off my development both as a researcher and an individual since the preceding years.

I wish to acknowledge the infrastructure and facilities provided by School of Electrical and Electronics Engineering, Lovely Professional University and Research department to guide me on timely basis regarding norms and guidelines.

I would like to thank our respected “Baba Sukhdeep Singh Bedi Ji” for his blessings. Without his blessings this work would not have been conceivable.

I might want to thank my Colleague Mr. Sukhminder Kaushal who also helped me a lot in my research work.

I am especially indebted to Mr. Sudhir Thakur, Head HRA, DoS, SCL, Mohali, Head of department Mr. Gurvinder Singh and his technical support team for Antenna Testing Department of Space, SCL Mohali for carrying out measurement facilities on vector network analyzer (VNA). My sincere gratitude towards my parents, wife Mrs. Prabhleen Kaur, Daughters Ms. Tanyapreet Kaur and Ms. Rabbanipreet Kaur who encouraged me and prayed for me throughout the time of my research. Their eternal moral support makes this work possible.

A word of thanks for all the authors of all those papers, books and other literature contents which I have referred during my thesis work. I might want to recognize my

Laptop and other essential resources. I need to say thanks to 'them' for their fundamental help in this venture, as, without them, the entirety of my work, from the perspective, to the creations, to the real reviewing, would not have been conceivable. They have allowed me the likelihood to do anything I desire, to investigate my considerations, to record my thoughts, and to impart them to the world. I realize they are simply bits of equipment to any other person, however to me, they are an expansion of my being and without them, it is difficult to be me.

TABLE OF CONTENTS

Declaration.....	ii
Certificate.....	iii
Abstract.....	iv
Acknowledgements.....	vi
Table of Contents.....	viii
List of Figures.....	xii
List of Tables.....	xvi
Acronyms and Abbreviations.....	xvii
List of Symbols.....	xix
CHAPTER-1.....	1
INTRODUCTION AND OVERVIEW OF ANTENNA.....	1
1.1 INTRODUCTION.....	1
1.2 NEED OF mm-WAVE.....	1
1.3 APPLICATIONS OF mm-WAVE SPECTRUM IN ANTENNA..	2
1.3.1 WRC-19 Suggestions.....	2
1.3.2 The Communication Spectrum.....	2
1.3.3 LTE.....	3
1.3.4 LTE-A.....	4
1.4 MICROSTRIP PATCH ANTENNA: AN OVERVIEW	5
1.5 ANTENNA SUBSTRATE.....	7
1.6 FEEDING TECHNIQUES TO MICROSTRIP ANTENNA.....	7
1.7 DESIGNING MODELS.....	8
1.8 CHARACTERISTICS OF MSPA’S.....	8
1.8.1 Merits of MSPA’S.....	8
1.8.2 Demerits of MSPA’S.....	9
1.9 ANTENNA PARAMETERS.....	10
1.9.1 Antenna Gain	10
1.9.1 Power Gain.....	10
1.9.1 Directive Gain.....	10
1.9.2 Directivity.....	11
1.9.3 Input Impedance.....	11
1.9.4 Return Loss.....	12

1.9.5 Radiation Intensity.....	12
1.9.6 VSWR.....	12
1.9.7 Bandwidth.....	13
1.9.8 Radiation Pattern.....	13
1.9.9 Envelope Correlation Coefficient (ECC).....	14
1.9.10 Diversity Gain.....	15
1.10 MOTIVATION.....	15
1.11 STATEMENT OF PROBLEM.....	17
1.12 SCOPE OF PRESENT WORK.....	17
1.13 THESIS OUTLINE.....	18
1.14 SUMMARY.....	19
CHAPTER -2.....	21
STATE OF ART WITH ANTENNA DESIGN METHODOLOGY AND SIMULATION TOOLS	21
2.1 INTRODUCTION.....	21
2.2 LITERATURE REVIEW.....	21
2.2.1 Shapes of antenna structures.....	22
2.2.2 Bandwidth Enhancement.....	22
2.2.3 Fractal structures of patch antenna.....	22
2.2.4 Multi-band antennas.....	24
2.2.5 Wideband and UWB antennas.....	24
2.2.6 L-band.....	24
2.2.7 S-band.....	25
2.2.8 Ultra Wide-Band.....	26
2.2.9 5G bands.....	27
2.3 STATE OF ART SUMMARY.....	29
2.4 ANTENNA DESIGN METHODOLOGY.....	31
2.5 SIMULATION TOOL USED.....	31
2.5.1 HFSS (High Frequency Structured Simulator).....	32
2.5.1.1 Structure Designing Process.....	33
2.5.1.2 Antenna Design steps.....	34
2.5.1.3 Simulation and Analysis of Antenna.....	34
2.5.2 VECTOR NETWORK ANALYZER.....	35
2.6 SUMMARY.....	37

CHAPTER – 3.....	38
WIDE BAND mm- WAVE ANTENNA DESIGN.....	38
3.1 INTRODUCTION.....	38
3.2 CLASSIFICATION OF mm-WAVE BANDS.....	39
3.3 HIGH GAIN ANTENNA AND ENHANCEMENT IN BANDWIDTH FOR mm-WAVE BANDS FOR PATCH ANTEN.....	40
3.3.1 Antenna Design Methodology.....	40
3.4 SIMULATED AND MEASURED ANTENNA RESULTS.....	45
3.5 PARAMETRIC ANALYSIS.....	47
3.6 SUMMARY.....	52
CHAPTER –4.....	53
mm-WAVE ANTENNA DESIGN UPPER FOR 5G BAND APPLICATIONS.....	53
4.1 INTRODUCTION.....	53
4.2 ANTENNA DESIGN METHODOLOGY.....	55
4.3 CURRENT DISTRIBUTION.....	60
4.4 PARAMETRIC ANALYSIS.....	62
4.5 ANTENNA FABRICATION.....	70
4.6 SIMULATED AND MEASURED ANTENNA RESULTS.....	71
4.7 MIMO ANTENNA DESIGN.....	72
4.8 SUMMARY.....	77
CHAPTER -5.....	78
mm–WAVE PATCH ANTENNA FOR HIGH DATA RATE COMMUNICATION APPLICATIONS.....	78
5.1 INTRODUCTION.....	78
5.2 ANTENNA DESIGN METHODOLOGY.....	79
5.3 CURRENT DISTRIBUTION.....	82
5.4 PARAMETRIC ANALYSIS.....	84
5.5 SIMULATED ANTENNA RESULTS.....	85
5.6 SUMMARY.....	88
CHAPTER -6.....	89
CONCLUSION AND FUTURE SCOPE.....	89
6.1 FUTURE SCOPE	90
Research Publications.....	91
Conference Certificate.....	92

APPENDIX A.....	93
A.1 CONNECTORS CONFIGURATION.....	93
A.2 MoU BETWEEN LPU AND DEPARTMENT OF SPACE (DoS), SCL, MOHALI.....	96
A.3 ANTENNA TEST PROCEDURE.....	100
A.3.1 Measurement of Return Loss Using VNA (ZVA-40).....	100
A3.1.1 Antenna Fabrication.....	100
A.3.2 Antenna Test Procedure.....	102
A.3.2.1 Return loss/VSWR measurement using VNA (ZVA40)	102
A.3.2.1.1 Return loss Test procedure	102
APPENDIX B.....	104
B.1 ANTENNA DESIGN EQUATIONS.....	104
Bibliography.....	105

LIST OF FIGURES

Figure 1.1: Example of D2D Communication using LTE.....	04
Figure 1.2: The view of microstrip patch antenna (MSPA).....	06
Figure 1.3: The basic radiating patch shapes of MSPA.....	06
Figure 1.4: VSWR measurement along Transmission line.....	13
Figure 1.5: Radiation Pattern of Antenna.....	14
Figure 2.1: ANSYS HFSS simulation procedure for Antenna designing.....	33
Figure 2.2: Practical two port Vector Network Analyzer.....	36
Figure 2.3: Setup for S-Parameter Measurement of DUT.....	36
Figure 2.4: S_{11} co-efficient representation for 2-port network.....	37
Figure 3.1: Antenna designs (a) Ant 1 (b) Ant 2.....	40
Figure 3.2: Simulated reflection co-efficient of Ant 1 and Ant 2.....	41
Figure 3.3: The current distribution of Ant 2 at (a) 4 GHz (b) 7 GHz (c) 10 GHz (d) 13.5 GHz.....	42
Figure 3.4: The antenna design Ant 3.....	42
Figure 3.5: Designed Prototypes (a) Front End (b) Back End.....	43
Figure 3.6: Simulated Vector current distribution of Ant 3 at (a) 5 GHz (b) 8 GHz (c) 15 GHz (d) 21 GHz (e) 25 GHz (f) 35 GHz.....	44
Figure 3.7: Simulated impedance of Ant 1 and Ant 2.....	45
Figure 3.8: Simulated gain of Ant 1 and Ant 2.....	45
Figure 3.9: Simulated and Measured reflection co-efficient of Ant 3.....	46
Figure 3.10: The antenna designs (a) Ant 3.1 (b) Ant 3.2 (c) Ant 3.3 (d) Ant 3.4.....	47
Figure 3.11: Simulated reflection co-efficient of Ant 3.1 and Ant 3.2.....	48
Figure 3.12: Simulated reflection co-efficient of Ant 3.3 and Ant 3.4.....	48
Figure 3.13: Simulated Impedance characteristics of Ant 3.....	49
Figure 3.14: Simulated S_{11} plots and gain characteristics of Ant 3 for n261-band (27.50-28.35 GHz).....	49
Figure 3.15: Simulated S_{11} plots and gain characteristics of Ant 3 for n260-band (38.6 – 40GHz).....	50

Figure 3.16: Simulated Radiation pattern (a) X-Z Direction (b) Y-Z Direction at 6 GHz.....	50
Figure 3.17: Simulated Radiation pattern (a) X-Z Direction (b) Y-Z Direction at 8 GHz.....	50
Figure 4.1: (a) Antenna Design Ant 1 (b) Simulated VSWR and Gain of Ant 1.....	56
Figure 4.2: Antenna design Ant 2 with 3-AHSS slot.....	57
Figure 4.3: Simulated VSWR on left y-axis and Gain on right y-axis of Ant 2.....	57
Figure 4.4: Antenna design Ant 3 with 3-AHSS and ITSS.....	58
Figure 4.5: Simulated VSWR-plot of Ant 3 and gain-plots of Ant 2 and Ant 3.....	58
Figure 4.6: Ant 4 Configuration etched with 3-AHSS, ITSS and 4 rectangular small slits.	59
Figure 4.7: Simulated Current distribution of Ant 1 (a) 30 GHz (b) 32 GHz (c) 34 GHz (d) 36 GHz (e) 38 GHz (f) 40 GHz	60
Figure 4.8: Simulated Current distribution of Ant 2 (a) 30 GHz (b) 32 GHz (c) 34 GHz (d) 36 GHz (e) 38 GHz (f) 40 GHz.....	61
Figure 4.9: Ant 2 with various etchings of (a) I-shaped slots (b) T-shaped slots (c) 2-AHSS (d) 3- AHSS	62
Figure 4.10: Simulated plots of Ant 2 as function of etched I-, T-, 2-AHSS and 3-AHSS (a) VSWR-plots (b) gain plots.....	63
Figure 4.11: Ant 2 etched with 3-AHSS (a) Simulated VSWR-plots as function of d_2 (b) Simulated Gain-plots as function of d_2	64
Figure 4.12: Ant 2 etched with 3-AHSS (a) Simulated VSWR-plots as function of L_0 (b) Simulated Gain-plots as function of L_0	65
Figure 4.13: Ant 2 with etched 3-AHSS (a) Simulated VSWR-plots as function of W_1 (b) Simulated Gain-plots as function of W_1	66
Figure 4.14: The plots of Ant 3 as function of etched 3-AHSS and ITSS with and without edge circles (a) Simulated VSWR-plots (b) Simulated gain-plots	67
Figure 4.15: Ant 3 etched with 3-AHSS and ITSS (a) Simulated VSWR-plots as	68

function of L_2 (b) Simulated Gain plots as function of L_2	
Figure 4.16: Ant 3 etched with 3-AHSS and ITSS (a) Simulated VSWR-plots as function of W_2 (b) Simulated Gain plots as function of W_2	69
Figure 4.17: The fabricated structure of Ant 4 (a) Front end (b) Back End.....	70
Figure 4.18: Simulated and measured VSWR-plots of Ant 4 on left y-axis and comparison of gain-plots of Ant 3 and Ant 4 on right y-axis.....	71
Figure 4.19: Simulated Gain-plots of Ant 4 as function of etched 2-AHSS, 3-AHSS and without upper slit.....	71
Figure 4.20: Simulated Radiation pattern (a) X-Z Direction (b) Y-Z Direction at 22.5 GHz.....	72
Figure 4.21: Simulated Radiation pattern (a) X-Z Direction (b) Y-Z Direction at 36 GHz.....	72
Figure 4.22: Two element (1 x 2) MIMO antenna array.....	73
Figure 4.23: Four element (1 x 4) MIMO antenna array.....	73
Figure 4.24: Simulated VSWR comparison of 1, 2 and 4 elements MIMO antenna.....	74
Figure 4.25: Simulated Gain comparison of 1, 2 and 4 elements MIMO antenna.....	74
Figure 4.26: Simulated ECC of 1 x 4 MIMO element array.....	75
Figure 5.1: Antenna designs (a) Ant 1 (b) Ant 2.....	80
Figure 5.2: Simulated reflection co-efficient of Ant 1 and Ant 2 at $\theta = 90^0$ and $\varphi = 90^0$	81
Figure 5.3: Simulated gain of Ant 1 and Ant 2 at $\theta = 90^0$ and $\varphi = 90^0$	81
Figure 5.4: The antenna design Ant 3.....	82
Figure 5.5: Simulated Current Distribution at (a) 30GHz (b) 34 GHz (c) 36 GHz (d) 40 GHz.....	83
Figure 5.6: Simulated Vector Current Distribution (a) 30GHz (b) 34 GHz (c) 36 GHz (d) 40 GHz.....	83
Figure 5.7: Simulated Parametric Analysis of reflection coefficient.....	84
Figure 5.8: Simulated Parametric Analysis of Gain.....	84
Figure 5.9: Simulated reflection co-efficient of Ant 2 and Ant 3 at $\theta = 90^0$ and $\varphi = 90^0$	85

Figure 5.10: Simulated gain of Ant 2 and Ant 3 at $\theta = 90^0$ and $\varphi = 90^0$	86
Figure 5.11: Simulated radiation efficiency of Ant 2 and Ant 3 at $\theta = 90^0$ and $\varphi = 90^0$	86
Figure 5.12: Simulated Radiation pattern (a) X-Z Direction (b) Y-Z Direction at 41 GHz	87
Figure 5.13: Simulated Radiation pattern (a) X-Z Direction (b) Y-Z Direction at 45 GHz	87
Figure 6.1: Snapshot of IEEE Conference Certificate.....	92
Figure A.1: Technical Datasheet of the Coaxial Connectors.....	94
Figure A.2: Coaxial Connectors and part no description.....	95
Figure A.3: Snap shot of Antenna Testing Permission Letter.....	96
Figure A.4: Snap shot of MoU between LPU and DoS, Mohali.....	97
Figure A.5: PCB Fabrication process.....	101
Figure A.6: Test setup for VSWR measurement.....	103

LIST OF TABLES

Table 1.1: Radio frequency bands as per IEEE standards.....	3
Table 2.1: Summary of the literature review.....	29
Table 3.1: mm-Wave bands classification.....	39
Table 3.2: The dimensions of final Ant 3. (in mm).....	43
Table 3.3: The comparison of proposed Ant 3 with other mm-wave based antennas	51
Table 4.1: Dimensions and optimized Parameters of the Proposed Antenna (in mm)	60
Table 4.2: Comparison of mm-wave antennas with the proposed antenna.....	76
Table 5.1: Dimensions of the proposed Patch Antenna (in mm).....	82
Table 5.2: The comparison of parameters of Ant1, Ant2 and Ant3.....	88
Table 5.3: The comparison of Previous Designs with Recent Antenna.....	88
Table A.1: Connectors configuration and Attributes.....	93
Table A.2: Apparatus used for Antenna parameter measurement.....	102
Table A.3: Antenna testing devices used for proposed antenna Measurement.....	102

ACRONYMS AND ABBREVIATIONS

Acronym	Description
2D	Two Dimensional
3D	Three Dimensional
3GPP	3 rd Generation Partnership Project
4G	4 th Generation
5G	5 th Generation
A-i-P	Antenna in Package
BW	Bandwidth
CCL	Channel Capacity Loss
CP	Circular Polarization
CPW	Coplanar Waveguide
D2D	Device – to - Device
DGS	Defected Ground Structure
DRA	Dielectric Resonator Antenna
DoS	Department of Space
ECC	Envelope Correlation Coefficient
eNB	Evolution Node B
FBR	Front to Back Ratio
FCC	Federal Communication Commission
FDD	Frequency Division Duplexing
FEM	Finite Element Method
FMCW	Frequency Modulated Continuous Wave
G	Gain
HFSS	High Frequency Structure Simulator
IEEE	Institution of Electronics and Electrical Engineers
IF	Iteration Factor
IMT	International Mobile Telecommunications
IO	Iteration Order
ISM	Industrial Scientific and Medical Band
ISRO	Indian Space Research Organization

ITU	International Telecommunication Union
IoT	Internet of Things
LTE	Long Term Evolution
LTE-A	Long Term Evolution Advanced
MIM	Metal Insulator Metal
MIMO	Multi Input and Multi Output
mm-Wave	Millimeter Wave
MMIC	Monolithic Microwave Integrated Circuit
MoM	Methods of Moment
MSPA	Microstrip Patch Antenna
OFDMA	Orthogonal Frequency Division Multiple Access
PCB	Printed Circuit Board
PCMA	Printed Circular Monopole Antenna
PDA	Personal Digital Assistant
PGP	Partial Ground Plane
PIFA	Planar Inverted F- Antenna
RF	Radio Frequency
RMFA	Rectangular Microstrip Fractal Antenna
RRP	Rectangular Radiating Patch
SCL	Semiconductor Limited
SIW	Substrate Integrated Waveguide
SMA	SubMiniature Version A
UMTS	Universal Mobile Telecommunications Systems
UWB	Ultra -wide Band
VNA	Vector Network Analyzer
VSWR	Voltage Standing Wave Ratio
WLAN	Wireless Local Area Network
WPAN	Wireless Personal Network
Wi-MAX	World Wide Interoperability for Microwave Access
Wi-Fi	Wireless Fidelity
WRC	World Radio Communication

LIST OF SYMBOLS

Symbol	Description
α	Tilted Angle
$\tan\delta$	Loss Tangent
β	Clipping Angle
θ	Angle for Gain and Reflection Co-efficient
ϕ	Angle for Gain and Reflection Co-efficient
λ	Wavelength
λ_g	Guided Wavelength
ϵ_r	Relative Permittivity
c	Speed of Light
f_r	Resonating Frequency
Z_0	Characteristic Impedance

CHAPTER-1

INTRODUCTION AND OVERVIEW OF ANTENNA

1.1 INTRODUCTION

With the increase in the usage of wireless communicating devices and the increasing demand of data traffic, the fifth generation (5G) technology seems to be the potential candidate to satisfy the requirements for high speed and congestion free networks. The 5G network and the supporting devices will be the revolution in the communication industry. Thus, one of the possible solutions is the millimeter wave (mm-wave) and its supporting device such as mm-wave antenna. In other words, antenna acts as a transducer which converts electrostatic (ES) signal into electromagnetic (EM) signal. But to design an antenna for the specific application is the most challenging task. So, to design an antenna for the support of 5G networks, there are certain prerequisites such it should be of smaller size with low tangential losses and low cost. With the above said properties, microstrip patch antenna (MSPA) is the most suitable choice to meet the above challenges. Microstrip patch antenna with suitable size performs in an efficient manner for the specific application and is therefore it is tremendously accepted throughout the world. As microstrip patch antenna supports mm-wave range and its applications, it will be the revolution for the upcoming 5G technology.

1.2 NEED OF mm-WAVE TECHNOLOGY

With the exponential growth of wireless data traffic due to the usage of digital devices such as laptops, PDA's, cell phones and other devices which results a severe network issues such as network load, congestion and interference problems. Therefore, to solve these kinds of issues, millimeter-wave (mm-wave) technology will work as a boon for high-speed data networks. Lots of research is continuing to support the radio architecture for mm-wave frequency ranges which varies from 30GHz – 300GHz. Therefore, in order to maintain the consistency for high data rate, antennas which can support mm-wave are highly required. The other perspective with the communication industry is to overcome the spectrum shortage which leads to the mm-wave band more prominent. This leads to explore the millimeter wave (mm-wave) frequency

range for futuristic 5G communications with high data rate connectivity for cellular, satellite, defense, medical, multimedia and many other area applications.

With these advantages mm-wave range communication system also adhere to some disadvantages such as sensitive to blockage and propagation losses suffers as it carries high carrier frequency. Therefore, to reduce these kinds of losses high gain antenna is the major requirement to support communication devices [1, 2, and 3].

1.3 APPLICATIONS OF mm-WAVE SPECTRUM IN ANTENNA

- ✚ Automotive Radar Applications
- ✚ Satellite Communication
- ✚ 5G cellular Communication
- ✚ WPAN/WLAN (IEEE 802.15.3c, 802.11ad/ay)
- ✚ Vehicular Applications
- ✚ Medical Applications (Tissue Diagnosis)
- ✚ Internet of Things (IoT) Applications
- ✚ Massive MIMO Applications
- ✚ Health Care Applications [1]

1.3.1 WRC -19 SUGGESTIONS

International telecommunications union (ITU) world radio conference (WRC-19) proposed new cellular bands for fifth generation (5G) at millimeter wave frequency. The new 5G bands which were under consideration for various countries despite various sharing issues are as follows [2]:

- ✚ 24.25–27.5 GHz
- ✚ 31.8–33.4 GHz
- ✚ 37–40.5 GHz
- ✚ 40.5– 42.5 GHz

1.3.2 THE COMMUNICATION SPECTRUM

The spectrum is defined as the RF assigned for communication systems. Over the time, guidelines for assigning the spectrum to wireless communication systems are modified to have high economic benefits and its efficient use. This

also helps to provide affordable spectrum to each person, high data speeds and more connectivity. The designated spectrum bands per standards Institute of Electrical and Electronics Engineering (IEEE) are given below:

Table 1.1: Radio frequency bands as per IEEE standards

S No.	Band Name	Frequency Bands
1	<i>L</i>	1-2 GHz
2	<i>S</i>	2-4 GHz
3	<i>C</i>	4-8 GHz
4	<i>X</i>	8-12 GHz
5	<i>K_u</i>	12-18 GHz
6	<i>K</i>	18-27 GHz
7	<i>K_a</i>	27-40 GHz
8	<i>V</i>	40-75 GHz
9	<i>W</i>	75-110 GHz
10	<i>G</i>	110-300 GHz

1.3.3 LTE (Long Term Evolution)

With the advancement of fourth and fifth generation, the development of data traffic is more prominent than multiple times has been anticipated, thusly in the impending years in excess of 10 Exabyte's of traffic development each month is expected across cell network. The third generation project partnership (3GPP) had started working in long term evolution (LTE) systems with its specific versions. Therefore, to obtain high speed interface with the involvement of orthogonal frequency division multiple accesses (OFDMA), release-8 includes high speed downlink packet access (HSDPA) and high speed packet access (HSPA) techniques. LTE in the communication system has been incorporated in favor of the decrease in cost per bit, adaptability to utilize novel and accessible bands, outdoors connections, and least utilization of power, congestion control and improved inclusion. As a result, current LTE devices are hence ready to accomplish high transmission rates of 150 to 300 Mbps, which have brought forth the usage of Internet of Things (IoT). Thus, LTE

in the today's scenario can be considered as the latest radio interface technology [3]. LTE supports band of 1920- 1980 MHz for uplink and 2110-2170 MHz for downlink for FDD.

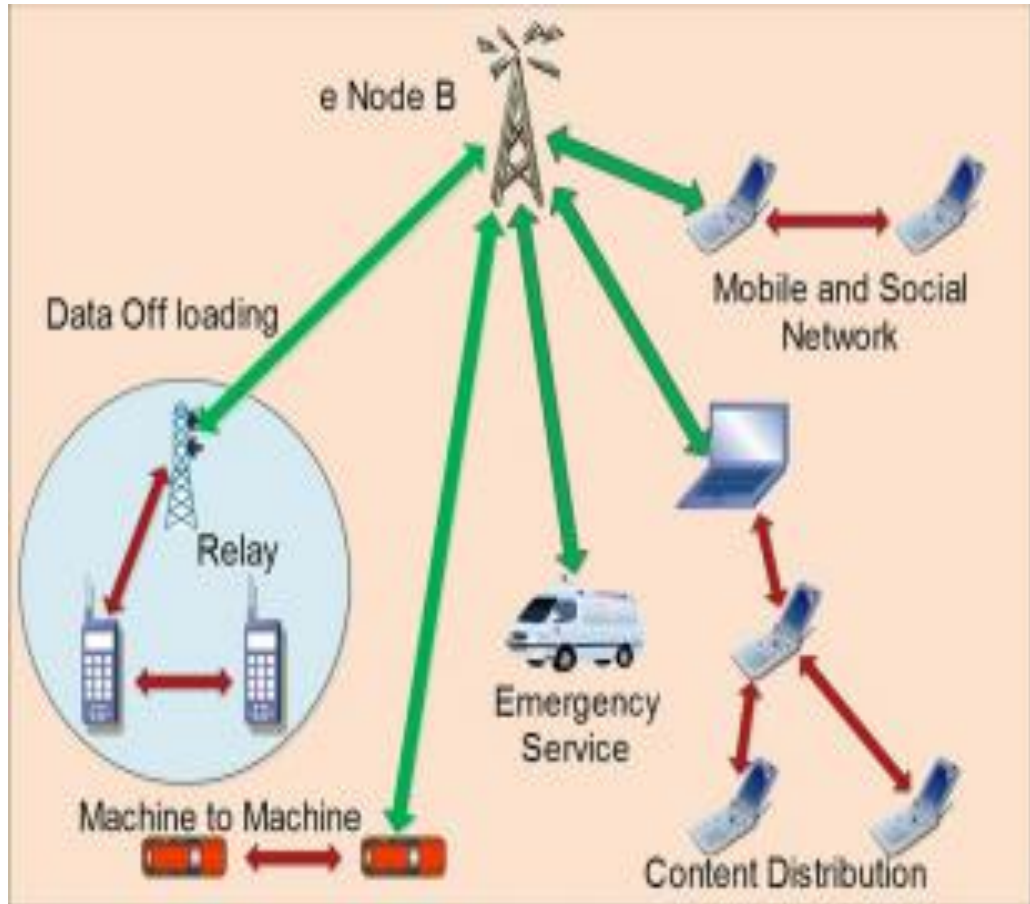


Figure 1.1: Example of D2D Communication using LTE

1.3.4 LTE-A (Long Term Evolution-Advanced)

With the quick advancement of 4G and beyond 4G advances (B4G), the 5G technology yet to gear up by the end of 2021. The innovative procedure shall improve the broadcasting capacities interface in addition to empower latest broadened applications which will be far contrast from the conventional advanced mobile and different appropriate gadgets. Therefore, current communication industry has been focusing on trustworthiness with provisions of improved network exposure and other prerequisites. Also, to guarantee that LTE-A can topographically oblige the accessible range for channel portion over 20 MHz, the prerequisites recommended by the ITU is that the transmission rate should be $> 1\text{Gbps}$ by the implementation of MIMO and

MU-MIMO. Therefore, LTE-A technology is focusing to reduce the problems there are being faced by the current 4G network thereby enhancing the network performance. Radio interface modeling can be accomplished with the LTE-A simulation tool and several other available simulators which must support the 5G network for the application level protocols. Numerous wireless performance parameters for 5G can thus be evaluated for the protocols with support physical and other layers in the diverse environment [3]. LTE-A has frequency band of 3400-3800 MHz for uplink and same frequency band for downlink communication. Therefore, the various releases are issued by the 3GPP with the new features and some of the features are as under:

- ✚ Enhances support to Machine to Machine (M2M) communications
- ✚ Evaluation of Small cell enhancements for interference mitigation, radio based synchronization for the improvement in spectrum efficiency.
- ✚ Focussed on power efficient, public safety Proximity services (Prose).
- ✚ Interoperability Features (SON's).
- ✚ Handover performance improvement in Het-Nets.

1.4 MICROSTRIP ANTENNA: AN OVERVIEW

The initial concept of MSPA was proposed by Deschamps [4] in 1953. In 1970, Munson [5] and Howell [6] demonstrated the MSPA in practical form. The researcher's community has shown the deep interest in MSPA over the passage of time because of its extraordinary advantages. The MSPA can be effortlessly fabricated on low-cost printed circuit board, thus MSPA is also known as printed antenna. The MSPA also have advantages as these are light-weight, small size, low cost and low-profile which leads to design of numerous MSPA to use in multiple applications [7]. Due to these advantages, the MSPA became extremely popular for small communication systems like Wireless Fidelity (Wi-Fi), Bluetooth, Worldwide Interoperability for Microwave Access (Wi-MAX), digital media broadcasting, personal and mobile communications.

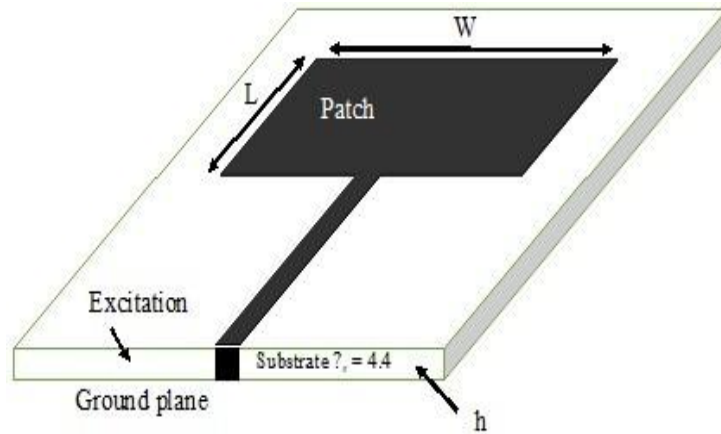


Figure 1.2: The view of microstrip patch antenna (MSPA)

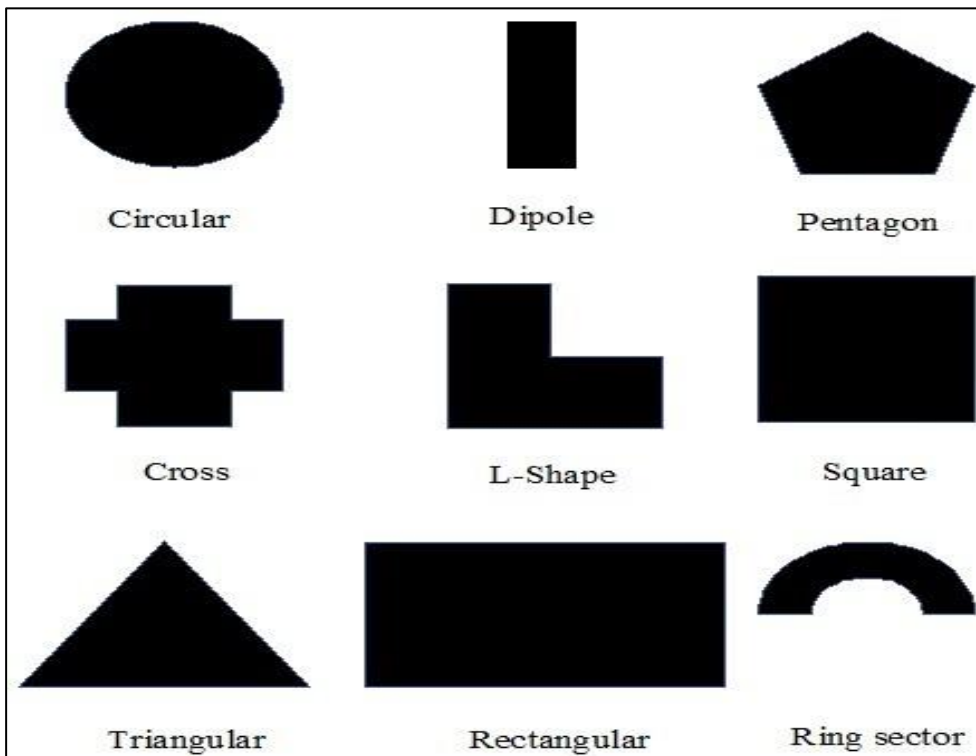


Figure 1.3: The basic radiating patch shapes of MSPA

The microstrip antennas are preferred over conventional microwave antennas because of its numerous extraordinary advantages for several practical applications. The patch antennas are most common type of the microstrip antennas that are used at microwave frequencies. The simplest form of MSPA comprises of a radiating patch on the dielectric substrate and a ground plane on the reverse side of it [8]. The thin copper foil coated with anti-corrosion metal like tin, nickel, gold etc. is used for patch and ground plane. The patch of microstrip

antenna from which energy is radiated known as radiating patch and it have many shapes like circular, dipole, pentagon, cross, L-shaped, square, triangular, rectangular, ring sector etc. The most common and preferable type is the rectangular shape and the antenna with this shape is known as rectangular microstrip antenna as shown in Figure 1.2. The other kinds of shapes for patch of microstrip antennas that are used in practical applications are shown in Figure 1.3.

1.5 THE ANTENNA SUBSTRATE

The substrate is of an insulating material such as Flame-Retardant-4 (FR4) and Rogers RT/Duroid 5880. These materials are most common used due to ease of availability depending upon the value of relative permittivity (ϵ_r), the substrate used for microstrip patch antenna is categorized as:

1. for $1.0 \leq \epsilon_r \leq 2.0$, substrate must be of honeycomb, polystyrene foam or air
2. for $2.0 < \epsilon_r \leq 4.0$ substrate typically made up of fiberglass reinforced Teflon
3. for $\epsilon_r > 4.0$ substrate is comprised of glass, marble, mica, gallium arsenide

To have better efficiency, wide impedance bandwidth and for overall good performance of MSPA, a thick substrate with lower dielectric constant is desirable [9].

1.6 FEED TECHNIQUES TO MICROSTRIP ANTENNA

The diversity of techniques is existed in literature to transfer radio frequency (RF) power from source to antenna; these techniques are known as feeding techniques. The existing feeding techniques are broadly categorized as non-contacting and contacting techniques [10–12]. In the case of non-contacting techniques, the RF power is transferred among RP and microstrip line by coupling electromagnetic field whereas, in the case of contacting techniques, RF power is directly fed through physical contact via microstrip line from source to RP. The MSPA is fed with four most popular common feeding techniques:

- Aperture coupling[9]

- Microstrip line[10]
- Coplanar feed (coaxial probe)[11]
- Proximity coupling[12]

Out of these, microstrip line and coaxial probe are contacting feeding techniques whereas proximity coupling and aperture coupling are non-contacting techniques. Feeding towards the microstrip line is quite uncomplicated implementation because it is fabricated while construction of antenna and the extension into array is also feasible.

1.7 DESIGNING MODELS

The various models for designing of MSPA's [13] are broadly classified as

- Transmission line model [13,14]
- Full wave analysis model[15]
- Cavity model[16]

1.8 CHARACTERISTICS OF MSPA'S

The dominant requirements of an antenna are to have wide impedance bandwidth, high gain, low weight, small size and embedded installation [17]. The MSPA offers many essential merits, however basic MSPA and its arrays also have some demerits. The merits and demerits of the MSPA are given below:

1.8.1 MERITS OF MSPA'S

- The MSPA's are of low profile, having the order of thickness not more than $0.03 \lambda_o$ (where λ_o is denoted as wavelength in the free space)
- The MSPA offers both circular as well as linear polarization
- The MSPA are light weight and very thin antennas, as they are constructed by placing perfectly electrical conductor (PEC) on the thin substrate.

- The MSPA's can be easily fabricated on inexpensive materials like FR4
- The operation in multiple frequency bands are also possible using MSPA's
- The active components can also be integrated with in the structure of MSPA due to its planar form
- The manufacturing process of MSPA is also easy as compared to conventional antennas

1.8.2 DEMERITS OF MSPA'S

Despite abundant merits of MSPAs over conventional antennas, the MSPA's also suffer from some demerits as follows:

- The MSPA have low radiation efficiency
- Due to surface waves, the higher modes may be excited which in turn reduces the antenna gain
- The MSPA's have relatively low power handling capability compared to conventional antennas
- Due to existence of higher horizontal component of surface current, the MSPA may have high cross polarization
- MSPA may have high feed network losses

The major restrictive factor for MSPAs is that the fractional impedance-bandwidth is in the range of 1–5 %, therefore the use of MSPA's for wide range of applications are not possible. Thus, the researchers got scope in this field and achieved [18] 70 % of fractional impedance bandwidth in the short span of past 20 years. Along with the improvement of fractional impedance-bandwidth in MSPA, there is also need to maintain fractional-gain-bandwidth, peak-gain, impedance, omnidirectional radiation patterns, and depth of return loss or through power (%).

1.9 ANTENNA PARAMETERS

Antenna performance is analysed on the basis of following parameters:

1.9.1 Antenna Gain: It may be is defined as the capability of the device to transmit and radiate in particular direction as compared to isotropic antenna. Directional antenna gives better performance in one direction than isotropic antenna. For transmitting antenna, gains are the factor of input energy conversion into radio waves in one direction and for receiving antenna gain defines how much radio frequency wave are converted into electrical signal. Antenna gain is basically functioning of antenna efficiency and directivity. Graphical representation of gain with respect to directivity is called radiation characteristics of antenna. Gain in terms of efficiency and directivity is given as follows:

$$G = \eta D \quad (1.1)$$

Here, D is directivity and η is efficiency of antenna which is unit less and lies between ($0 \leq \eta \leq 1$), and $\eta=1$ for lossless antenna. Practically gain of antenna at all times not more than directivity.

Gain is of two types:

- (a) Power gain (G_p)
- (b) Directive Gain (G_d)

Power Gain (G_p): It is defined as the ratio of radiation intensity in particular given direction to the total average power input power applied across antenna.

$$G_p = \frac{U(\theta, \phi)}{P_t/4\pi} = \frac{4\pi U(\theta, \phi)}{P_t} \quad (1.2)$$

Here, P_t is the total power and $P_t = P_r + P_i$, P_r is the Radiated power and P_i is the ohmic loss in antenna

Directive Gain (G_d): It is expressed as the ratio of antenna radiation intensity in given headed direction to the average antenna radiated power.

$$G_d = \frac{U(\theta, \phi)}{P_r/4\pi} = \frac{4\pi U(\theta, \phi)}{P_r} \quad (1.3)$$

Directive gain is independent of radiated power and antenna losses, so maximum value of Gd is directivity of antenna.

$$G_p = \pi G_d \quad (1.4)$$

1.9.2 Directivity: Antenna directivity is defined as the measurement of how directional any antenna has its radiation pattern. Antenna directivity is defined in terms of decibels (dB). Radiation pattern of antenna will be more focused or concentrated in one particular direction if antenna directivity is high and will travel long distance. Omnidirectional antenna that radiates equally in all directions has 0 dB directivity. Directivity is defined in terms of antenna gain and electrical efficiency. It is maximum value of its directive gain and is represented by

$$D(\theta, \phi) = \frac{U(\theta, \phi)}{P_{tot}/4\pi} \quad (1.5)$$

Here, θ and ϕ are the zenith angle and azimuth angles respectively. Also, Directivity is defined in terms of ratio of maximum power density to average value of power observed in far field over S-sphere.

$$D = P(\theta, \phi)_{max} / P(\theta, \phi)_{av} \quad (1.6)$$

Directivity value D lies between 1 and ∞ . For isotropic antenna directivity can be calculated below:

$$D = \frac{4\pi}{\Omega_A} = \frac{4\pi}{4\pi} = 1 \quad (1.7)$$

1.9.3 Input Impedance: Antenna input impedance is defined as “the impedance presented by an antenna at its terminals or the ratio of the voltage to the current at the pair of terminals or the ratio of the appropriate components of the electric to magnetic fields at a point”. It is defined by following mathematical expression;

$$Z_{in} = R_{in} + jX_{in} \quad (1.8)$$

Where Z_{in} is the antenna input impedance, R_{in} antenna resistance and antenna reactance at the terminals is specified by X_{in} respectively.

How much power is stored in antenna near field, is presented by imaginary part of input impedance X_{in} . R_{in} in the resistive part of input impedance which consists of two components further, Radiation resistance R_r and loss resistance R_L . The actual power radiated by antenna is the power associated with radiation resistance, and power dissipated in terms of heat is the power loss due to dielectric or antenna conducting losses.

1.9.4 Return Loss: It is the function of transmitted power and reflected power in dB. It is mostly measured at the input of the coaxial cable connected to the antenna. If P_t is the source transmitted power and P_r is the reflected power than ratio of P_r/P_t is termed as return loss. Of return loss should be very small to transfer maximum power. Return loss is mainly presented in negative and should be as large a negative number. Large negative is the value, good will be the return loss. The required value to transfer the power of its maximum R_L should be as low as probable. It is expressed in dB as follows:

$$RL \text{ (dB)} = -20 \log_{10} |\Gamma| \quad (1.9)$$

Where $|\Gamma|$ is the reflection coefficient

1.9.5 Radiation Intensity: It may be defined as power radiated from antenna with respect to per unit of solid angle U that is independent on that part of the sphere surface in both horizontal and vertical planes. Antenna radiation intensity is related to beam direction and beam efficiency in that direction. It is used to measure radiation from antenna due to its independence on measurement range. Radiation intensity can be measured w.r.t isotropic antenna and given as;

$$\text{Radiation Intensity } U = \frac{W}{4\pi} \quad (1.10)$$

By plotting radiation intensity with different directions radiation pattern can be achieved.

1.9.6 VSWR: This parameter is used to measure how efficiently antenna impedance is matched with transmission line to deliver maximum power. To transfer maximum power between source and load, impedance of both terminals should be matched. Also, when transmission line is not properly terminated, then travelling wave is

reflected back completely or partially at the termination end. So, the combination of these incident and reflected waves give rise to voltage standing waves along the transmission line. This ratio of maximum to minimum amplitude of voltage is called VSWR [4] as given in Figure 1.4 below.

$$\text{VSWR} = V_{\max}/V_{\min} \quad (1.11)$$

VSWR is defined in terms of reflection co-efficient that defined how much power is reflected back from antenna.

$$\text{VSWR} = \frac{1+|\Gamma|}{1-|\Gamma|} \quad (1.12)$$

VSWR value lies between 1 to ∞ . If VSWR value is small, antenna is matched properly with transmission line and more power is delivered and there is no reflection.

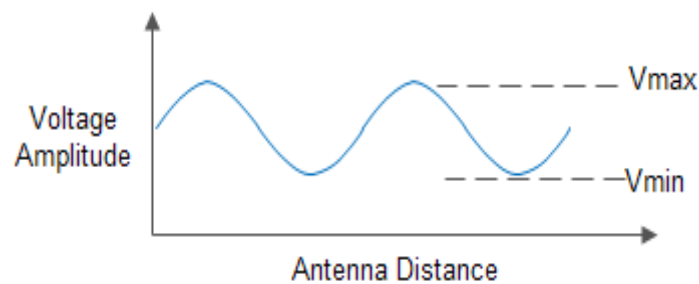


Figure 1.4.VSWR measurement along Transmission line

1.9.7 Bandwidth: It is expressed as “the range of frequencies within which the performance of the antenna, with respect to some characteristic, conforms to a specified standard.” It is considered as the range of frequencies on both side of cut of frequency where antenna performance parameters like input impedance, radiation pattern, polarization and beam-width should be within acceptable value with respect to central frequency.

1.9.8 Radiation Pattern: Antenna radiation pattern or far field describes the dependence of radio waves strength from antenna or other sources over angular direction [33]. Radiation patterns are graphical representation of antenna distributed power radiated from antenna if antenna is transmitting and incoming energy if

antenna is receiving as function of direction angles. It can be 3-D or 2-D plot. It has three following parameters:

- **Main lobe:** It is the major or main lobe which represents the major portion of radiated energy over larger area as shown in Figure 1.5. Maximum energy exits in this portion only which indicates directivity of antenna also.
- **Side lobe:** Antenna power distributed side ward with respect to main lobe is called minor or side lobes. Most of antenna power is wasted in this region.
- **Back lobe:** Antenna power radiation lobe that is opposite to main lobe known as back lobe. Antenna power is also wasted in this lobe as it reflects energy in opposite direction.

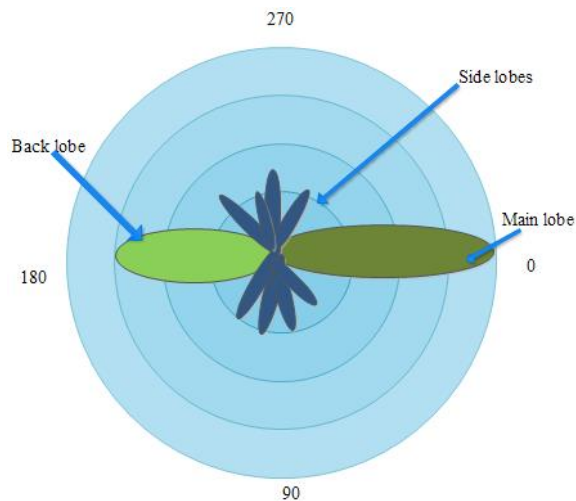


Figure 1.5: Radiation Pattern of Antenna

In Antenna, following radiation patterns are used most commonly

- **Omni-directional pattern/non-directional pattern:** It resembles figure of eight in if observed in two-dimensional view and give doughnut geometry in 3-D view.
- **Pencil-beam pattern:** The beam has a sharp directional pencil shaped pattern.
- **Fan-beam pattern:** The beam has a fan-shaped pattern.

1.9.9 Envelope Correlation Co-efficient (ECC): The envelope correlation coefficient (ECC) is the vital parameter to characterize MIMO antenna. Basically, this is a measure of isolation level among various MIMO antenna ports. The calculation of

ECC is based on radiation patterns which show the effect in terms of mutual coupling of various antenna elements that are operating simultaneously. Typically, its value should be less than 0.5 for good operational characteristics.

1.9.10 Diversity Gain: Diversity gain is related to the number of transmitters receives signals over different channels. It is also related with the signal to noise ratio (SNR) and gain enhancement and can be calculated by $DG = 10 \times \sqrt{1 - ECC}$ and for good operation of MIMO antenna diversity gain should be ≤ 10 dB.

1.10 MOTIVATION

With the recent advancements in this technological era there is a need of compact and handier devices which can support heavy data traffic for wireless communication systems. Therefore, to support this miniaturized mm-wave antenna has played a vital role. To reduce the overall dimensions of such systems, antenna optimization are therefore also becomes necessary. For wireless communication with high transmission data rates, highly efficient miniaturized wide band mm-wave antennas are needed with improved performance characteristics. Currently, the wireless devices are supporting communication by working on different wireless frequency standards, so wideband mm-wave antenna characteristics that have been suggested by international Telecommunication Union (ITU) and world Radiocommunication Conference (WRC-19) are seeking much attention of researchers. In literature, plethora of techniques are available to achieve mm-wave range such as fractal, defected ground structures (DGS), multiband, ultra wide band (UWB), Arrays, Multi Input Multi Output (MIMO) and several other techniques along with usage of expensive materials.

These are some of the theories used to achieve such behavior in microwave and antenna engineering field component designing. Another partial ground plane (PGP) technique offers the achievement of wide band characteristics as suggested by the WRC-19. With the partial ground plane wide band characteristics along with multiple resonances can be achieved in antenna and it also increase the length of flow of electric current without increasing the overall dimensions of device which leads to more compact structure. Also tapered feeding technique along with the partial ground plane in the slot antenna with different shape and size can increase the antenna's impedance matching, gain bandwidth and peak gain. Wireless communication standards like Wi-Fi, Bluetooth, Zigbee, GSM, GPS, LoRA, IoT, WiMAX, LTE/5G

are most adopted standards for wireless application in field of home automation, medical, industries etc. for wireless data sharing. So, there is huge demand for single fed low profile compact wide band antennas with high and stable gain, wide impedance bandwidth, and good radiation efficiency.

Microstrip patch antennas are generally considered as narrowband devices. Antenna dimensions and performance highly depends on the frequency of operation and wavelength. So, antenna design parameters like gain, input impedance, radiation pattern, surface current distribution etc will face changes due to shift in frequency of operation. Antenna dimensions are taken as quarter wavelength as per frequency of operation, and these basic design rules are taken care while designing antenna. But this is still a serious issue in antenna designing to obtain compact designs with respect to frequency. To deal with this problem, partial ground plane geometries can be used and further can be extended to array, MIMO designing to meet minimum requirements of wireless communication systems. The reason is that to overcome the load on lower 5G spectrum mm-wave bands are highly required and extend wide impedance bandwidth from 20GHz onwards so as to reach K- and K_a- bands.

Therefore, the methodology of PGP has been opted to enhance antenna parameters like operating impedance bandwidth, peak gain, radiation efficiency, return loss etc. PGP with different shapes and sizes can be configured so to divert the current distribution which actually changes the reactive characteristics of the circuit likes inductance and capacitance. Current distribution along with its component's direction and propagation through ground plane can be controlled by properly with suitable slots with the optimized dimensions and shapes which further controls electromagnetic wave's generation and transmission through supporting specific substrate material. Also, due to changes in inductive and capacitive properties of ground plane, additional frequency bands and resonances can be achieved which proves to be very useful in wireless communication devices.

In this thesis, wide-band microstrip patch antennas of high gain with high radiation efficiency are designed with partial ground planes for wireless applications like automated radar, satellite communication, health care, Internet of Things (IoT), LTE, LTE-A with frequency range of operation from 5 GHz to 40 GHz. Two different antenna prototypes are designed and tested on VNA based on partial ground plane geometry to obtain wide Impedance bandwidth characteristics. First antenna is designed with 3 point semi circular arc on the ground plane with tapered feeding point

on the inexpensive FR4 substrate. Wide impedance bandwidth of (5.86 GHz – 40 GHz) is achieved by exciting multiple resonant frequencies with the higher gain in n-260 and n-261 bands. Second simulated, fabricated and tested antenna design is also based on the partial ground plane by using Epoxy FR4 substrate. The inverted T-shaped slot along with 3-armed patch covers K_a-band (26.5 - 40 GHz) band applications. A compact design of antenna 3 covers high data rate communication applications with the achievement of wide impedance bandwidth of 30.86GHz–46GHz. Proposed mm- Wave antenna structures are fabricated on in expensive material with additional features like wide bandwidth, high gain and high radiation efficiency characteristics. Thus, mm-Wave antenna designs found to be useful in the futuristic wireless communication applications and standards.

1.11 STATEMENT OF PROBLEM

Based on the literature review, it has been concluded that still a lot of work has to be done by academia and industry. So the research gaps which require consideration and to be settled for the futuristic communication system in terms of communication system support prototype are as follows:

- ✚ Improvement in impedance bandwidth of the antenna is required.
- ✚ Further enhancement of gain for mm-wave antenna is required for futuristic communication bands.
- ✚ Miniaturization of antenna is required for futuristic communication bands.
- ✚ Coverage of 5G impedance BW is still needed according to World radio communication conference (WRC-19) for the mm-wave antenna.

1.12 SCOPE OF PRESENT WORK

Scope of present work is mainly to Design and Fabrication of mm-Wave Patch antenna for 5G futuristic wireless communication applications. Therefore, it is also necessary to optimize the antenna parameters like resonant frequency, Voltage Standing Wave Ratio (VSWR), Bandwidth, return loss, directivity and gain etc. for proposed antenna using HFSS simulation software and following steps are taken to design wide-band antenna using partial ground planes.

- ✚ Study and analysis of the existing Micro-strip antennas design for 5G Technology.
- ✚ Design of the wideband Microstrip antennas for futuristic 5G communication system.
- ✚ Optimization of parameters of designed antennas in terms of return loss, VSWR, gain and radiation efficiency.
- ✚ Fabrication of optimized and designed wide band Microstrip antennas using PCB Fabrication Machine.
- ✚ Finally, analysis and comparison of the simulated results with measured results of fabricated antennas with the measuring instruments.

1.13 THESIS OUTLINE

This thesis report provides detailed explanation about different types of microstrip antennas and methodologies used in literature for the improvement in several antenna parameters. Partial ground techniques used to analyze, design, optimize, fabricate and test wide-band microstrip antenna for wireless applications and complete process to achieve desired goal is divided into following chapters:

Chapter-1: This chapter provides the detailed explanation about the need of mm-Wave and its supporting wireless communication system technologies used and need of microstrip patch antenna. It also provides the information about the different applications based on mm-Wave and recommendations suggested by WRC-19. This chapter presents the overview of antenna, antenna performance parameters like Gain, Impedance, Bandwidth, Radiation pattern, Return loss etc. It also describes microstrip patch antenna structure with different feeding method used and different analysis techniques used for microstrip patch antennas. The problem statement, aim and motivation of thesis are also explained in this chapter.

Chapter-2: Presents extensive literature review on microstrip patch antenna used for wireless communication techniques. It provides detailed explanation about different methods and techniques used by researchers to improve antenna efficiency in terms of antenna parameters like gain, bandwidth, return loss, radiation patterns etc. and advantages and disadvantages of these methods. This chapter also explains about tools needed for antenna designing, simulations and to extract the performance parameters

for antenna performance analysis. Testing tools like Vector network analyzer are explained in detail in terms of their working principle, types and procedure followed for antenna parameter measurements.

Chapter-3: In this chapter, detailed explanation is presented for the millimeter wave (mm-wave) antenna design. It has also been explained with the help of literature survey that what the earlier techniques are used for antenna designing with the different shapes and sizes such as fractal, defected ground structure geometries etc. As several mm-wave antennas are available as per the literature survey, therefore in this chapter augmentation in bandwidth and gain has been achieved as the spectrum specified by the third generation partnership project (3GPP). Also, microstrip patch antenna with partial ground plane technique with clipped edges design methodology is elaborated with simulated and measured results comparative analysis.

Chapter-4: Explains about mm-wave wide band microstrip patch antenna design methodology and parametric study. Antenna performance has been analyzed in terms of return loss, gain, bandwidth and VSWR to investigate antenna proposed structures possibility for wireless applications. Simulated results for proposed prototype are verified and validated by testing and measurement.

Chapter -5: In this chapter, a compact mm-wave microstrip antenna design is analyzed with effective radiation efficiency.

Chapter-6: In this chapter, explanation is given about conclusions drawn from this research work and suggestions are intended for upcoming investigations.

Appendix: It accomplishes the different methodologies and procedures followed for the design of antenna from simulation to fabrication using Printed Circuit Board technology and setup used for the measurement of the different antenna parameters such as return loss, VSWR with the vector network analyzer (VNA).

1.14 SUMMARY

This section initiates by means of impression of wireless communication technology and different wireless technologies used with different frequency bands and bandwidth needed for efficient communication. Subsequently, it informs about need of microstrip patch antenna in wireless applications and it is realized that how concept of partial ground structures comes into picture for microstrip antenna performance and efficiency improvement. This chapter also explains the basics of microstrip patch

antenna, structure, characteristics, merits and demerits. Further the fundamentals of Antenna and Transmission line theory along with its performance parameters with mathematical expression are also discussed. Also, different types of feeding methods used to improve gain and bandwidth of patch antenna with different analysis methods used in Antenna simulation electromagnetic solver software's like HFSS, CST. To sum up, this chapter laid emphasis on microstrip patch antennas. Brief discussion has been done in the succeeding chapters. These chapters give the outline of research work.

CHAPTER -2

STATE OF ART WITH ANTENNA DESIGN METHODOLOGY AND SIMULATION TOOLS

2.1 INTRODUCTION

The recent and important developments in wireless communication systems, emerges out the need of efficient antenna, to transmit and receive signal wirelessly. The prime reasons for the rapid growth of wireless systems include easy to use, flexible and moreover it is cheaper compared to its wired counterpart. The miniaturization of wireless system technology results in the invention of novel devices such as cell-phone and Bluetooth etc. and the development of new network technologies such as Worldwide Interoperability for Microwave Access (Wi-MAX), Wireless Fidelity (WiFi) based on wireless local area (WLAN) networks. For these high-end applications, the multi-frequency and multimode antennas are required and in recent years, the demand of these antennas also increases several times. The prime requirements of such antennas are small size, wide impedance bandwidth, multi-purpose and high gain. The important factors of an antenna affecting the performance of wireless communication system are radiation patterns, polarization, peak-gain, and impedance-bandwidth and mismatch loss. To meet these requirements and improving the performance of antenna with many important factors, the various type of antennas exist in literature are wired, aperture, array, reflector and lens antenna [14]. Although, these are highly efficient antennas however they are large and not compatible with the compact communication devices. Due to compact in size, low cost, ease of fabrication and low profile, the microstrip antenna may be considered the best solution. Henceforth, a lot of research has been done to develop and modify the microstrip antennas.

2.2 LITERATURE REVIEW

The very first micro-strip antenna is proposed by Deschamps [4] and later demonstrated by Munson [5] and Howell [6]. Over the last decade, the numbers of microstrip antennas [19–22] were developed. These antennas were manufactured using a low-cost substrate of material called Frame Redundant (FR4) and patch and ground planes are made up of copper film. Since the microstrip antennas were planar structures and thus also known as printed antennas. In these printed

antennas many active components such as varactor diodes or pins, [16, 23, 24] were added as load to the patch to make the designed antenna more versatile.

2.2.1 Shapes of antenna structures

In the past few years, researchers had designed various microstrip antennas that have different shapes or structure. These were categorized as Spiral slot antenna [25], Vivaldi antennas[26], circular disc [27], elliptical [28],Spherical annular [29], stack patch [30], crescent-shaped [31],V-shaped [32], rectangular [33], triangular [34], half elliptical [35], hexagonal [36], fractals antenna [37], etc.

2.2.2 Bandwidth Enhancement

One of the main advantages of microstrip antenna is that they have compact size, due to which it can be efficiently installed in real time environment without using much space. The other advantages include ease of fabrication, low cost, low profile etc. Despite of many advantages, microstrip antennas have prime disadvantage of narrow impedance bandwidth [14]. At very beginning, addition to narrow impedance bandwidth, the major disadvantages of microstrip antenna designed were low power handing capability, high quality factor (Q) and low radiation efficiency. Therefore, these narrow band microstrip antennas can be used only for limited number of applications. Therefore, to improve the bandwidth and efficiency, the researchers had increased the height of the substrate [38] as one of the solution. With the use of thicker substrate, the undesired surface waves were introduced which results in low power generation of space waves. The new techniques were introduced to suppress the surface wave such as by using cavities [39], and stacking [40]. Though these methods bandwidth of antenna is enhanced and surface waves were eliminated.

2.2.3Fractal structures of patch antenna

The fractal structures are the one of efficient designing techniques adopted to boost the bandwidth of microstrip antenna. Therefore, in last decade, a strong interest has been generated on fractal structures of antenna to optimize the performance. The fractals are self-similar structure having same shape and different scaling factor. The various types of fractal antennas such as Sierpinski

carpet [41], Sierpinski gasket [42], Minkowski fractal [43], Koch fractals [44], Hilbert curve [45], Cantor set fractal structure [46], Vicsek shape fractals [47] has been introduced in the past years.

2.2.4 Multi-band antennas

Several compact size multiband antennas were reported in the past literature. Afrough *et al.* [48] designed a compact size of $17 \times 20 \text{ mm}^2$ dual band antenna with the use of multi-layered substrate composed of FR4 and air/foam with an antipodal parasitic element. The presented antenna exhibited the good radiation patterns with 2.39–2.5 GHz and 5.1–6.05 GHz with 10 dB return loss bandwidth. Anguera *et al.* [49] presented a triple band microstrip Sierpinski fractal antenna with a broadside radiations patterns. The method of movement coding was adopted to design the antenna and it provides high efficiency. Chang *et al.* [50] proposed dual band circular fractal slot antenna with CPW feeding based upon the synthesis configuration and design map. The authors have presented first dual band half wavelength design which provides fractional impedance bandwidth of 47.4 % and 13.5 % and peak-gain of 3.58 dBi and 7.28 dBi. The second presented dual band design is of quarter wavelength which provides fractional impedance bandwidth of 75.9 % and 16.1 % and peak-gain of 3.58 dBi and 7.28 dBi. The omni-directional radiation patterns were also figure out by applying the Contour distribution patterns. Moreover, the EM characteristics were also verified by depicting the simulated current distributions. Hu *et al.* [51] presented a miniaturized tri-band antenna realized by introducing L-shaped slot edge and E-shaped coupled edge resonators at edges of the monopole to field independent resonant frequencies. Further to reduce the size of designed antenna a symmetric co-planar strip feeding method is employed to feed monopole antenna. The presented antenna is suitable for WLAN and Wi-MAX applications. Hung *et al.*[52] Proposed a dual band reconfigurable slot antenna on a folded slot loads deployed with inductors and capacitors, which results in affected the phase of edged currents. Kumar *et al.* [53] has designed a multi-band hybrid fractal antenna with combination of Koch curved at idention angle of 60° and Minkowski curve at idention angle of 90° . The author has claimed the designed antenna has exhibited seven multi-bands with the value of 10 dB return loss i.e. GPS, ISM,

WLAN, mobile satellite, four bands for navigation. The presented hybrid fractal antenna is compact in size of $28 \times 15 \text{ mm}^2$ return loss for two fractal iterations were presented and compared. The maximum gain of designed antenna was 4.16 dBi. Li *et al.* [54], have designed a triple band microstrip antenna by using a toothbrush-shaped patch (TSP), inverted U-shaped patch (IUSP) and a meandered line (ML) for WLAN and Wi-MAX, however the antennas presented are designed only for certain frequency instances that too for specific applications. Song *et al.* [55] proposed a multiband perturbed fractal Sierpinski gasket antenna in which two methods of switching of impedance with port were discussed. An expected ratio of 0.5 is improved by using microstrip feed technique from the value of 0.35 as used in conventional feeding. Another outcome of designed antenna is that the antenna is not a frequency independent design. Tsachtsiris *et al.* [56] presented a dual band (2.4 GHz and 5.2 GHz bands) Sierpinski Gasket antenna printed on the surface of the dielectric lamination which is extended beyond the circuit of the device. The author claimed that without need of the matching network antenna possessed high efficiency, Medical and Industrial scientific bands even retaining small size of the printed antenna.

2.2.5 Wideband and UWB antennas

Instead of narrow band or multi-band antennas, a wide-band and ultra wide band are likely to be suitable by extending bandwidth of multiband and narrowband antennas, which is potential candidate to successful cognitive wireless task in these days. In current satellite, portable and remote correspondence frameworks, the correspondence inside S-band and UWB is considered significant on the grounds that utilizing a little omnidirectional radio wire of the size of only couple of centimeters can viably get/emanate the sign. The microstrip patch antennas are amazingly main-stream for S-band and UWB communication due to minimal expense, low profile, reduced estimate and can undoubtedly be imprinted on circuit board

2.2.6 L-band

The different shapes for L band include quasi yagi, slot and micro strip patch antenna [57–60]. The antennas in these bands were optimized to improve the

bandwidth, directivity. Different shapes for the patch antennas have been discussed for the improvement in bandwidth [61].

Antennas were also designed which can operate in the multiple bands also. Obviously, their applications range and frequency will be wider than other antennas which were designed to operate in the single band. These antennas namely PIFA (Planar inverted F antennas), low power active antenna, quadruple inverted which is totally based on the patching technique. The objective is to make the size more compact which is suitable for the applications in wireless communications [62–64].

Interference in the wireless communication system is the major problem but it can be overcome by using circular polarized antenna. It may be single path or multipath. As wireless communication devices are operating on the multiple frequencies so interference is the major problem during communication. The base for the antennas which are to be designed is the patch. CPA provides the diversity and reduces transmission losses due to the misalignment between the terminals [65].

2.2.7 S-band

In recent literature, many authors have presented several compact size antennas for S-band applications. Cai *et al.* [66] designed a reconfigurable polarized omnidirectional antenna, which is designed by inserting PIN diode on the slots. The diode is controlled by using a single diode; if only positive (negative) polarity is applied left (right) handed circular polarization (L/RHCP) is obtained with wide impedance bandwidth of 19.8 % in frequency band of 2.09–2.55 GHz. Khanna *et al.* [67] has designed a gap coupled antenna with efficiency of 97.56 %, impedance bandwidth 1.68–4.16 GHz and gain 3.31 dBi for S-band applications. Li *et al.* [68], have designed a double layered structure compact polarization microstrip antenna in S-band to achieve left and right hand circular polarization with impedance bandwidth of 24 % i.e. S_{11} less than -15 dB. Nascetti *et al.* [69] designed a novel circularly polarized patch antenna for earth-observing Cubesat in S-band. The proposed antenna yields impedance bandwidth 1.7–3.2GHz, gain of 7.3 dBi, directivity of 8.3 dBi and 60° 3dB beam-width. Nikfalazar *et al.* [70] designed a beam steered phased antenna array (PAA) in which fully printed

components are made with loaded line phase shifter that are both compact and PAA adaptable. The disadvantage of the presented antenna is that due to resonance of the virtual ground radial stub, therefore the operation bandwidth is limited to 2.4–3.3GHz. [25] has designed a dual wide band printed monopole antenna, in which the impedance bandwidth has been increased with the use of trapezoid conductor-backed plane to cover the bands 2.5/3.5/5.5 GHz for WiMAX and 2.4/5.2/5.8 GHz for WLAN. Qu *et al.* [71], have designed a cavity-backed folded triangular bowtie antenna for S-band to achieve impedance bandwidth of 92.2 % for reflection coefficient less than -2. The designed antenna shows the larger bandwidth, stable radiation patterns and less fluctuations of input impedance as compared to cavity-backed ordinary TBA. Wang *et al.* [72] designed a wideband monopole antenna for the height of non-ground portion of 8 mm which results in lumped high pass matching filter for octa-band WWLAN/LTE mobile phones. Zhang *et al.* [73] designed a wide-band patch antenna array having dual polarization that achieves through I-shaped strip line and balun feeding with parallel strip line to replace 180° phase shifter which in turn provides good isolation for wide band of frequencies and small phase error within working band of 1.88–2.99GHz (41.7 %). Zhao *et al.* [74], used dual band antenna fed with a substrate integrated meandering (SIM) probe, which is designed to achieve low cross-polarization in S-band.

2.2.8 Ultra Wide-Band

Authors of [54] suggested a twin layer based Electromagnetic band hole (EBG) configuration array that joins straight directing radiating area along with gaps synchronized with its reverse side. Suggested configuration demonstrates with the purpose of detachment along with the multiple antennas which is can be enhanced by putting cuts on its reverse side. Federal Communication Committee (FCC) [75] has assigned a license free UWB band that has bandwidth of 3.1–10.6GHz, which increases the numerous free applications in this range. Hence, the designing of antennas in UWB band is an important area of research. The microstrip based UWB antennas [76] have turned to be the first choice of researchers because of special properties [77] such as portability, printability and low cost etc. However, these antennas have narrow impedance bandwidth and

gain bandwidth. In recent literature, many authors have presented techniques to enhance the impedance bandwidth. Chitra, *et al.* [78] offered a twin L- shaped slot printed radiating array for Wi-MAX and WLAN bands. The authors claimed that by using two dissimilar slits, high-quality matching of impedance along with bandwidth can be achieved however there is $VSWR \geq 2$ at certain frequencies. Rectangular stepped slot antenna with bore sight radiation pattern design for ultra wide band. The researchers have achieved several parameters through which the performance can be analyzed from this antenna. Though, it depicts that the size of the prototype is $57 \times 32 \text{mm}^2$, which is overall measured as vast size. Srivastava *et al.* [79] projected a compact (MIMO) antenna for impedance bandwidth of 3.1–12GHz for communication applications. The designed device provides remoteness with no decoupling network, envelope correction coefficient (ECC) and channel capacity loss (CCL). The author's claimed that the calculated peak gain of the prototype is constant and is esteemed approximately 4dBi.

2.2.9 5G bands

However, to cover upcoming 5G services such as massive Ultra-reliable and Low Latency Communication, Machine Type Communication and enhanced Mobile Broadband, [80] the more bandwidth is needed. In the World Radio communication Conference-15 (WRC-15) there is proposal many spectrums for 5G applications, one of them is allocated for mobile and IMT identification (31.8–33.4 GHz) [80, 81]. In recent years, various techniques have been testified in literature to broaden the impedance bandwidth to cover 5G applications. Abdel-Wahab *et al.* [82] presented an aperture-coupled V-shaped (60GHz-band) patch antenna to enhance the radiation efficiency above 98 % by using substrate integrated waveguide (SIW) technology. The authors have claimed that the presented antenna covers unlicensed 57.66 GHz band with peak-gain of 6.8 dBi. Chin *et al.* [83] proposed a 60GHz wideband antenna array fabricated with a low temperature multi layered co-fired ceramic substrate. The backed substrate-integrated waveguide (SIW) cavity was used to enhance the front radiations. Further, the authors applied a parasitic patch to improve both bandwidth and gain of presented antenna. The author also claimed that four elements of antenna array

provide gain of 9 dBi in the frequency band of 57–64 GHz. Deng *et al.* [81] enhances the fractional-bandwidth from 69.1 % (2.53–5.2GHz) to 164 % (2.4–24.3GHz) of a monopole antenna for mobile communication. The author restructures the antenna as M-shaped notched rectangular RP at bottom, a T-shaped GP in the notch and exponential tapered GP out of notch. Emadian *et al.* [76] presented a rectangular slot antenna with dual notches for super ultra wideband of 159.38 % (2.6–23GHz). The designed antenna had been improved by bevelled corners of RP and with the etching semi-circular slots at current irregularities in the GP, which results in improvement in the impedance bandwidth. Haraz *et al.* [85] proposed a broadband elliptical slot ring dual band antenna for 5G cellular communication systems. The presented antenna design covered frequency band of 20–40 GHz and peak gain of 4dBi and 5dBi for 28 and 38band of applications. Lin*etal.*[86] Broadened the impedance-bandwidth by 193.59 % (0.57–35 GHz) of a strip fed tapered slot antenna by using irregular slot-line cavity. Mak *et al.* [87] presented a miniaturized 5G mobile phone antenna which is 44.8 % smaller in size as compared to half wavelength conventional patch antenna. The authors claimed that the antenna provides bandwidth of 10 % and 3dB axial-ratio in band of 3.05 %. The half beam-width was also enhanced to 1240 by supported metallic block and by surrounded the dielectric substrate to the radiating patch. Park*etal.* [88]Proposedanovel5Gantennawhichproducedradiationon an inclined direction by combining a waveguide aperture and multiple microstrip patch. The author claimed that the fractional impedance bandwidth of 5.4 % in frequency band of 27.2–28.7 GHz and gain of peak gain of 7.41 dBi, however, the beam is widely spread across azimuthal plane. Yang *et al.* [89] proposed a compact antenna array for 60 GHz band. The differential feeding technique with the use of parallel series feeding network was employed to boost simultaneously bandwidth and gain. The authors claimed that the designed antenna array provided peak gain of 15.6 dBi and impedance-bandwidth in frequency band of 55–68 GHz. Moreover, many printed antennas [90–92] have been testified for various 5G bands as proposed in WRC-15 [80, 81]. Huang *et al.*[93] designed dual pole vector synthetic dipole

antenna which can work upto 3.3 – 3.6 GHz 5G band based on MIMO technique. The authors claimed that high isolation of >25 dB, low cross polarization of < -24.5 dB and high front to back ratio can be achieved with small electrical size. The antenna was further extended to a 4x4 array by assigning weighting factor and phase for each element. Saif *et al.* [94] proposed the F shaped patch antenna for lower 5G band. The authors claimed that the antenna can cover 2GHz – 12GHz all lower 5G bands. The designed antenna provided the reflection coefficients of -35dB and -32.5dB at 5.2 GHz and 9.2GHz respectively with overall return loss under-10dB. Jaiswal *et al.* [95] designed the microstrip patch antenna for 60 GHz. The designed antenna with recessed ground plane enhanced the bandwidth of 9.47%. Khaleghi *et al.* [96] designed the microstrip patch antenna for Ku band applications. The authors introduced epsilon near zero (ENZ) impedance matching circuit for 50Ω, 100Ω and 150Ω which enhanced the bandwidth of 8 – 15%.

2.3 STATE OF ART SUMMARY

The following summarized table provides comparison of the information of the basic antenna parameters such as Impedance Bandwidth and Gain of the previous literature review:

Table 2.1: Summary of the literature review

S.No	#	Impedance BW (GHz)	Gain (dBi)
Multiband Antennas			
1	[48]	2.39–2.5 GHz and 5.1–6.05	4.5 dB
2	[49]	1 – 3 GHz	--
3	[50]	0-8 GHz	3.58 dBi and 7.28 dBi
4	[51]	2.37 – 5.96 GHz	1.98 dBi
5	[52]	0.5 -4.5 GHz	2.9 dBi
6	[53]	1.2 – 9.6 GHz	4dB
7	[54]	2.4/3.5/5.2/5.5/5.8 GHz	3.0 dBi
8	[55]	0- 10 GHz	5.83 dBi
9	[56]	2.4 / 5.33/ 10.2 GHz	---

WIDEBAND AND UWB ANTENNAS			
10	[57]	1.2 – 2 GHz	4.5 dBi
11	[58]	1 – 2 GHz	8 dBi
12	[59]	1.3- 1.7 GHz	14 dBi
13	[60]	1.884 GHz	5.7 dBi
14	[61]	1.56- 2.12 GHz	9.86 dBi
15	[62]	2.4–2.63 GHz and 5.04–6.04 GHz	---
16	[63]	VHF (174–216 MHz), UHF (470–806 MHz), and L-band (1450–1492 MHz).	3–4 dB
17	[64]	1.1 – 1.7 GHz	2 dBic
18	[65]	1.8 – 2.4 GHz	4 dBi
14	[66]	2.09–2.55 GHz.	2.5 dB
15	[67]	1.68–4.16	3.31 dBi
16	[68]	2.33 —2.97 GHz	---
17	[69]	1.7–3.2GHz	7.3 dBi
18	[70]	2.4–3.3GHz	12.5 dB
19	[71]	1.86 - 5.04 GHz	9.5 dBi
20	[72]	(0.69–0.98 GHz) and (1.63–2.74 GHz)	5.6 dBi
21	[73]	1.88–2.99GHz.	9.4 dBi
22	[74]	2.34–2.57 GHz and 3.5–3.83 GHz	5.8 dBi and 6.8 dBi
ULTRA WIDE AND 5G BANDS			
24	[76]	2.6 -23 GHz	5 dBi
25	[78]	2 – 6 GHz	8 dBi
26	[79]	3.1 - 12 GHz	4 dBi
27	[82]	57 – 66 GHz	6.8 dB
28	[83]	57 – 64 GHz	9 dBi
29	[84]	2.4–24.3GHz	4.4 dBi
30	[85]	20–40 GHz	4 dBi and 5 dBi for 28 band and 38 band
31	[86]	0.57–35 GHz	---
32	[87]	3.6 – 4 GHz	5.5 dBi
33	[88]	27.2–28.7 GHz	7.41 dBi
34	[89]	55–68 GHz	15.6 dBi
35	[90]	2 – 18 GHz	---
36	[91]	5.07 - 5.95 GHz	9 dBi
37	[92]	26.5–38.2 GHz	5.8 dBi
38	[93]	3.3 – 3.6 GHz	8 dBi
39	[94]	2 – 12 GHz	4.5 dBi
40	[95]	58.2 - 65 GHz	6.9 dBi
41	[96]	12 – 16 GHz	6.7 dBi

dB: dB(decibel) as a standalone unit represents a level (e.g. loss or gain)

dBi: dBi is antenna gain w.r.t. the isotropic antenna.

dBic: dBIC is decibel above the gain of a isotropic antenna as a reference where the isotropic antenna has the same circular polarization as the antenna of which the gain is expressed. From the above table, it can be concluded that the single miniaturized antenna for the mm-wave band is required which provide enormous impedance bandwidth along with high stable gain.

2.4 ANTENNA DESIGN METHODOLOGY

Designing antenna is an exceptional and iterative process that involves optimized multiple steps to attain final design that consist of diverse steps like design of antenna in the specific software with the help of simulations followed by the fabrication and testing process. This chapter discusses the methodology involved and kind of tools usage for the mm-wave antenna design, analysis, and fabrication and testing of proposed antenna.

For the design of simple antenna like dipole, methodology which adopted is quite simple and antenna's current distribution for the specific structure can be easily calculated and measured with realistic accuracy due to which it is easy for designer to calculate antenna performance parameters like Gain, Bandwidth, VSWR and radiation patterns etc. But for complex and mm – wave based high frequency antenna structures, the current densities are difficult to analyze, so simulation tools which can support at very high frequency are required to analyze antenna performance. Commercially, various electromagnetic solver antenna design tools are available to analyze the performance. Mainly, techniques used are Finite Difference Time Domain (FDTD), Method of Moments (MoM), and finite element method (FEM). The basic difference of these techniques is discussed as below:

The Method of Moment (MoM) operation is performed on the basis of linear partial differential equations (PDEs), which are formulated as integral equations (IEs). This technique solves for surface currents which are further helpful to analyse radiation patterns.

Finite difference time domain (FDTD) uses full-wave solving technique partial-differential versions of Maxwell's equations. This differential time-domain method solves for the electric field and then the magnetic field.

The Finite Element Method (FEM) uses adaptive meshing, numerical solving by subdividing a large system into smaller, simpler parts that are called finite element. Finally, it recombines all sets of component equations into a overall system of equations for the concluding computation.

2.5 SIMULATION TOOL USED

2.5.1 HFSS (HIGH FREQUENCY STRUCTURED SIMULATOR)

HFSS is an elite full-wave electromagnetic (EM) solver field test system for a self-assertive 3D volumetric latent gadget displaying that exploits the natural Microsoft Windows GUI (Graphical User Interface). The electromagnetic solver integrates simulation process by doing calculations at the back end and visualization of simulation process at the front end in an easy learning environment and EM solutions can accurately be obtained. The ANSYS HFSS 15.0 is used for scheming and recreating high recurrence electronic designs like antennas, RF and microwave segments filters, connectors and printed circuits boards to use in communication systems, Satellites, Radar systems, Internet of things (IoT) and other digital devices. It contains versatile solvers and GUI (Graphical User Interface).

Apart from the design of antenna systems HFSS gives a influential and whole Multiphysics investigation of electronics components through interaction with Ansys thermal, structural and fluid dynamics tools to ensure their thermal and structural reliability. It is the Electromagnetic tool used for research and development and virtual prototype designing. It is standard tool used for 3D modelling for high frequency design. Professor Zoltan Cendes developed it initially developed with his students at Carnegie Mellon University in year 1990. This tool consists of combination of simulation, visualization, automation and solid modelling. This software uses Finite Element Method (FEM), excellent graphics and meshing to provide good performance. Users have the flexibility to choose the solver as per their design requirements. High Frequency Structure Simulator (HFSS) is a 3D electromagnetic field solver simulation tool used to design a extensive range of high frequency antennas, filters, and IC packages.

Electromagnetic solvers are based on finite elements and other IE methods supported by high performance technology that enables to perform quick and truthful design of high-frequency and electronic components.

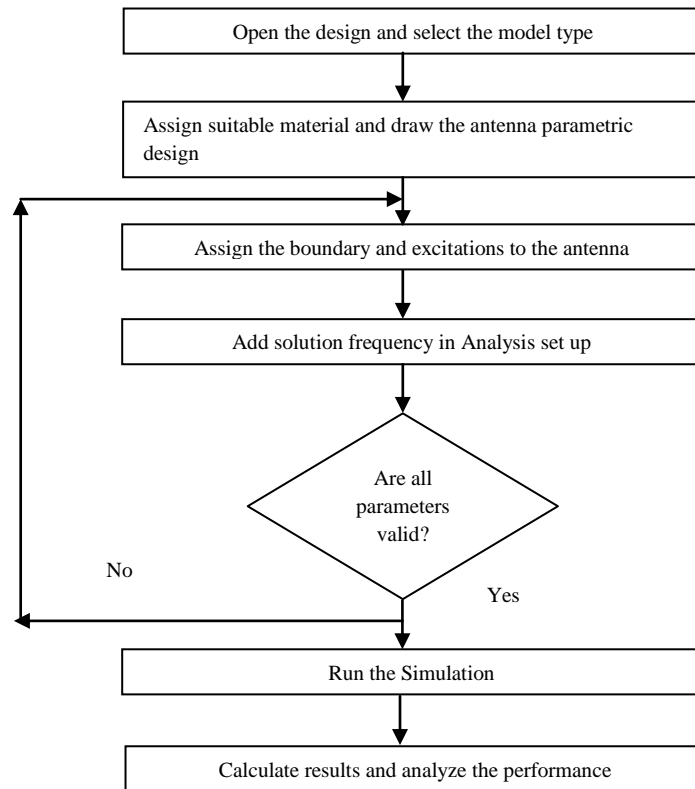


Figure 2.1: Ansys HFSS simulation procedure for Antenna designing

2.5.1.1 Structure Designing Process

The flow chart in Figure 2.1 illustrates the step by step process to prepare antenna design and analyse its performance using HFSS tool. Initially by selecting the modeler type designer can design the geometric model. Afterword's, proper dielectric material is assigned to designed antenna structure like FR4 Epoxy, Rogers RT Duroid 5880 with desired thickness and dielectric constant. In the next steps, source (port line lumped and wave port) assigning and boundary conditions are provided like perfect E to patch, ground and Radiations to Radiation box.

In HFSS simulator, after defining the boundary condition to all sheets and solids, a port either wave or lump is required to excite antenna structure. After structure modelling and validation check, the structure solution is setup. After that solution

frequency is assigned and frequency sweep is added to generate the solution frequency across the desired frequency range. Far field setup is added to calculate far field parameters like antenna gain and radiation patterns. After analysing the design, antenna performance parameters can be calculated in terms of S11, VSWR, Gain, 2D-3D Radiation patterns and Directivity etc. in graphical, table or smith chart form.

2.5.1.2 Antenna Design steps:

1. Create the ground plane
2. Create the substrate and assign dimensions after calculating with mathematical expressions
3. Assign dielectric material
4. Create the patch and assign dimensions
5. Create feed line with proper dimensions
6. Unite the structure i.e. Patch with feed-line
7. Assign perfect E boundary conditions to patch, ground plane
8. Assign port (Lumped or Wave) to antenna structure to couple electromagnetic energy
9. Create radiation box and assign Radiation boundary to radiation box.

2.5.1.3 Simulation and Analysis of Antenna

- To analyse the different parameters of designed antenna, the analysis setup is created first and desired solution frequency is assigned.
- ❖ **Go to HFSS design-Analysis-Right Click-Add Solution Setup-Assign Solution frequency-provide maximum number of passes**
- After assigning the solution frequency, the next step is to add the frequency sweep which is used to generate the solution frequency across the frequency ranges.
- ❖ **Go to HFSS design-Analysis-Right Click on Setup-Add frequency Sweep-Select Sweep Type (Discrete)-Assign Start and stop frequency with desired step size**
- After that far field radiation setup is used to analyse the gain and radiation pattern of designed antenna.

- ❖ **Go to HFSS design-Radiation-Right Click on Radiation-Insert far field setup-Infinite Sphere-Enter start and stop values for Phi and Theta in degrees.**

Execute analysis setup and compute results in terms of antenna parameters as follows:

S₁₁ / Reflection Co-efficient parameters:

Go to HFSS Design-Results-Right Click-Create Modal Solution Data Report-Rectangular Report-Select S₁₁ parameters in dB

VSWR:

Go to HFSS Design-Results-Right Click-Create Modal Solution Data Report-Rectangular Report-Select VSWR parameters in dB

Gain:

Go to HFSS Design-Results-Right Click-Create Far field report-Rectangular Report-Gain-Gain Total (dB)

Radiation Efficiency:

Go to HFSS Design-Results-Right Click-Create Far field report-Rectangular Report-Antenna Parameters-Radiation Efficiency

2.5.2 VECTOR NETWORK ANALYZER

Vector Network Analyzer is used to measure the frequency response of active or passive components or networks or it is sensitive and costly electronic instrument that is used to measure the frequency dependent properties of device under Test (DUT) as shown in Figure 2.2. This measurement can be carried over a range of frequencies starting from a few kilohertz to hundreds of gigahertz.

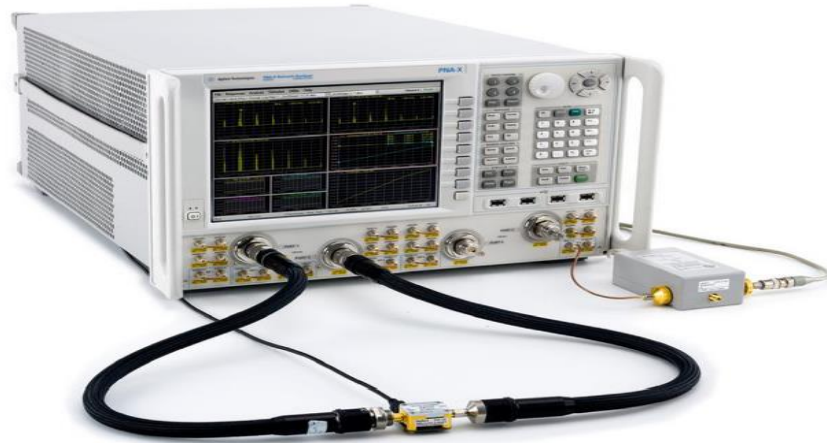


Figure 2.2: Practical two port Vector Network Analyzer

VNA measures then power going into and reflected back from a component and network at high frequencies. A signal electrical property can be analysed in terms of incident, reflected and transmitted signals, so, impedance of DUT can be calculated. The ratio of incident and reflected waves are defined in form of S parameters, also called S-Matrix or scattering parameters. Using VNA, both amplitude and phase of frequency signals can be measured at each frequency point. Also, insertion loss and return loss of device under test can be visualized by computer used in VNA in different formats like real and imaginary, magnitude and phase and Smith chart. For S_{11} parameter measurement following setup as given in Figure 2.3 is considered using 2-port VNA to measure S-Parameters of DUT.

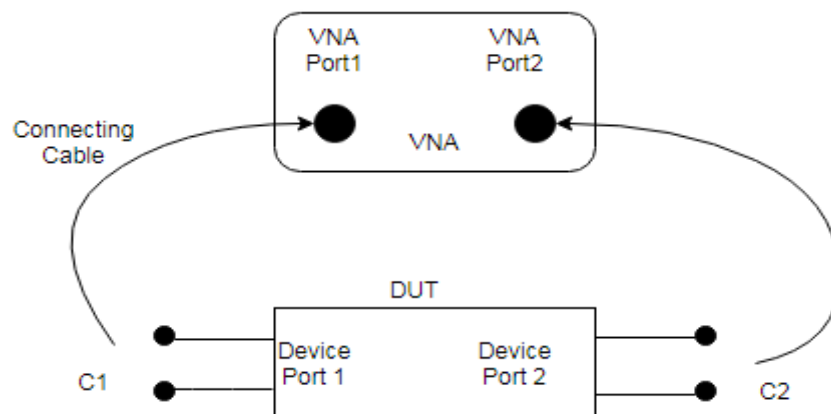


Figure 2.3: Setup for S-Parameter Measurement of DUT

Before performing measurement of device under test in VNA, it should be calibrated. Calibration means, all the undesired signal reflections, those will occur due to connecting cables and end terminals of connectors C1 and C2 as shown in Figure,

must be considered and nullify. After calibration, measurement can be done. When Port1 can be used as source for RF and a_1 is considered as incident voltage wave on DUT than b_1 and b_2 will be the reflected waves and transmitted waves through DUT respectively. Incident wave propagates from analyzer to DUT and reflected wave travels in opposite direction from DUT to analyzer. Also, phase and amplitude of a_1 is known, phase and amplitude of b_1 and b_2 can be measured using VNA. S-parameters give very accurate representation of the linear characteristics of device under test under ambient temperature conditions. It basically describes how the device interacts with other devices when cascaded with them. Reflection co-efficient (Γ) or S_{11} is given as follows in Figure 2.4:

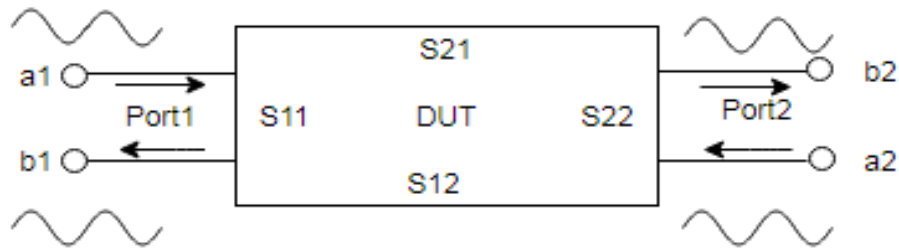


Figure 2.4: S_{11} co-efficient representation for 2-port network

$$S_{11} = \left. \frac{b_1}{a_1} \right|_{a_2=0} S_{12} = \left. \frac{b_1}{a_2} \right|_{a_1=0}$$

$$S_{21} = \left. \frac{b_2}{a_1} \right|_{a_2=0} S_{22} = \left. \frac{b_2}{a_2} \right|_{a_1=0}$$

$$S_{11} \text{ (Reflection co-efficient)} = \frac{b_1}{a_1} \quad (2.1)$$

$$\text{and Transmission co-efficient (T) or } S_{21} = \frac{b_2}{a_1} \quad (2.2)$$

2.6 SUMMARY

In this chapter, antenna designing, simulation and testing tools are explained. Antenna structure can be designed using High Frequency Software Simulator (HFSS) and antenna designing steps are represented using flow diagram. Steps are explained to analyse designed antenna performance in terms of return loss, gain, radiation efficiency using 2-D and 3-D plots. Also, antenna testing tools are used to measure antenna return loss performance, VSWR, gain and radiation efficiency working principle, features and types are also explained in detail.

CHAPTER -3

WIDE BAND mm- WAVE ANTENNA DESIGN

3.1 INTRODUCTION

With the constant growth of data traffic due to the usage of handheld and other digital devices and therefore requirements of spectrum globally, there is requirement of communicating devices like antenna is also noteworthy requirement in today's research scenario. Also, the nearby wireless communication networks suffer from latency, network load, severe infrastructure and other several network related issues. The massive frequency range like mm-wave spectrum may be optimum resolution to handle this necessarily trend of data growth and channel capacity [3, 80]. Therefore, WRC [2] constantly recommended for the setting up of the mm-wave spectrum for majority of applications from time to time. Recently, a variety of microstrip antennas [97–112] were reported to cover these mm-wave range applications. Jilani et.al [97] proposed a wearable Polyethylene Terephthalate (PET) based substrate compact inkjet flexible antenna to achieve Ka-band spectrum. Kao et.al [98] and Tighezza et.al [99] reported mm-wave antennas by using flexible diverse substrate in order to attain wider bandwidth. However, the elevated gain was also be achieved by deploying arrays having switchable beam scanning [100–103]. Also, fourth generation (4G) and fifth generation (5G) convenient supporting array antennas were designed in [104, 105] in order to achieve pertinent gain and radiation efficiency. Furthermore, apart from array and sub arrays, Multi Input and Multi Output (MIMO), Dielectric Resonator antennas (DRA) compatible techniques [106–110] were also reported to accomplish high gain for 5G applications. Correspondingly, antennas reported in [111, 112] were designed to acquire the moderate gain by using single and dual feeding techniques. Conversely, the antennas discussed in [97–112] were state of art structures to augment bandwidth and gain in mm-wave or 5G applications by utilizing diverse methodologies, though none of them covers lower 5G band from 5GHz to mm-wave applications i.e. 40GHz. Also, the reported antennas were large in size and have moderate gain.

In this chapter, a compact antenna of dimension $27.5 \times 20 \text{ mm}^2$ is designed to achieve wide bandwidth of 5.86–38.3GHz and gain-bandwidth of 27–39.54GHz with peak gain of 10.8 dBi. The three Ka-bands namely 28 GHz (27.50–28.35GHz) n261-band

and 37 GHz (37–38.6GHz) and 39 GHz (38.6–40GHz) n260–bands with a peak-gain of 8.76 dBi, 10.8 dBi and 9.92 dBi respectively have been achieved successfully. The massive bandwidth has been achieved by etching two symmetrical slots at a tangential angle $\alpha = 15^\circ$ for efficiently diverting the elliptical periphery current to the central portion of the antenna. Due to this smoothly diversion of current, the electrical dimensions of antenna are lengthened that resultant the improvement in radiation phenomena.

3.2 CLASSIFICATION OF mm-WAVE BANDS

Table 3.1: mm-Wave bands classification

S.No	Name of the band	Range	Applications
1.	X	10 – 12	Device to Device Communication, Medical Imaging, Security and Healthcare, Internet of Things (IoT)
2.	K _u	12 – 18	Aircraft, Spacecraft and Satellite-based Communication Systems
3.	K	18 – 26	Radar and Satellite communications
4.	K _a	26.5 – 40	Radar, Cellular and Satellite Communication and Internet of Things (IoT)
5.	Q	33 – 50	Radar, Cellular and Satellite Communication and Internet of Things (IoT)
6.	60 GHz	57 – 64	WPAN / WLAN (IEEE 802.15.3c, 802.11ad / ay)
7.	V	40 – 75	Wireless local area network (WLAN) 802.11aj, WiGig unlicensed band, 802.15, 802.11 ad
8.	W	75 – 110	Automotive Radar, Point to Point Licensed communication links, 1.25Gbps to 10Gbps (Planned), Imaging Radar, Airport ground control

3.3 HIGH GAIN ANTENNA AND ENHANCEMENT IN BANDWIDTH FOR mm-WAVE BANDS FOR PATCH ANTENNA

3.3.1 ANTENNA DESIGN METHODOLOGY

The basic (i.e. Ant 1) and modified designs (i.e. Ant 2) of microstrip printed antenna are shown in Figure 3.1. This basic design has formed on rectangular radiating patch (RRP), partial ground plane (PGP), microstrip tapered feeding line printed on (Flame Redundant) FR4 substrate having relative permittivity (ϵ_r) of 4.4, tangent loss ($\tan(\delta)$) of 0.02 and height (h) of 1.6 mm as illustrated in Figure 3.1(a). The basic dimensions of rectangular radiating patch (RRP) are of length (L_p) mm and width (W_p) mm are considered according to [113–116]. The partial ground plane (PGP) is constructed by merging a rectangle with three (3) point semi-arc. The Ant 1 offers bandwidth of 3.57–10.68GHz that covers complete C–band, however near to X–band. Therefore, the inferior edges of rectangular radiating patch (RRP) are progressively clipped away to improve the impedance matching with the aim of appreciably extend the bandwidth towards higher frequency range. The progressively clipping of inferior corners of rectangular radiating patch (RRP) and tapered microstrip line gives smooth flow of current and modified design is said to be Ant 2. Therefore, due to this extract, the impedance bandwidth of Ant 2 is improved to 10.77 GHz (3.43–14.20GHz) from 7.11 GHz of Ant 1 as illustrated in Figure 3.2. It is obvious that Ant 2 provides 3.66 GHz additional bandwidth than Ant 1 and it covers entire C– and X–band applications.

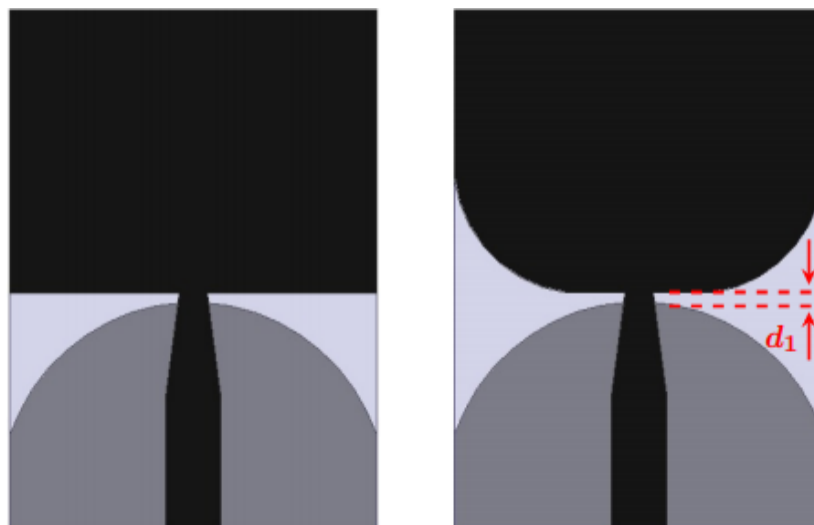


Figure 3.1: Antenna designs (a) Ant 1 (b) Ant 2.

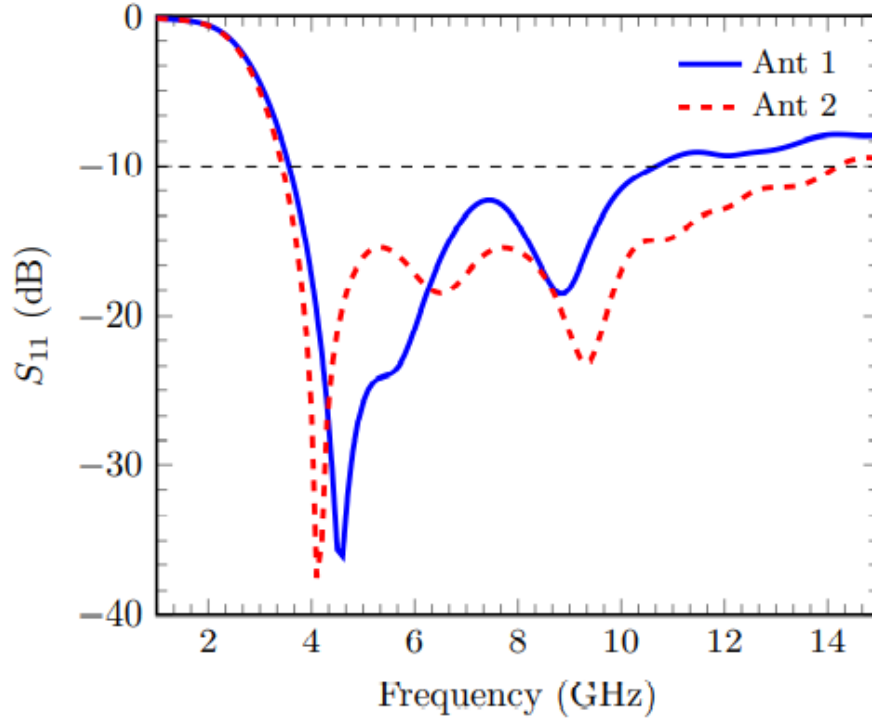


Figure 3.2: Simulated reflection co-efficient of Ant 1 and Ant 2.

The main purpose of this chapter is to expand the bandwidth of examination antenna from C-band to mm-wave spectrum. Consequently, in order to widen the bandwidth in mm-wave range, the Ant 2 is further customized by embedding two tilted slots at an angle α in patch. To understand the phenomenon of the embedding tilted slots, current distribution of the Ant 2 is studied as depicted in Figure 3.3. As per the literature study [117] the current is mostly intense on the surrounding area of elliptical antenna as compared to the interior central portion. Therefore, any change in the edges of patch will appreciably influence the impedance bandwidth. As per previous contemplation, the gradually clipping of lower corners in Ant 2, makes the antenna design nearly elliptical at lower corners. Henceforth, the current is largely disseminated on the vicinity of Ant 2 as shown in Figure 3.3. To utilize the peripheral current of Ant 2 and significantly participation of central patch in radiations, two tilted slots at an angle $\alpha = 15^\circ$ are embedded at vertical edges of the Ant 2. These slots will divert vicinity current towards central portion of the patch abundantly.

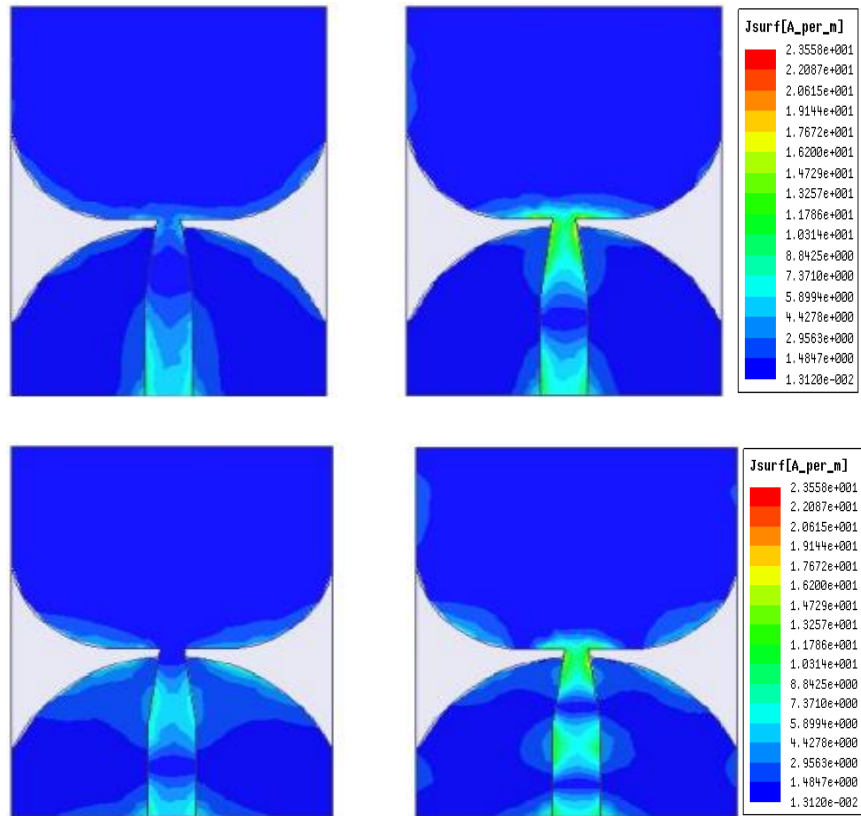


Figure 3.3: Simulated current distribution of Ant 2 at (a) 4 GHz (b) 7 GHz (c) 10 GHz (d) 13.5 GHz.

Due to this diversion a noteworthy effect on performance of antenna in terms of gain and bandwidth is observed. In addition, the upper corners of Ant 2 are triangularly clipped away at an angle $\beta = 45^\circ$ in order to smooth flow of current in the upper portion of the antenna. The extracting of upper corners significantly improves the peak-gain and gain-bandwidth due to the copper losses minimization. Consequential antenna is said to be Ant 3 as illustrated Figure 3.4 in and the final dimensions are publicized in Table 3.2.

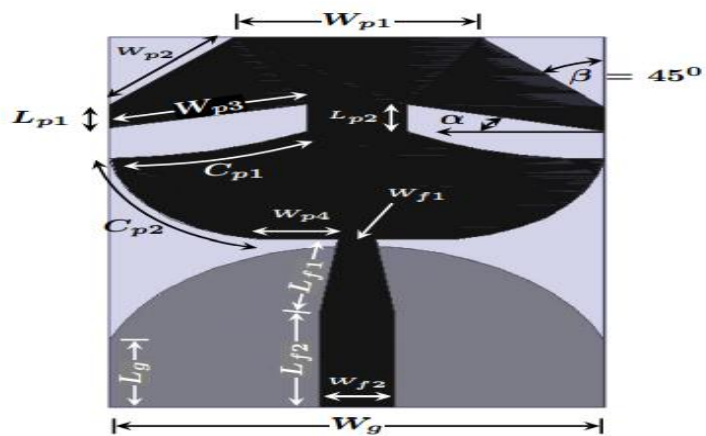


Figure 3.4: The antenna design Ant 3

Table 3.2: The dimensions of final Ant 3. (in mm)

L_s	27.5	W_{p1}	8	L_{p1}	2	L_{f2}	7
W_s	20	W_{p2}	7.81	L_{p2}	2	W_{f1}	1.5
C_{p1}	9.13	W_{p3}	8.25	L_g	5	W_{f2}	3
C_{p2}	8.32	W_{p4}	3.25	L_{f1}	5.55	W_g	20

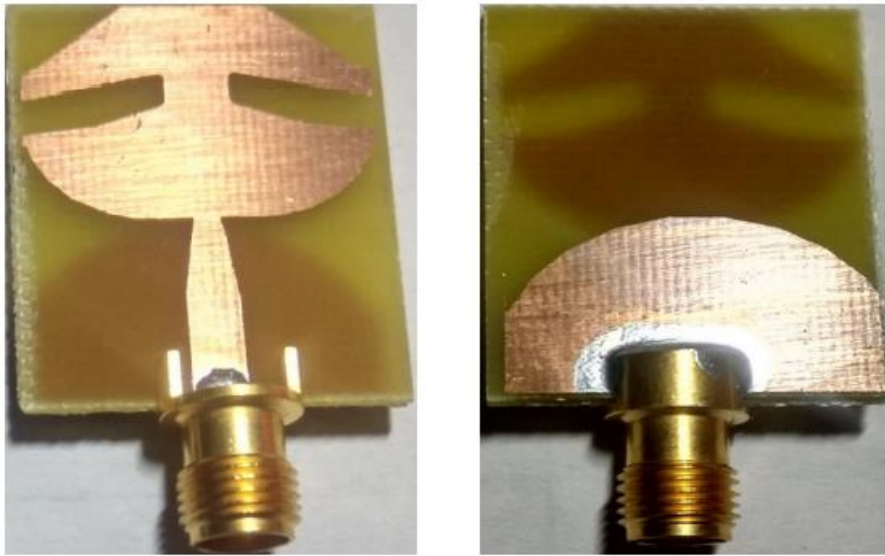


Figure 3.5: Designed Prototypes (a) Front End (b) Back End

Figure 3.5 shows the front and back sides of prototype of Ant 3. A 50 Ω female type 2.92 mm end launch co-axial or K-type connector is soldered to microstrip line for feeding purpose. It is here required to be mentioned here that SMA connector cannot be used while measuring any parameter for mm-wave antennas as it will not support the high frequency measurement and as result losses will be more as compared to the desired results.

However, the front and back side of the connector is perfectly soldered, the variation in simulated and measured results may be observed due to differ in the practical measuring condition, minor change in dimensions during fabrication, connection point etc. from the ideal simulations modal.

The component of current distribution of Ant 3 is also studied to clarify the diversion of current on the patch. Therefore, from Figure 3.6, it can be noticed that the two

embedded tilted slots at an angle α efficiently redirect the current towards central portion of the patch; as a result strength of current at vicinity is consistently disseminated over central and upper portion of the patch. Hence, the overall patch is participating in radiation phenomenon.

As a result input impedance is considerably improved as well as additional resonance modes of frequency are excited, which in turns, overall wider impedance bandwidth in mm-wave is achieved. This improvement covers especially upper 5G frequency bands such as 28 GHz, 32 GHz and 38 GHz bands of mm-wave as per discussed in WRC-19 [3].

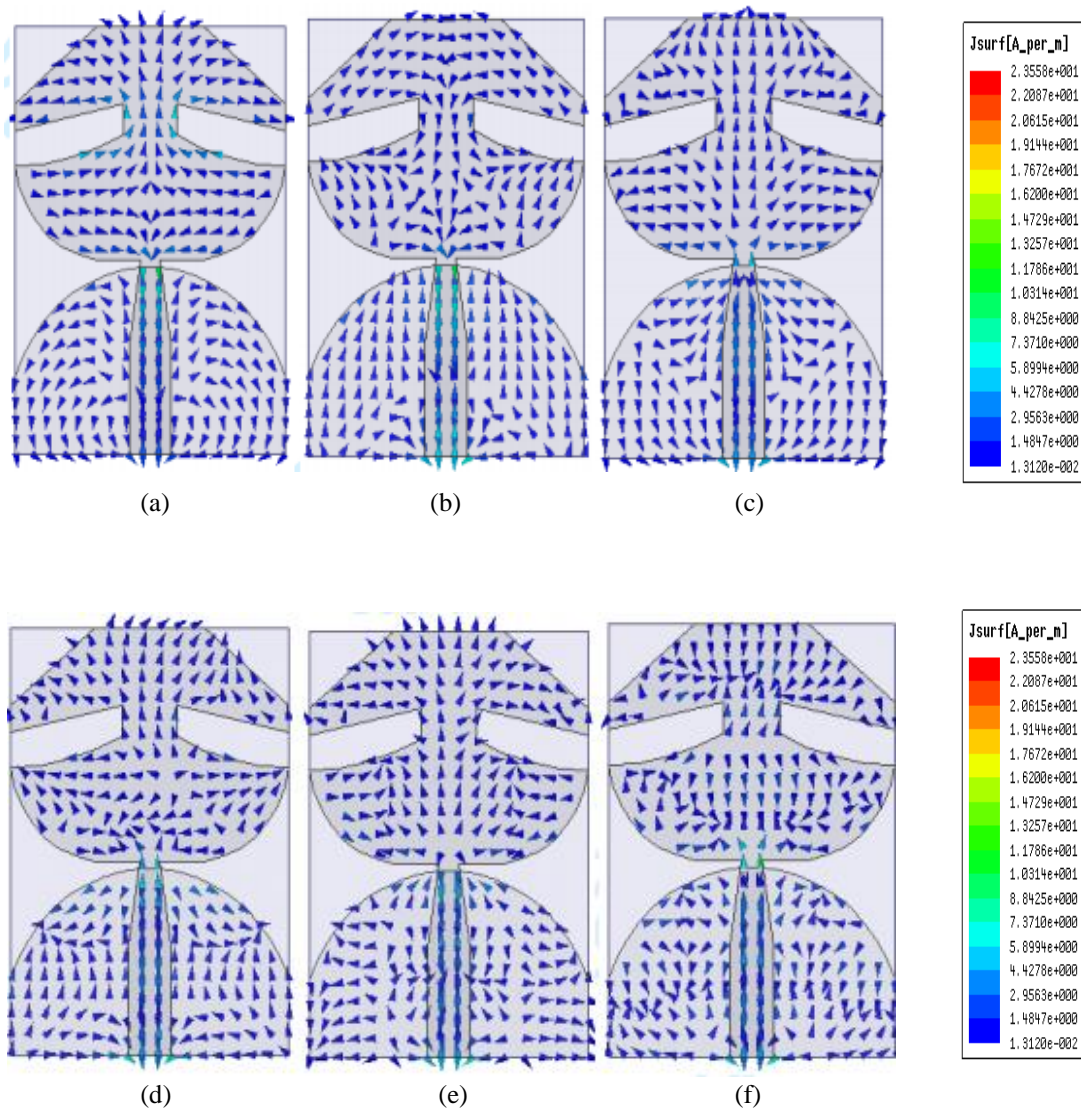


Figure 3.6: Simulated Vector current distribution of Ant 3 at (a) 5 GHz (b) 8 GHz (c) 15 GHz (d) 21 GHz (e) 25 GHz (f) 35 GHz

3.4 SIMULATED AND MEASURED ANTENNA RESULTS

Figure 3.7 compares the real and imaginary impedance parts of Ant 1 and Ant 2. It is depicted that both parts are oscillating about the preferred values of 50Ω and 0Ω respectively w.r.t frequency. For Ant 2, it is also observed that the values of both parts are oscillating more closely to the desired wide range of frequency as compared to the Ant 1. Therefore, it can easily be observed that gradually extracting of lower corners improves the impedance matching for wider range.

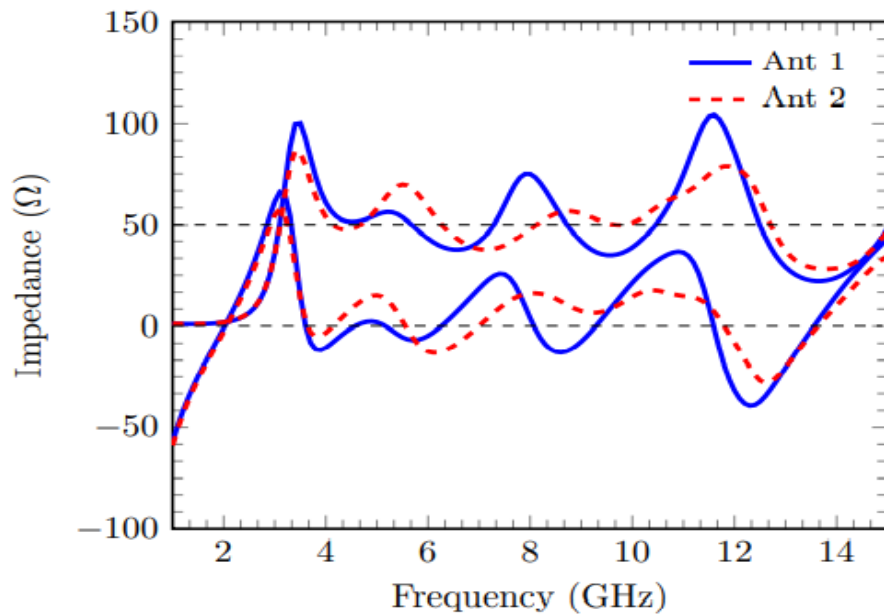


Figure 3.7: Simulated impedance of Ant 1 and Ant 2.

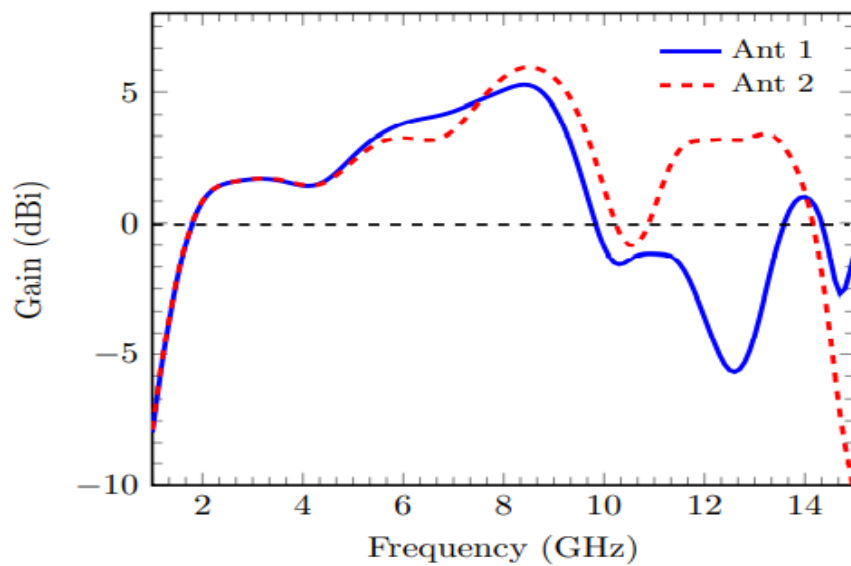


Figure 3.8: Simulated gain of Ant 1 and Ant 2

Figure 3.8 compares the simulated gain of Ant 1 and Ant 2. It is noticed here that the peak-gain of Ant 1 and Ant 2 is 5.26 dBi and 5.95 dBi at 8.26 GHz and 8.5 GHz respectively. It is also depicted that gain-bandwidth of Ant 2 is 12.36 GHz (i.e.1.79–14.157GHz) excluding a narrow band of 10.23–10.89GHz and gain-bandwidth of Ant 1 is 8.04 GHz (i.e. 1.79–9.83GHz).

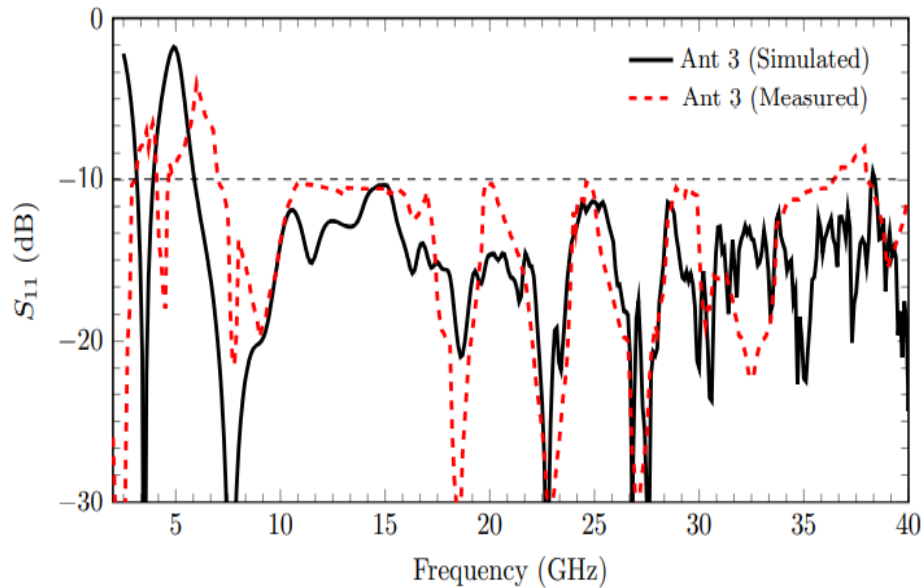


Figure 3.9: Simulated and Measured reflection co-efficient of Ant 3.

Figure 3.9 demonstrates the simulated and measured S_{11} of Ant 3. It is also found that wide impedance bandwidth of 38.44 GHz in the band of 5.86–38.3GHz is achieved. The designed prototype antenna covers lower 5G frequency spectrum to wide mm-wave range of applications. Further, it is also noticed that a band of 3.94–5.86GHz is attenuated due to destructive interference, and therefore current is stored in both the interior and exterior portions of the embedded slots for the defined frequency spectrum. In addition to above, it is also observed that the frequency gets lowered due to the increase in electrical dimensions of the antenna due to inclusion of slots in the patch.

A narrow frequency band of 1.92 GHz (3.14–3.94GHz) is also obtained for the same antenna structure. Furthermore, a good agreement in simulated and measured results for reflection co-efficient of the Ant 3 is observed. The resonating values are different in simulated and measured reflection co-efficient due to its ideal and varying practical testing conditions. The designed prototype covers lower and upper mm-wave bands namely C-, X-, Ku-, K- and Ka-band with majority of suitable diverse applications.

3.5 PARAMETRIC ANALYSIS

The parametric analysis is performed on dimensions of Ant 3 in order to find that with which specific shape and dimension the widest mm-wave impedance bandwidth can be achieved. From this analysis, the dimensions of antenna structure are optimized to final design (i.e. Ant 3). The various designs are demonstrated in Figure 3.10 and their comparative results are depicted in Figure 3.11 and Figure 3.12.

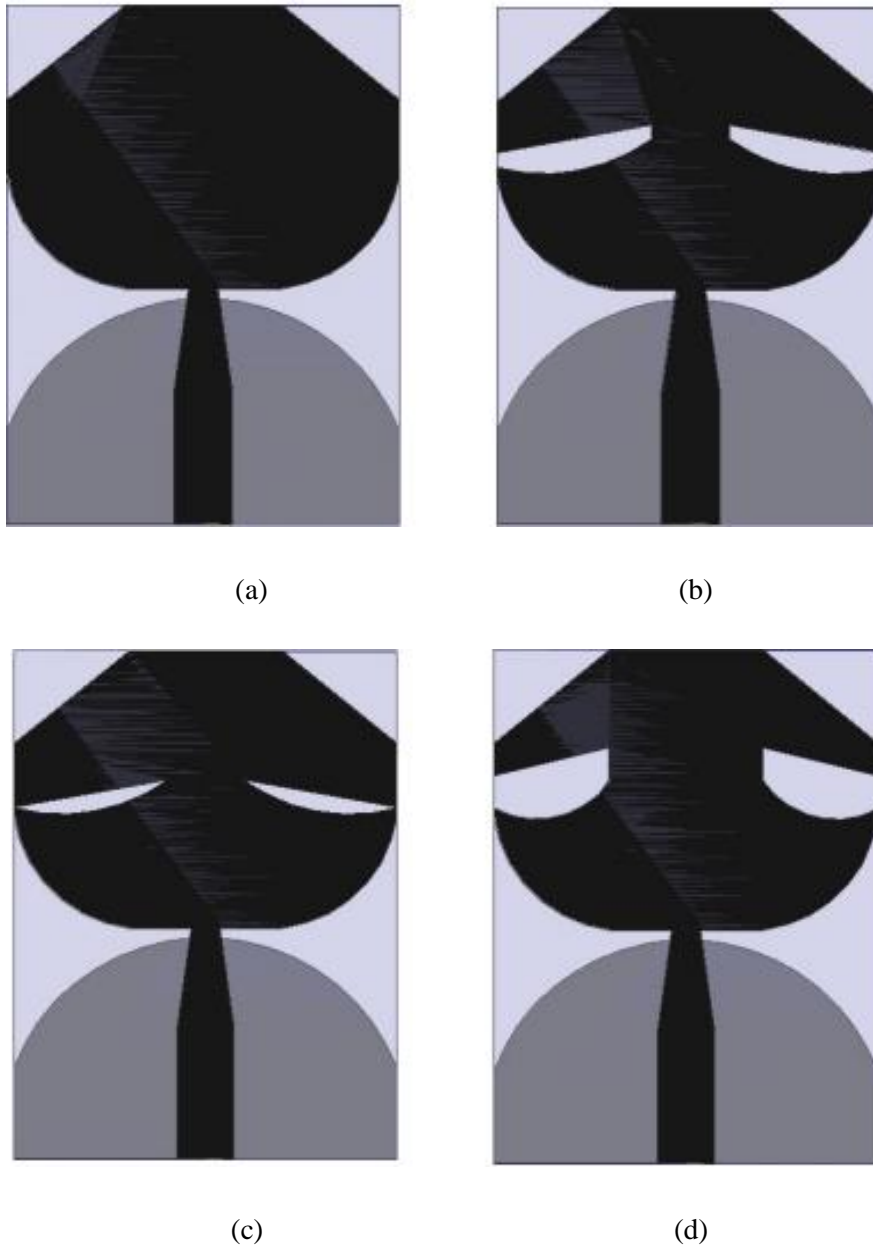


Figure 3.10: The antenna designs (a) Ant 3.1 (b) Ant 3.2 (c) Ant 3.3 (d) Ant 3.4

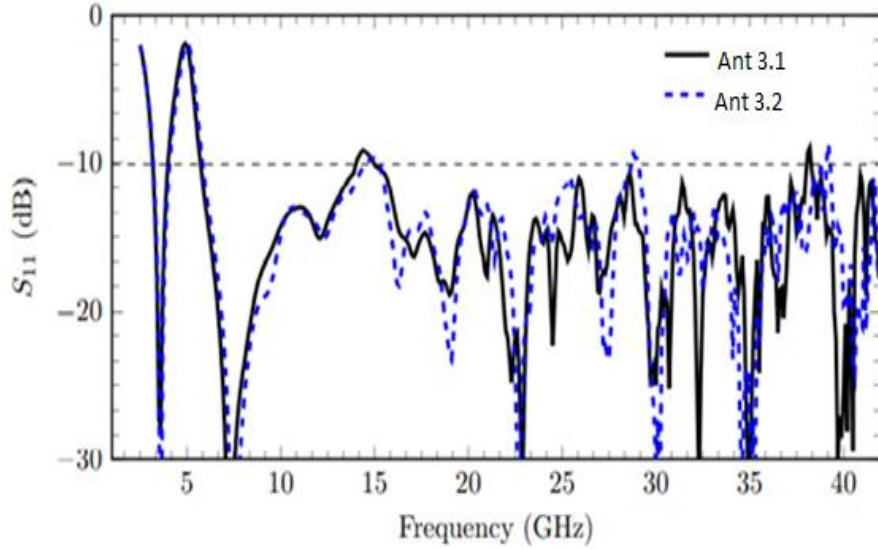


Figure 3.11: Simulated reflection co-efficient of Ant 3.1 and Ant 3.2.

Figure 3.11 and 3.12 demonstrates the reflection co-efficient with the variation of width of the tilted slits with the step size of 0.1mm of Ant 3.1, Ant 3.2, Ant 3.3 and Ant 3.4 and it is observed that the values of S_{11} are also above - 10 dB around 15 GHz.

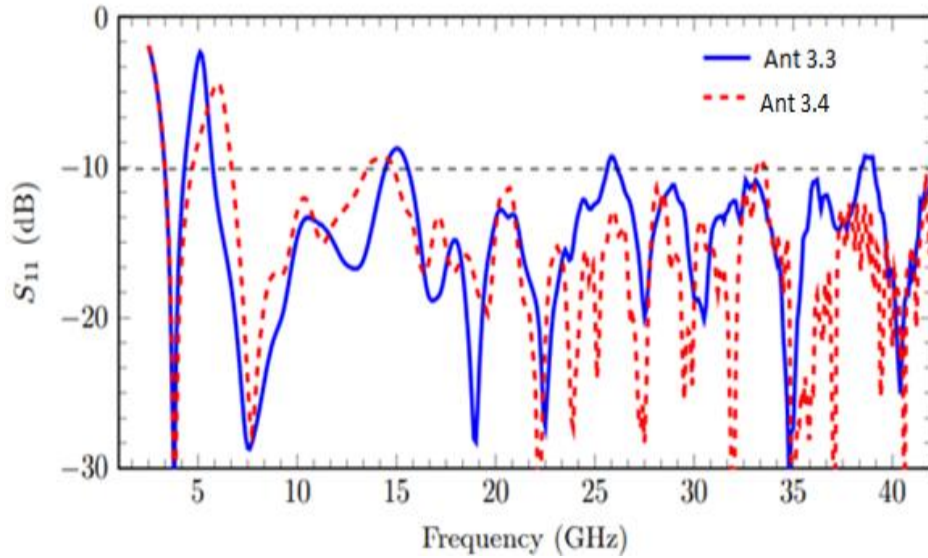


Figure 3.12: Simulated reflection co-efficient of Ant 3.3 and Ant 3.4

Figure 3.13 illustrates the impedance characteristics of Ant 3. It is observed that the real and imaginary parts of impedance are oscillating about 50Ω and 0Ω respectively. The high mismatching is also observed at 3.94–5.86GHz band due to

destructive interference of tilted slots in patch. For complete range of 5.86–38.3GHz, the real and imaginary parts are oscillating about 50 Ω and 0 Ω respectively.

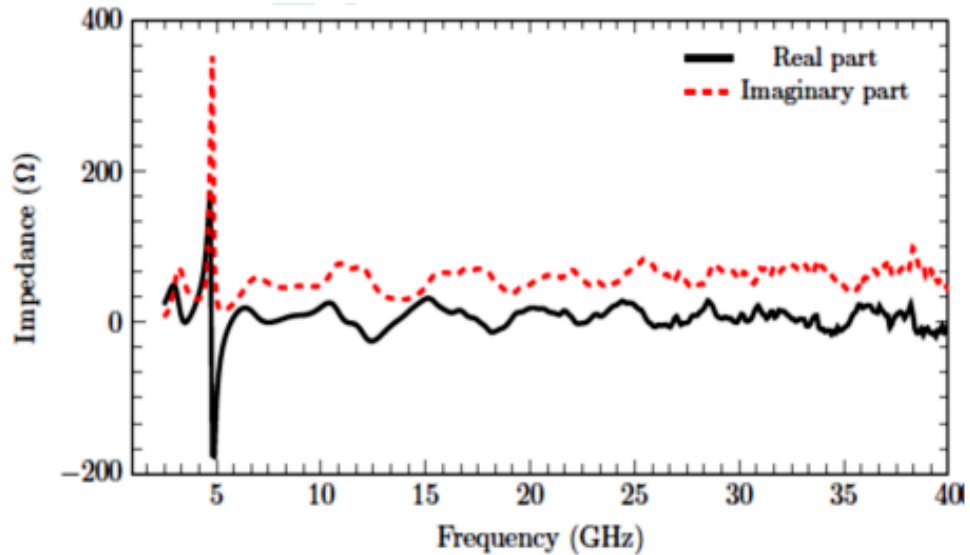


Figure 3.13: Simulated impedance characteristics of Ant 3

Figure 3.14 illustrates the zero (0) dBi gain of the final prototype Ant 3. It is seen that the gain–bandwidth of 27–39.54GHz is obtained from Ant 3. There are numerous peak gains i.e. 10.8 dBi at 37.75 GHz, 11 dBi at 30.5 GHz are depicted in figure.

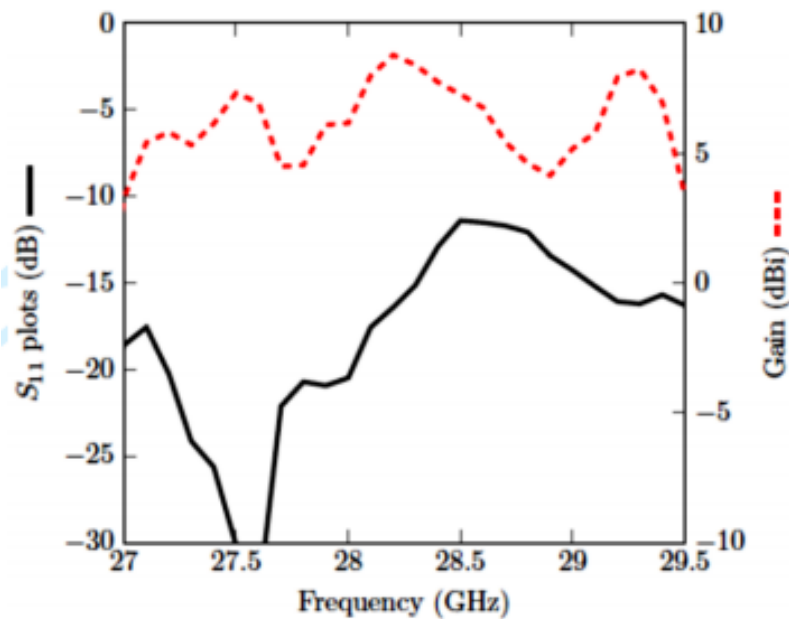


Figure 3.14: Simulated S_{11} plots and gain characteristics of Ant 3 for n261–band (27.50–28.35 GHz)

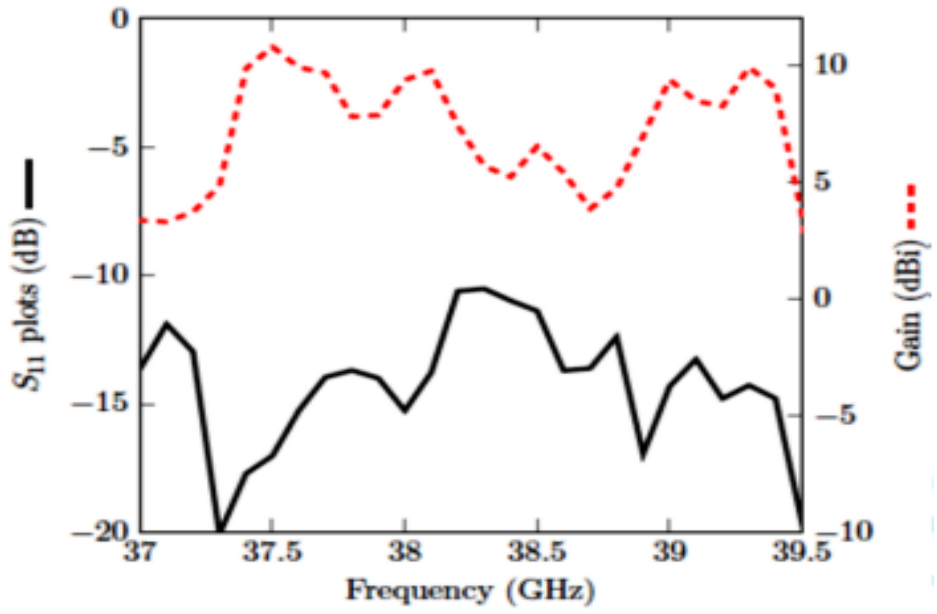


Figure 3.15: Simulated S_{11} plots and gain characteristics of Ant 3 for n260–band (38.6 – 40GHz)

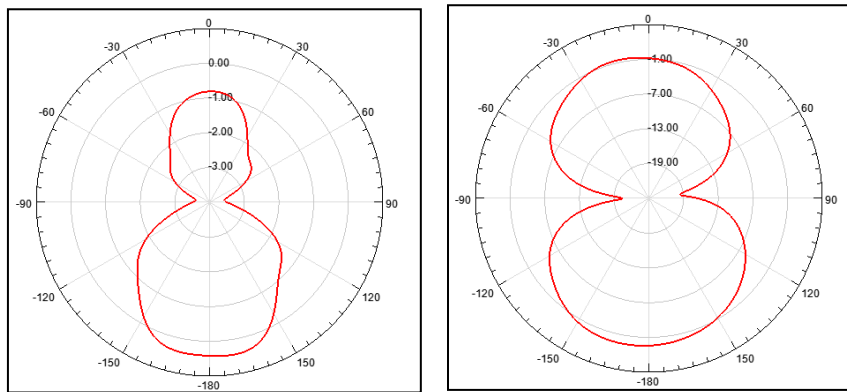


Figure 3.16: Simulated Radiation pattern (a) X-Z Direction (b) Y-Z Direction at 6 GHz

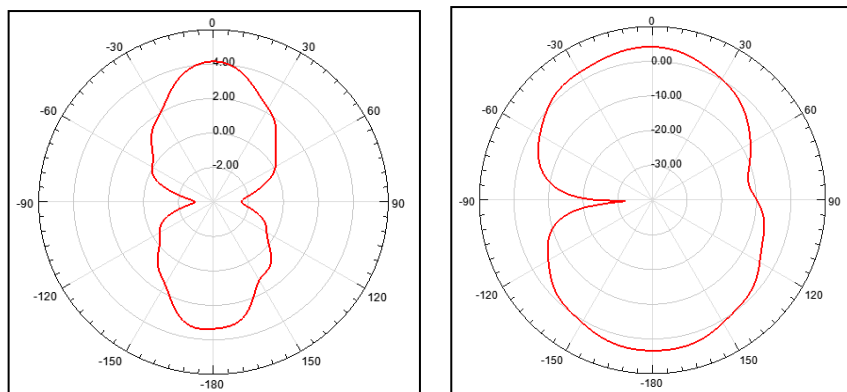


Figure 3.17: Simulated Radiation pattern (a) X-Z Direction (b) Y-Z Direction at 8 GHz

Figure 3.16 and 3.17 illustrates the radiation patterns both in X-Z and Y-Z directions at 6 and 8 GHz. The relevant broadside patterns are observed in both the planes at such higher frequencies.

Table 3.3: The comparison of proposed Ant 3 with other mm-wave based antennas.

#	Size (mm ²)	Bandwidth (GHz)	Bandwidth (%age)	Gain (dBi)	Substrate used	Loss Tangent	Category
97	12 × 12	25.1–37.5	39.62	10.6	Rogers RT Duroid 5880	0.0009	Expensive
98	13.2 × 4.2	26–33	23.73	6.2	Liquid Crystal Polymer	0.005	Expensive
99	60 × 75	7–13	60	5	Polyethylene Terephthalate	0.022	Expensive
100	110 × 55	21–22	4.65	10	Nelco N9000	0.0009	Expensive
101	19.9 × 30	27.2–28.7	5.37	7.41	Taconic TLY-5	---	Expensive
102	40 × 19.22	26.04–30.63	16.20	11.24	Rogers RT Duroid 5880	0.0009	Expensive
104	110 × 75	24.4–29.3	18.25	10.29	Rogers RTDuroid 5880	0.0009	Expensive
105	70 × 50	25–30	18.18	15	RO-5880	0.0009	Expensive
106	16 × 16	26–40	42.42	7.44	Polyethylene Terephthalate	0.022	Expensive
108	20 × 20	27.25–28.59	4.80	--	Rogers RT Duroid 5880	0.0009	Expensive
109	11.5 × 11.5	25.1–26.6	5.80	7.9	Rogers RT Duroid 5880	0.002	Expensive
111	36 × 36	8.95–19	71.91	6.9	Rogers RT Duroid 5880	0.0009	Expensive
This Work	27.5 × 20	5.86–40	148.89	10.8	FR4	0.02	Inexpensive

The other high cost materials are available in the market. However, the low cost FR4 is intentionally selected in order to keep the overall cost of communication system low.

In Table 3.3, the proposed antenna is compared with the state of art antennas. It can be clearly observed that the Ant 3 provides widest impedance bandwidth among the references cited above. It is also observed that the Ant 3 is compact in size as compared to [99–102, 104, 105, and 111]. However, antennas shown in [97, 98, 106,

108, and 109] are more compact than the Ant 3, though it provides less wide bandwidth and peak gain than Ant 3.

3.6 SUMMARY

A low cost compact mm-wave antenna is proposed to cover the C-band to mm-wave applications. The enormous bandwidth of 5.86 – 38.3GHz is achieved by diverting the patch peripheral current to the central portion of the radiating patch. Diversion is done by placing two slits at an angle $\alpha = 15^\circ$. With these techniques the current is uniformly distributed and hence enhanced the radiations in mm-wave range as a result, gain-bandwidth of 27–39.54GHz and peak-gain of 10.8 dBi is successfully achieved. The proposed antenna is suitable for K_a- band applications.

CHAPTER – 4

mm-WAVE ANTENNA DESIGN FOR UPPER 5G BAND APPLICATIONS

4.1 INTRODUCTION

These frequency spectrums have approximately no interference with the VHF and UHF bands and will be used in the world for many applications like satellite communications, radar services and earth observations [2]. Therefore, with the endless demand of high speed wireless communication systems, the mm-wave systems are likely to solve problems of limited bandwidth, gain and other network related issues which are being faced by the current 4G networks [3, 97]. Experimental results in [99] suggested wearable flexible printed antennas that cover the scope in area of biomedical applications for the lower 5G spectrum. The mm-wave will anticipate the 5G communication systems that by fulfilling the demand of high speed, negligible congestion rate and high gain as the lower 5G available bandwidth was already promoted by the various countries [118]. In order to achieve the higher bandwidth and other essential parameters, researchers from the industry, academia has shown more interest for the development of appropriate applications convention in mm-wave communication spectrum [119]. Therefore, it becomes necessary to introduce such devices that can handle and support the mm-wave networks. Wide-band microstrip antennas are promising candidates to play a vital role for these networks. These antennas can provide wide impedance bandwidth with low 15 profile and high stable gain [120]. World radio communications (WRC-19) and Federal communication commission (FCC) [6] has jointly proposed upper 5G cellular bands for many countries within the range of 24–42.5GHz. Therefore, such developments and usage of communication systems and its prototype will create a positive potential impact on the economies, equipment development in entire world. Thus, mm-wave microstrip antenna has a potential to compete with the 5G communication network challenges due to its attractive features such as low profile and cost, easy to fabricate and light weight [2, 112].

In recent years, several studies on mm-wave microstrip antenna have been carried out due to its merits like low profile structure and cost efficient nature. In the associated

literature for 5G applications based on antenna design, planar log– periodic antennas based on poly strata process with 3 stages which 30 covers 2–110GHz bandwidth forming 11 layers with the impedance of 160Ω . A dual band antenna has also been urbanized which covers K–Q and W– band with the viable gain of 9 and 8 dBi respectively [121]. However, these antennas appear to be of very large size and complex. The authors of [122, 123, and 124] specify the application of upper band mm–wave for the cellular communication, handsets which efficiently deploy the antenna arrays, MIMO technique and packages respectively. The printed flexible antenna array based on sintering technique for mm–wave with orthomorphic applications provides stable gain for the upper band throughout the range [125]. Authors of [133] have designed helical shaped wearable mm-wave antenna with moderate gain that partially covers K_a -band in an axial mode. Authors also claimed that the proposed antenna is handmade and a futuristic human body communication device. Two higher TE_{115} and TE_{119} modes were investigated to curb tolerance problem in fabrication for slot fed with mode operation in mm-wave dielectric resonator antenna (DRA) in [134]. In [135], an mm-wave dielectric resonator antenna (DRA) that covers partial dual bands namely K- and K_a -band was designed. Dielectric resonator that operates in diverse TE modes was also aimed to achieve the better matching of impedance and circular polarization. The mm-wave dual feed antenna (DFA) [136] focuses on the reduction of transmission losses in the 5G networks and efficiency improvement but failed to achieve the prospective gain. In [137], authors presented an integrated tapered slot multiband MIMO antenna which supports L and S band for 4G and K_a -band for 5G hand held prototypes. As the designed MIMO antenna is a multi band antenna with its good directive radiation patterns, but fails to achieve the throughout stable gain for its configured band. In [138], MIMO antenna was designed and optimized using CST and HFSS electromagnetic solvers to obtain dual band characteristics for K_a -band. However, the gain in the two bands i.e. 27 / 39 GHz was 5 and 5.7dBi respectively. Therefore, keeping in view implementing for practical application where high gain is the major requirement in which MIMO antenna is lagging. In [139], an integrated MIMO antenna with array for 4G and 5G handsets was proposed with the limitation of moderate gain and larger size. A flexible 5G MIMO flexible reconfigurable antenna with switching technique for K_a -band was proposed for suitable wearable applications with the adoption of distinct modes feasible for multi channels [140]. Flexible substrates are also suitable for mm-

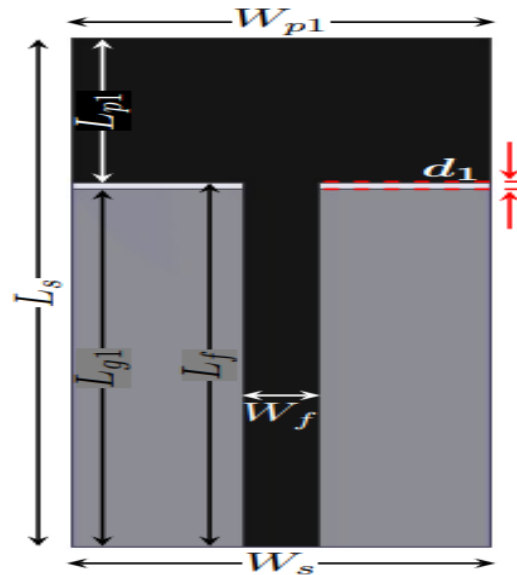
wave applications due to its feasibility, compactness and these can be also be used on dissimilar surfaces. The paper [141] primarily focuses on the solution that a single handset can accommodate the multiple LTE and K_a- range frequency band without affecting each other's performance. This simply increases the usage of smart phones in a commercial manner with assorted applications. However, to avoid complexity with larger array elements and handset size, gain of Vivaldi array antenna has been compromised. A dual polarized metallic phone comprises of antenna array design for partial K_a-band with restricted gain presented in [142]. In [143], the gravitational search algorithm (GSA) and particle swarm optimization (PSO) techniques were implemented to design array antenna of 32 elements with conical frustum configuration in order to control polarization and directivity for multi-beam patterns for dual bands of 5G.

In this chapter, a novel design of microstrip line fed with partial ground plane is designed to suit the futuristic 5G communication applications. It offers high peak-gain of 8.06 dBi, gain bandwidth of 20–36.5GHz and -10 dB impedance bandwidth of 17.33–40GHz. Both are achieved by etching rectangular and circular shaped slots in the patch. Further, the parameters are enhanced by optimizing the dimensions of slots with pattern search technique. The fabricated prototype is soldered with a special edge mount 2.92 mm 50Ω coaxial type connector and results are measured by using Rohde and Schwarz (ZVA-40) Vector network Analyzer.

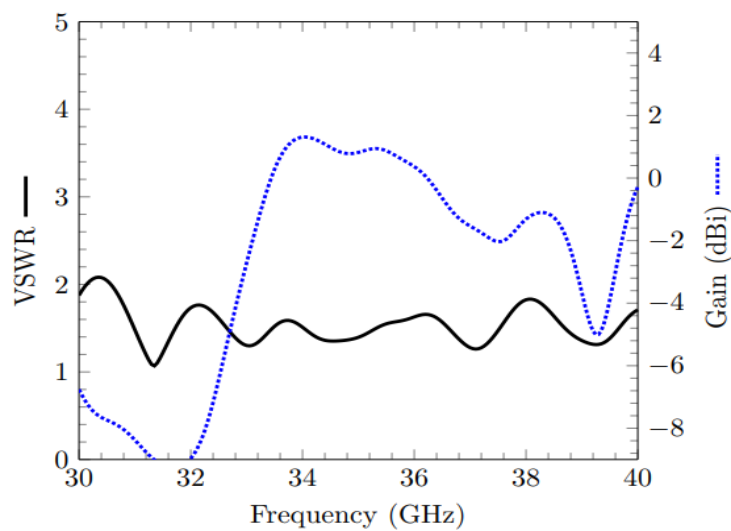
4.2 ANTENNA DESIGN METHODOLOGY

The proposed rectangular microstrip antenna is illustrated in Figure 4.1 (a), is printed on FR4 substrate ($h = 1.6$ mm, $r = 4.4$ and $\tan(\delta) = 0.02$) is fed by 50 Ω microstrip feeding line. The dimensions of the rectangular slot antenna are calculated according to [114]. Initially, basic antenna i.e. Ant 1 having partial ground plane and rectangular patch is designed and performance is examined by simulating it. Figure 4.1 (b) demonstrates voltage standing wave ratio (VSWR) on left y-axis and gain of Ant 1 on right y-axis and it is seen that Ant 1 excites the multiple resonances for a wide bandwidth of 30.68–40GHz. This shows that the lower 5G spectrum is not included in the resulted frequency range. It can also be observed that the gain-plot with the peak gain of 1.31 dBi at 34.05 GHz and 0 dBi gain-bandwidth of 2.78 GHz for Ant1 is impractical for the utilization of mm-wave applications. Therefore, various

modifications are performed on the antenna patch in order to include the bandwidth for lower 5G spectrum by embedding H-shaped slots in it. The optimization is also carried out to adjust the dimensions and positions of the embedded slots for enhancement of bandwidth and gain. Henceforth, the modified Ant 1 is said to be Ant 2.



(a)



(b)

Figure 4.1: (a) Antenna Design Ant 1 (b) Simulated VSWR and Gain of Ant 1

From the previous contemplation [115, 116, 126, 127], it has been seen that additional resonances can be excited by embedding various slots in the patch. Therefore, two triangular slots are clipped away on lower sides of the rectangular patch. Also, 2-

armed H-shaped slots (2-AHSS) are symmetrically embedded on the upper portion of it as illustrated in Figure 4.2. These H-shaped slots excite new resonance frequencies for lower mm-wave spectrum i.e. 25.7–30.5GHz in addition to Spectrum of Ant 1. Consequently, the bandwidth is enhanced to 25.53–40GHz for Ant 2 as illustrated in Figure 4.3 and it is 5.15 GHz more than that of Ant 1 and covers the complete K_a-band (26.5–40GHz).

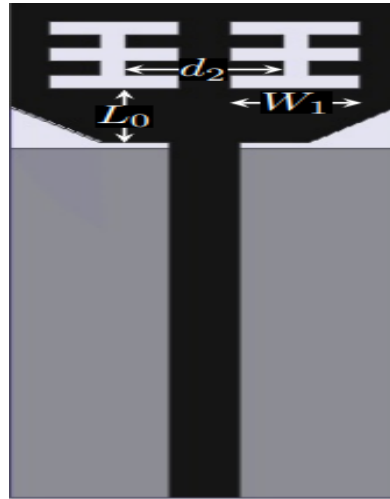


Figure 4.2: Antenna design Ant 2 with 3-AHSS slot.

Another observation can be made that with the etching of 3 armed H-shaped slots (3-AHSS) in the patch and without changing the physical dimensions; the electrical dimensions of antenna are increased thereby increasing the path of surface current on the patch which in turn lowers the values of VSWR at lower edge of the spectrum. Thus, the modification from Ant 1 to Ant 2 depicts that embedding of H-shaped slots excites new mode of resonance.

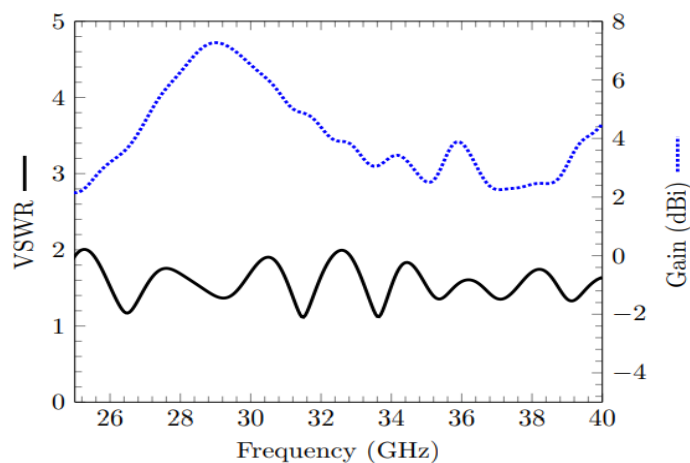


Figure 4.3: Simulated VSWR on left y-axis and Gain on right y-axis of Ant 2.

Figure 4.3 demonstrates the gain performance of Ant 2 in the band of 25.3–40 GHz. It is also observed that the peak value of gain obtained is 4.7 dBi respectively.

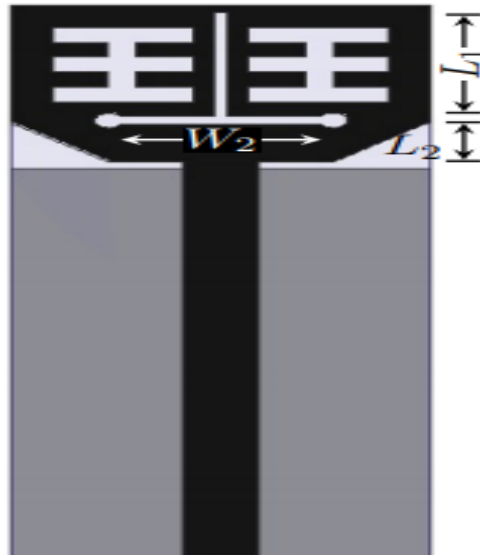


Figure 4.4: Antenna design Ant 3 with 3-AHSS and ITSS

Hereafter, an inverted T-shaped slot (ITSS) with circular edges is also embedded at center of patch as exhibited in Figure 4.4. Henceforth, now onward Ant 2 with improved bandwidth is said to be Ant 3. The geometrical parameters and position of embedded patch slots are optimized by Genetic Algorithm by keeping the step size of 0.1 mm.

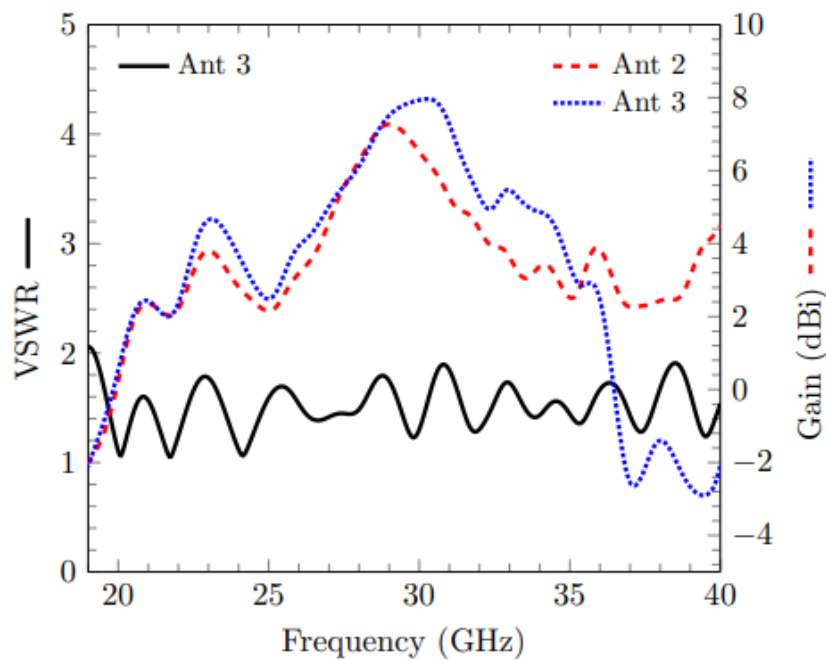


Figure 4.5: Simulated VSWR-plot of Ant 3 and gain-plots of Ant 2 and Ant 3

Figure 4.5 compares the gain of Ant 2 and Ant 3 on the right y-axis and VSWR plot on the left y-axis. It depicts that by etching of inverted T-shaped slot (ITSS) on patch enhances additional spectrum of 6.34 GHz to Ant 2 and 19.19–40GHz bandwidth is achieved by Ant 3. This etching of slot nearby feeding point of patch lengthened the electrical dimensions of Ant 3. Therefore, resonant frequency is lowered to widen the bandwidth. It is noticed that Ant 3 covers complete K- and Ka-band [1]. From figure 4.5 for Ant 3, improvement in gain is observed over Ant 2 in terms of 3dBi and 5dBi with the gain bandwidth of 9.72 GHz and 5.21 GHz respectively. Also, peak-gain of 0.7 dBi is enhanced over Ant 2.

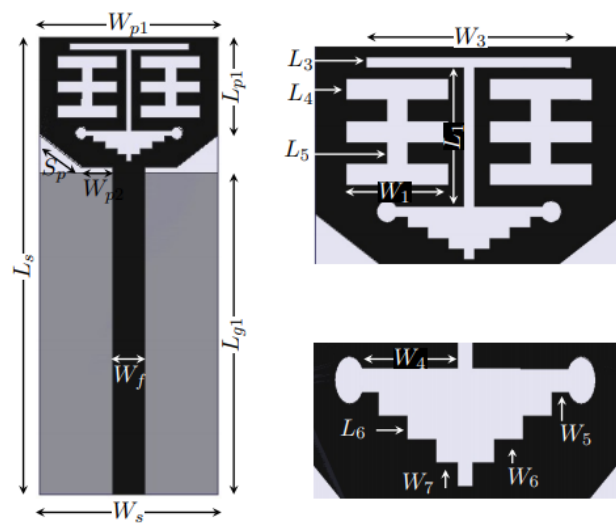


Figure 4.6: Ant 4 Configuration etched with 3-AHSS, ITSS and 4 rectangular small slits

Furthermore, in order to improve the gain, there is need to suppress the horizontal component of current by smooth transition of it from feeding location to overall structure of patch. To achieve the said characteristics, small multiple slits (here 4 in number) are embedded at the lower portion of inverted T-shaped slot (ITSS). Consequently, the vertical component of current is improved to contribute the radiation phenomenon. Moreover, a thin rectangular strip is also etched to the base of inverted T-shaped slot (ITSS) in order to divert the concentrated current at upper portion of patch back to the center of it. Therefore, with these arrangements of multiple strips and thin rectangular strip, the uniform distribution of current on patch is achieved and this effectively improves radiation phenomena. The final dimensions of Ant 4 are shown in Table 4.1. The results of Ant 4 are illustrated in figure 4.18.

Table 4.1: Dimensions and optimized Parameters of the Proposed Antenna (in mm)

L_s	37	S_p	4.375	W_1	10
W_s	15	L_1	6.5	W_2	5
L_{g1}	26	L_2	0.5	W_3	3.06
L_{p1}	7.875	L_3	1	W_4	0.56
W_{p1}	15	L_4	1	W_5	1
W_{p2}	3	L_5	1	W_6	0.5
W_{p3}	2.69	d_1	1	d_2	3

4.3 CURRENT DISTRIBUTION

The phenomenon of radiating mechanism has been influenced by the patch as it is an integral part of an antenna. These elements determine the behavior of radiation which further determines the effect on bandwidth enhancement and high stable gain. The simulated surface current distributions of the radiating element at different frequencies are illustrated in Figure 4.7 and 4.8.

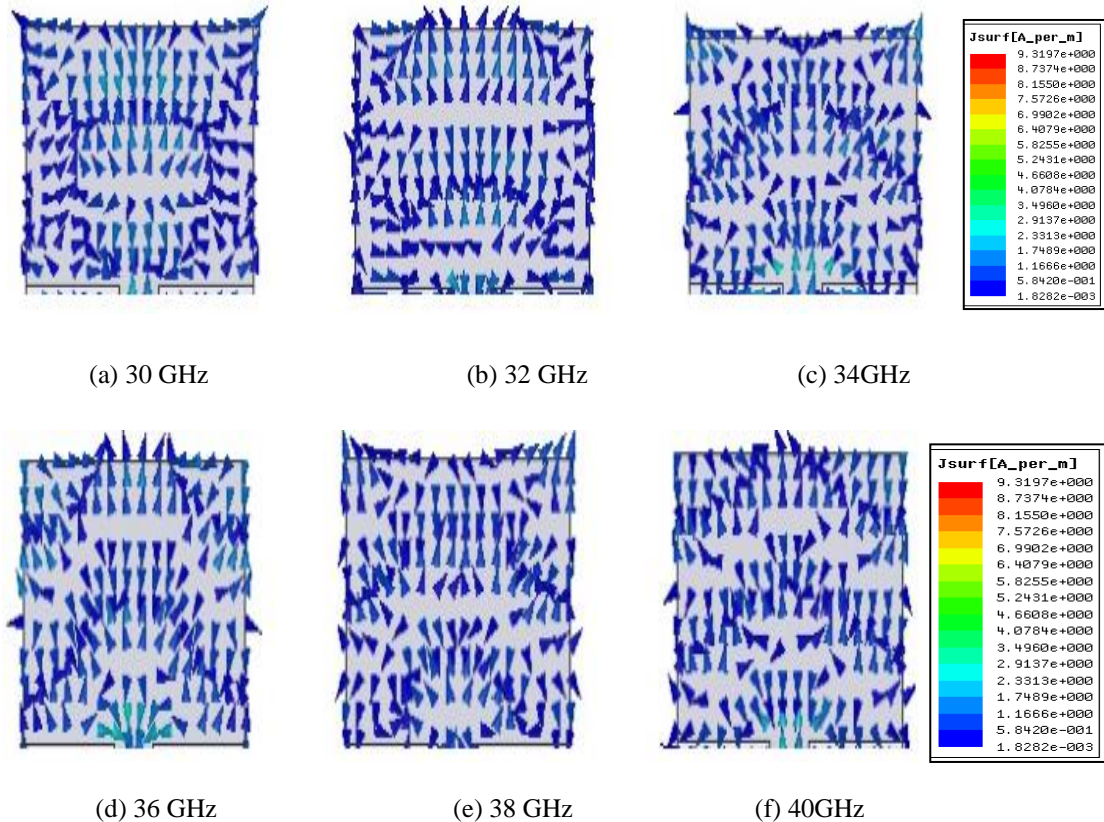


Figure 4.7: Simulated Current distribution of Ant 1 (a) 30 GHz (b) 32 GHz (c) 34 GHz (d) 36 GHz (e) 38 GHz (f) 40 GHz

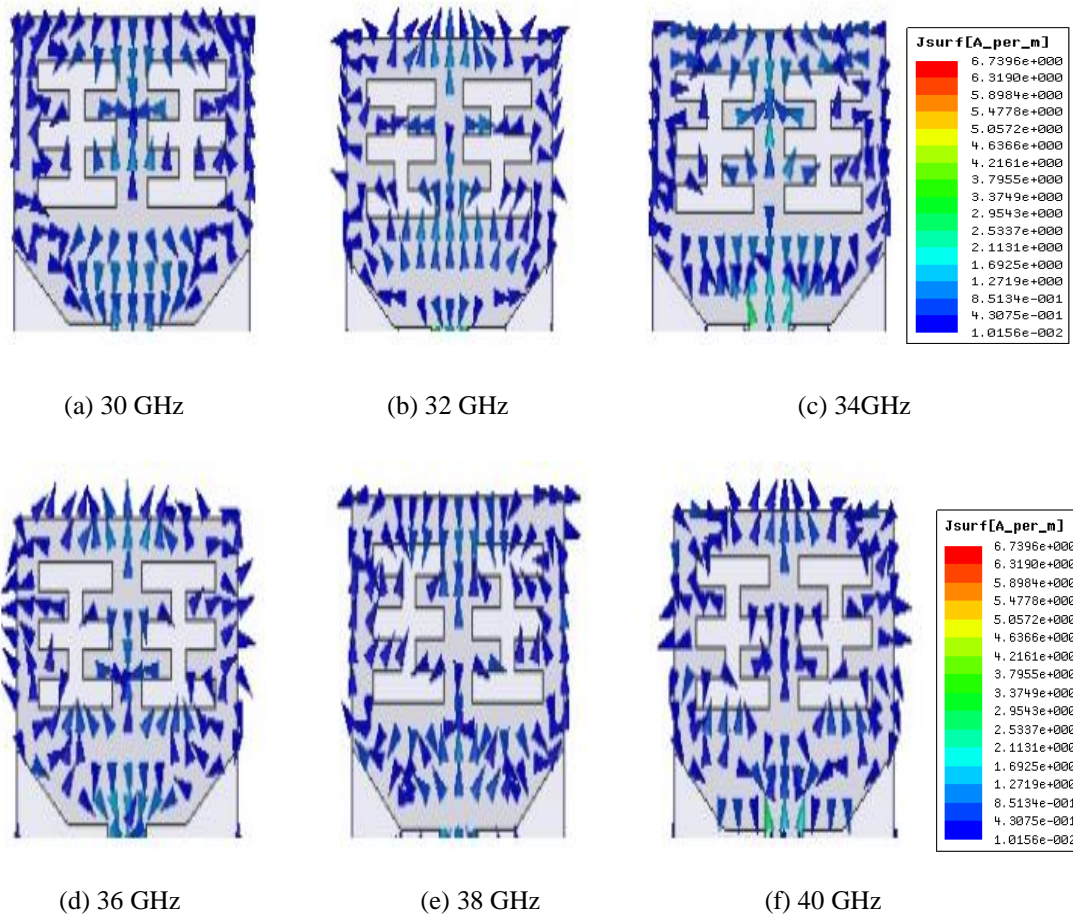


Figure 4.8: Simulated Current distribution of Ant 2 (a) 30 GHz (b) 32 GHz (c) 34 GHz (d) 36 GHz (e) 38 GHz (f) 40 GHz.

Figure 4.7 and 4.8 depicts the current distribution of Ant 1 and Ant 2 at 30 GHz, 32 GHz, 34 GHz, 36 GHz, 38 GHz and 40 GHz. It can be clearly observed that the surface current path of patch is increased in Ant 2 when compared with Ant 1. The significant improvement in the enhancement of bandwidth and gain is based on the phenomenon of embedding the rectangular 3 armed H- shaped slots (3-AHSS). Therefore, with the embedment of these slots, surface currents are diverted exactly towards the middle of these slots thereby balancing the horizontal and vertical currents on the patch.

4.4 PARAMETRIC ANALYSIS

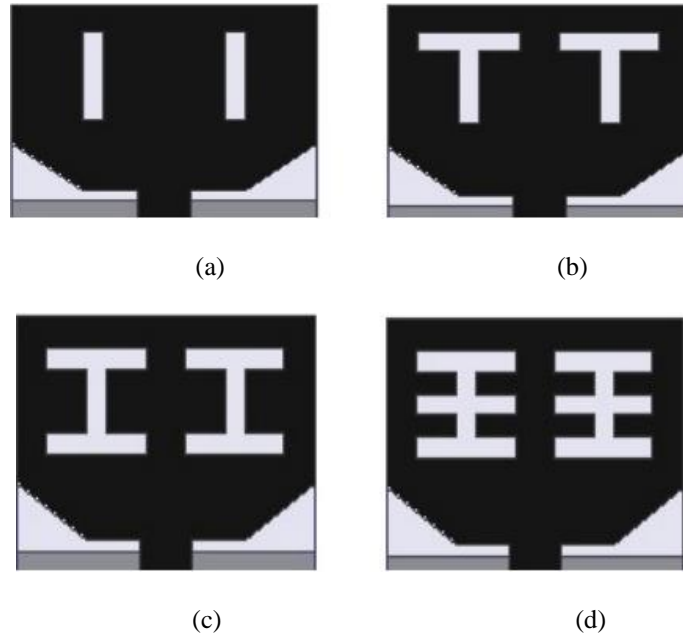


Figure 4.9: Ant 2 with various etchings of (a) I-shaped slots (b) T-shaped slots (c) 2-AHSS (d) 3-AHSS

To obtain the desired results which is suitable for the mm-wave antenna applications, parametric analysis is done with different shapes and sizes of slots on the patch. Therefore, etching of slots on patch is selected with diverse shapes like I-, T-, 2-armed H-shaped slots (2-AHSS) and 3-AHSS as shown in Figure 4.9.

Further, in order to achieve the better gain and impedance bandwidth, the dimensions of the 3-armed H shaped slots on the patch are finalized after the optimization parameters like L_0 , d_2 and W_1 . Figure 4.10(a) and 4.10(b) illustrates the comparison between the VSWR- and gain plots of the above said optimization parameters respectively. It can be observed from the figure 4.10(a and b) that for I-shaped slot, performance of the VSWR degraded approximately at 30.4 GHz but gain degrades throughout the bandwidth. For T-shaped slot, impedance matching is improved whereas gain remains still inadequate for the mm-wave applications. The improvement in both the parameters can be observed for 2 and 3-AHSS in the bandwidth of 25–30GHz. Also, it is noticed that the electrical dimensions are more lengthened for 3-AHSS than 2-AHSS. As a result, Ant 2 also covers the complete K_a-band. From figure 4.10 (b), it is exhibited that for 2 and 3-AHSS, 3 dBi gain-bandwidth is obtained within the multiple bands such as in (27.18–29.96GHz) and (25.81–34.60GHz) is peak-gains of 5.01 dBi and 7.26 dBi are obtained respectively.

Also, the gain-bandwidth for 5dBi within the band of (27.20–31.20GHz) is also obtained for etched 3–AHSS. This shows that with the etched slots of 3–armed H shaped offers suitable and high gain-bandwidth and peak-gain for mm-wave applications.

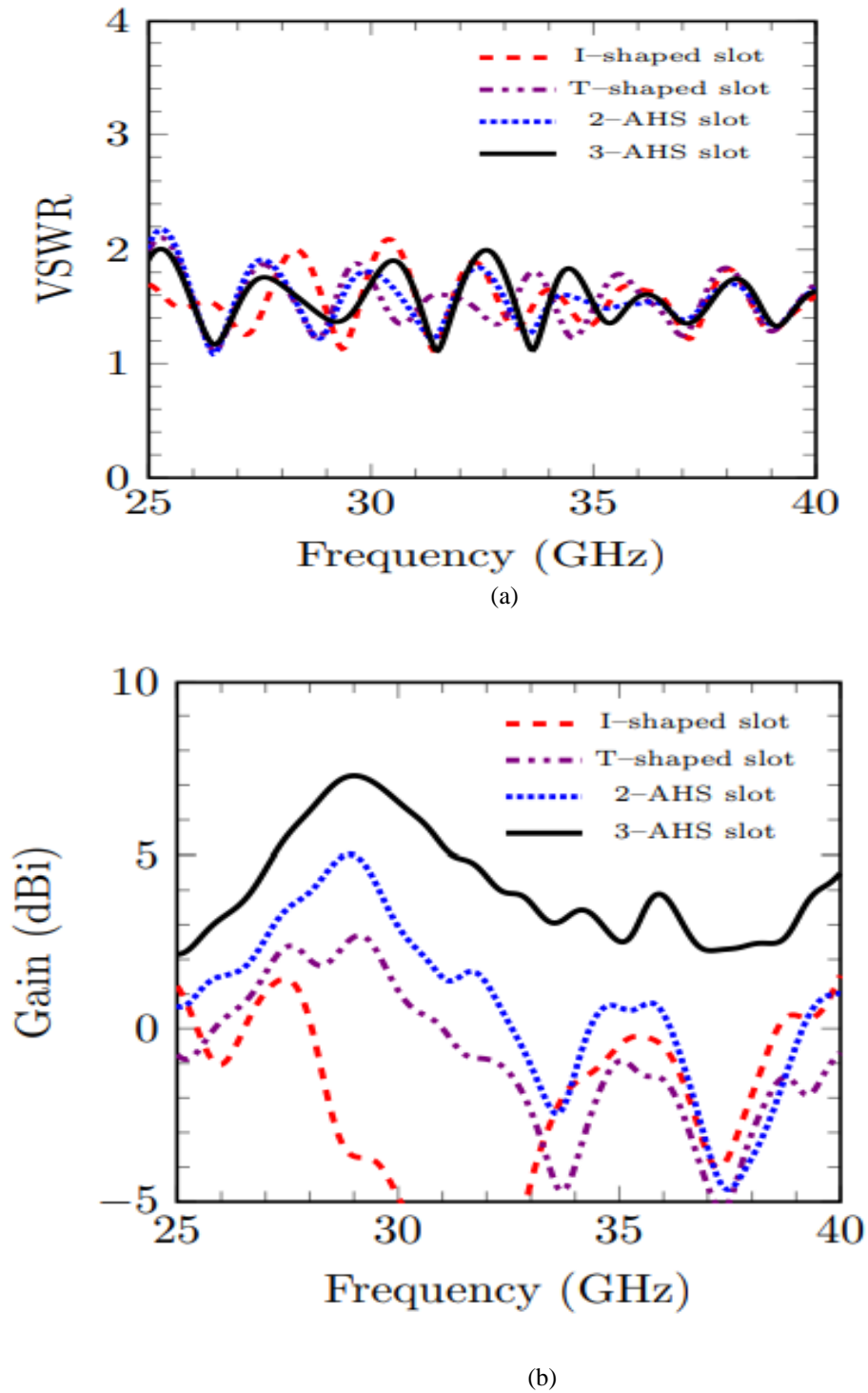
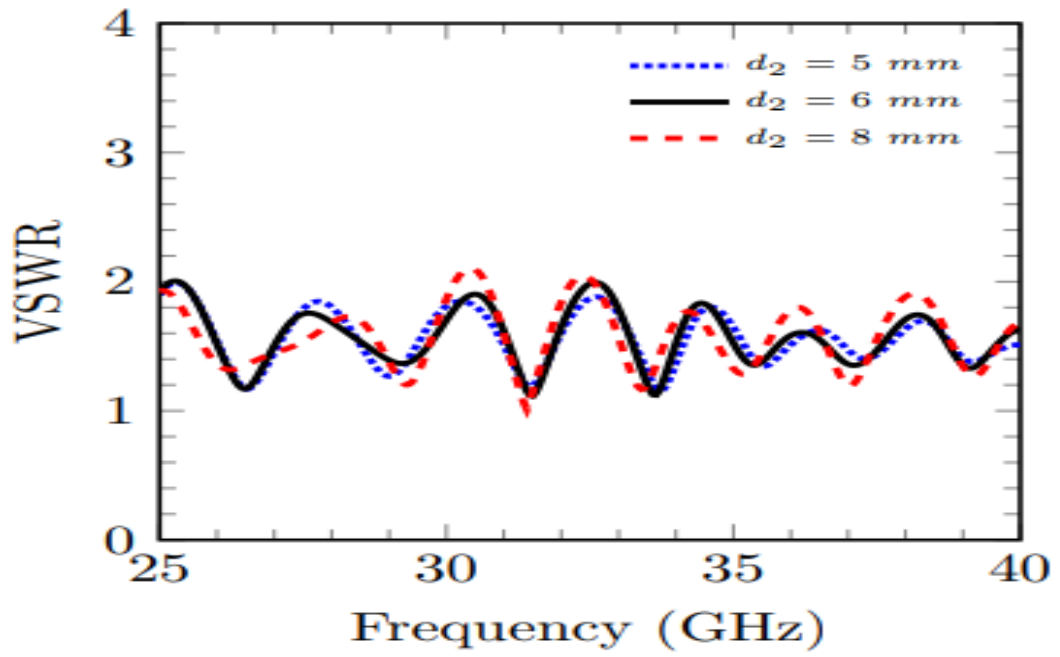
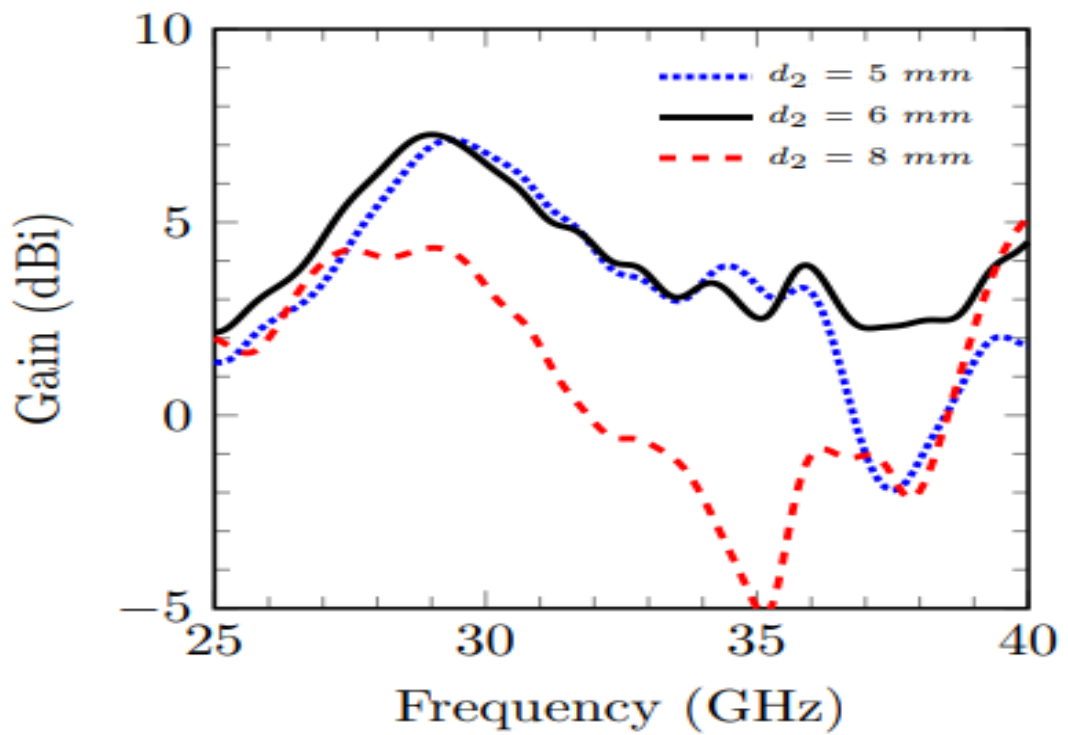


Figure 4.10: Simulated plots of Ant 2 as function of etched I-, T-, 2-AHSS and 3-AHSS (a) VSWR-plots (b) gain plots.



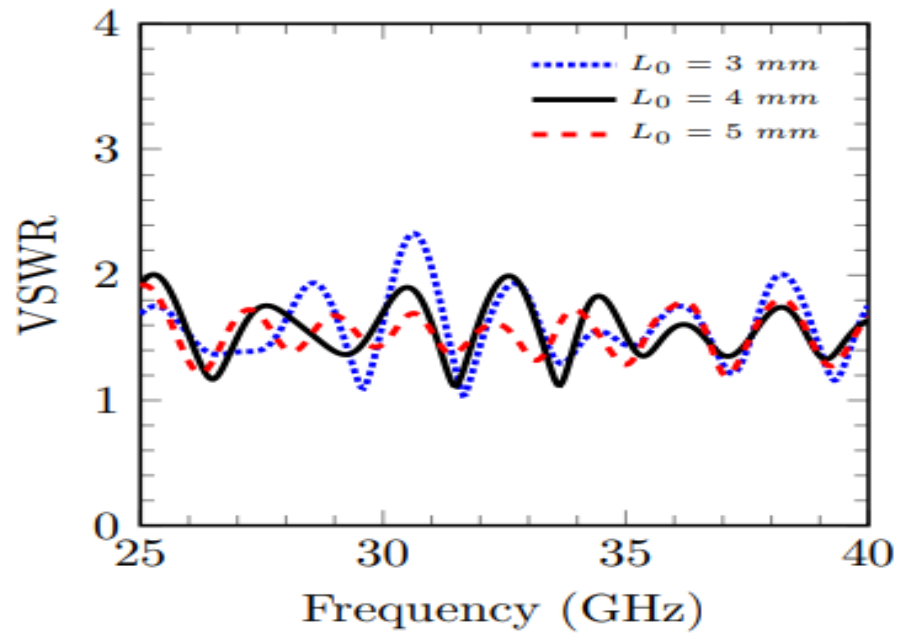
(a)



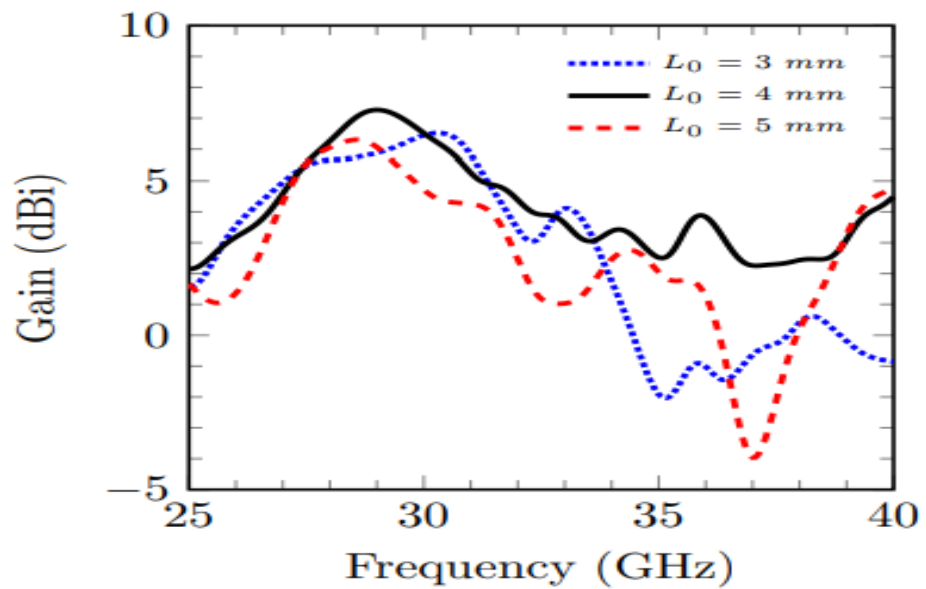
(b)

Figure 4.11: Ant 2 etched with 3-AHSS (a) Simulated VSWR-plots as function of d_2 (b) Simulated Gain-plots as function of d_2 .

Figure 4.11 (a and b) demonstrates the optimized effect of varying parameter distance (d_2) for 3-AHSS on VSWR- and gain-plots respectively. It can be noticed that with the high value of d_2 , impedance matching and gain gets deteriorated, however both optimized parameters have insignificant effect at lower values of d_2 i.e. $d_2 = 5$ mm.



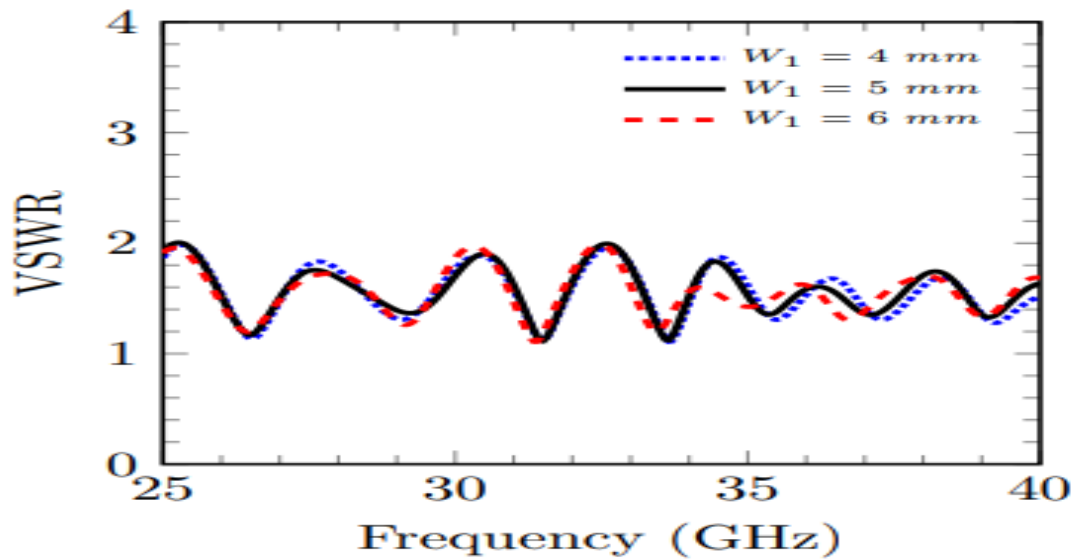
(a)



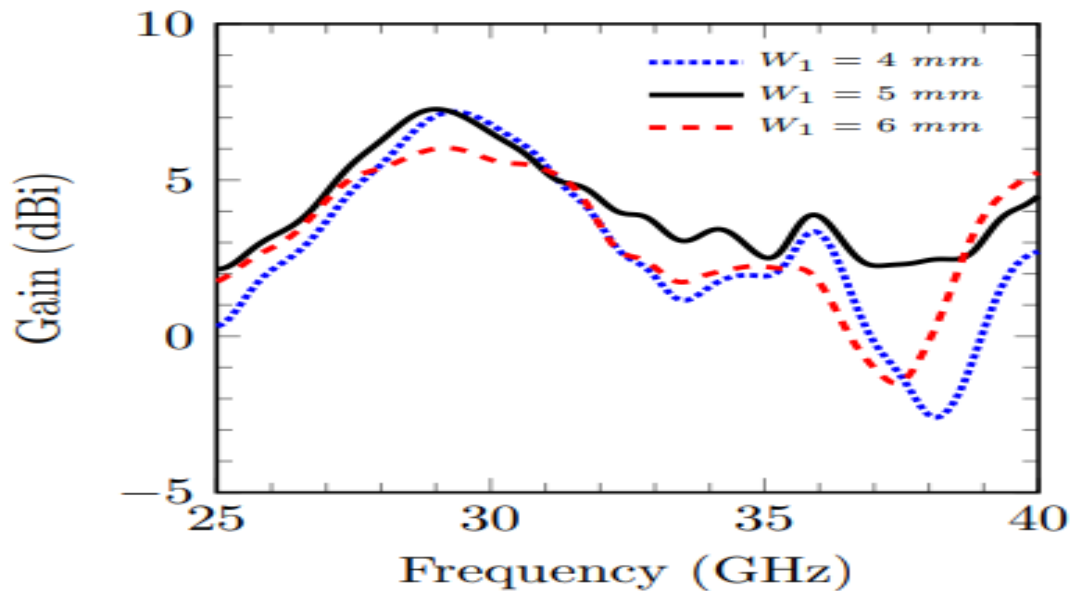
(b)

Figure 4.12: Ant 2 etched with 3-AHSS (a) Simulated VSWR-plots as function of L_0 (b) Simulated Gain-plots as function of L_0 .

Figure 4.12 exhibits that for both VSWR- and gain-plots are function of L_0 optimization parameter for 3-AHSS from bottom edge of patch respectively. It is illustrated that with the increase in value of L_0 from 3 mm to 5 mm, the VSWR is significantly improved and tends to its ideal value of 1.22; however, gain is not varying as much it was required. The noteworthy gain is obtained at $L_0 = 4$ mm.



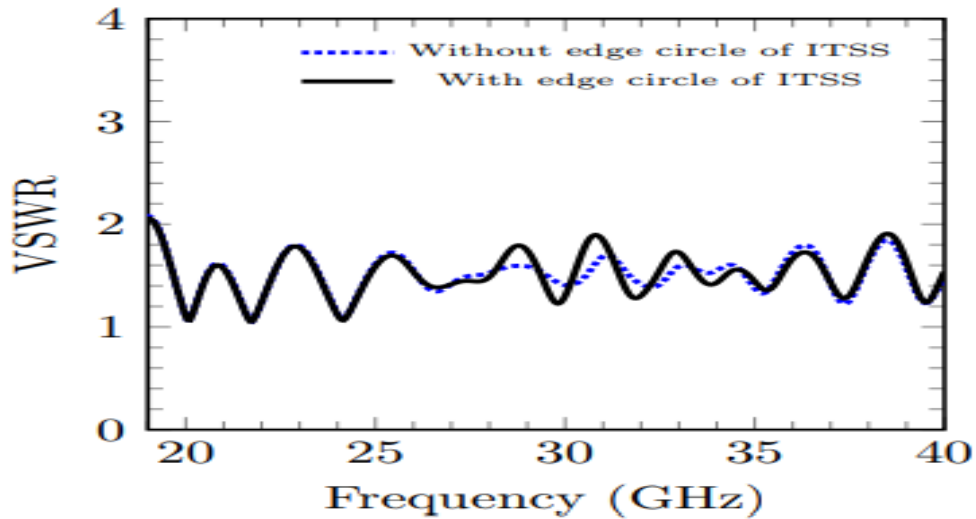
(a)



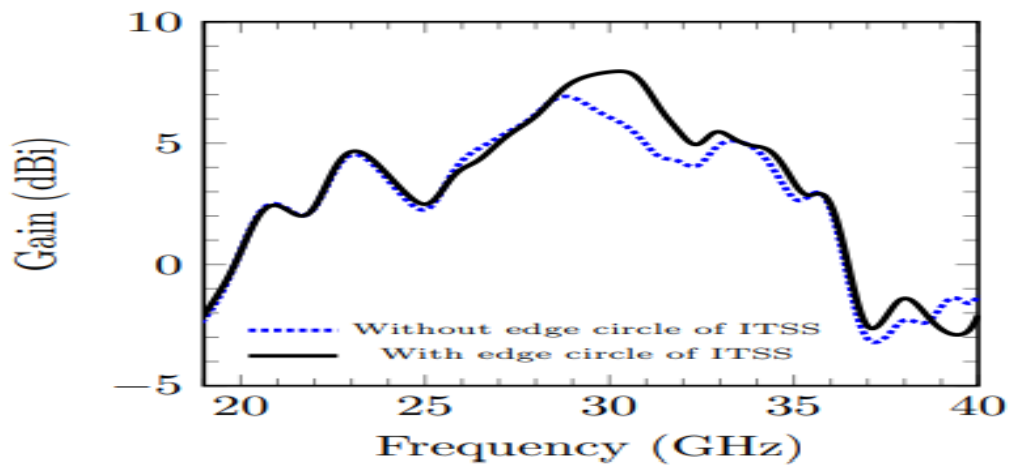
(b)

Figure 4.13: Ant 2 with etched 3-AHSS (a) Simulated VSWR-plots as function of W_1 (b) Simulated Gain-plots as function of W_1 .

Figure 4.13 demonstrates the effect of optimized variations of width (W_1) for one arm of both 3-AHSS on VSWR- and gain-plots respectively. It is observed that with the increase in value of W_1 results in gain deterioration.



(a)



(b)

Figure 4.14: The plots of Ant 3 as function of etched 3-AHSS and ITSS with and without edge circles
(a) Simulated VSWR-plots (b) Simulated Gain-plots.

The geometrical parameters L_1 , L_2 and W_2 and position of ITSS on patch is selected after optimization process. The Genetic Algorithm with step size of 0.1 mm is used for parametric analysis. The comparison of the above said parameters of etched ITSS on patch is also analyzed for with and without circles at edges as demonstrated in Figure 4.14. It is also observed that the values of gain-bandwidth remains almost

identical, however, gain values deteriorates significantly for spectrum of 29–34GHz due to abrupt changes in surface currents of antenna. The VSWR remains ineffective for entire range.

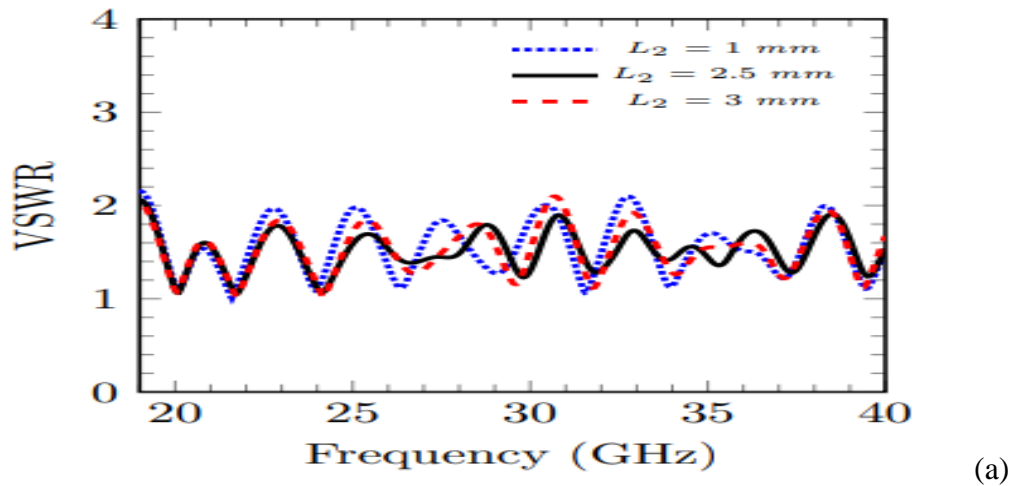
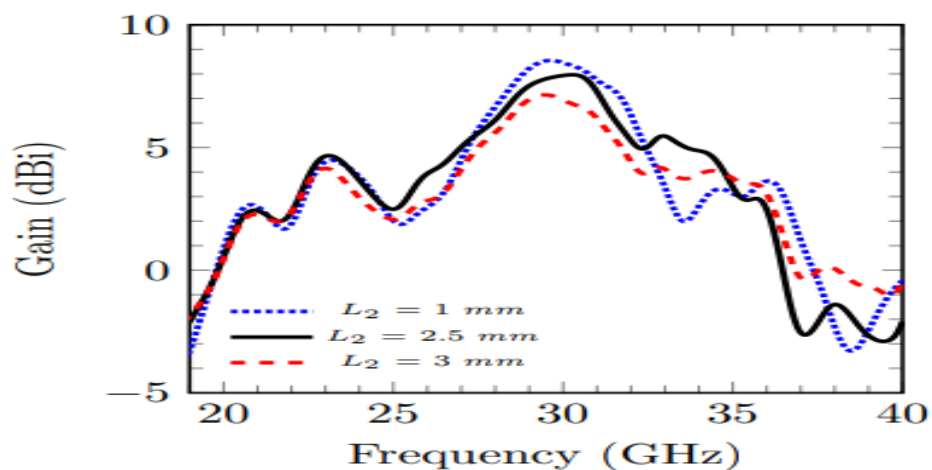
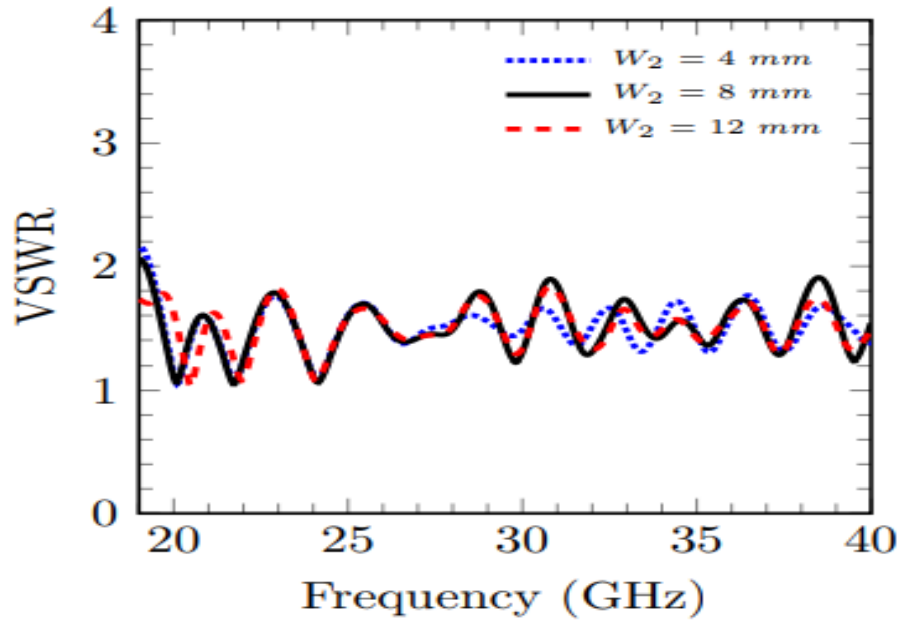


Figure 4.15 illustrates the impact of variation in L_2 on VSWR– and gain-plots. It is observed that impedance matching get inferior at perpendicular positions of $L_2 = 1$ mm and $L_2 = 3$ mm, conversely, matching of impedance is good at $L_2 = 2.5$ mm as depicted in Figure 4.15 (a). It can also be observed from Figure 4.15 (b) that if L_2 increases from 1 mm to 3 mm, the peak-gain of antenna decreases. The 3 dBi gain-bandwidth also depreciates at upper and lower range of frequencies. The optimal peak-gain and 3 dBi gain-bandwidth is achieved at $L_2 = 2.5$ mm.

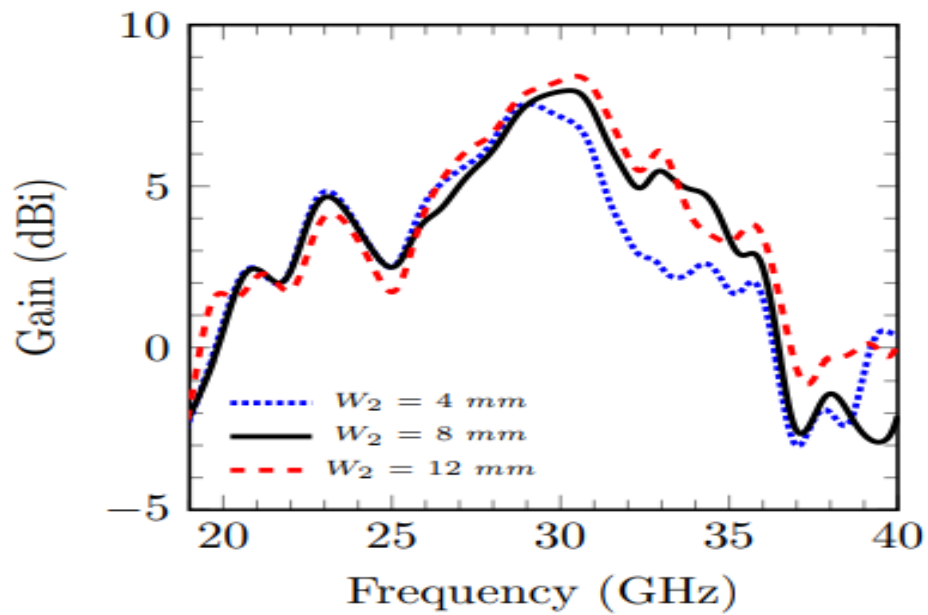


(b)

Figure 4.15: Ant 3 etched with 3–AHSS and ITSS (a) Simulated VSWR–plots as function of L_2 (b) Simulated Gain plots as function of L_2 .



(a)



(b)

Figure 4.16: Ant 3 etched with 3-AHSS and ITSS (a) Simulated VSWR-plots as function of W_2 (b) Simulated Gain plots as function of W_2 .

Figure 4.16 depicts the outcome of W_2 variation on VSWR- and gain-plots w.r.t frequency. From Figure 4.16 (b), it can be easily observed that with increment in W_2 , the gain is improved for the bandwidth of 30–40GHz. The additional noteworthy improvement in gain is experienced with increment in value of W_2 from 4 mm to 8

mm and furthermore, approximately at 25 GHz the values of gain deteriorates with increase in W_2 from 8 mm to 12 mm.

4.5 ANTENNA FABRICATION

Figure 4.17 shows the fabricated prototype with front patch and ground at opposite side of Ant 4. A specific female 2.92 mm end launch coaxial connector of 50Ω is also soldered to microstrip line for feeding purpose. It is here particular that K-type edge mount connector supports measurement for mm-wave configured antennas. It is worth to be mentioned here that SMA connector doesn't support measurements because these are available at frequencies upto 12 GHz and not available for very high frequencies such as mm-wave. Therefore, for higher frequencies more accurate 2.92mm K-type connector is used in this case. However, the measured results may vary from the simulated due to practical fabrication methodology, soldering of high frequency supporting connector and measuring conditions which are superlatively different from the simulation scenario.



Figure 4.17: The fabricated structure of Ant 4 (a) Front end (b) Back End

4.6 SIMULATED AND MEASURED ANTENNA RESULTS

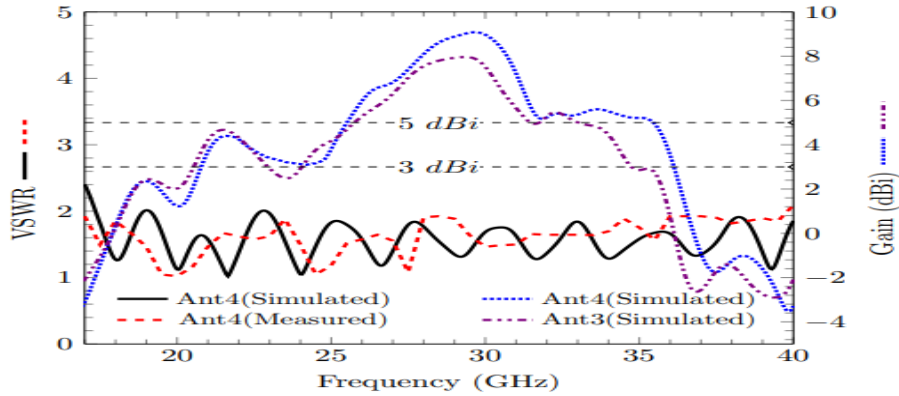


Figure 4.18: Simulated and measured VSWR-plots of Ant 4 on left y-axis and comparison of gain-plots of Ant 3 and Ant 4 on right y-axis.

Figure 4.18 demonstrates the simulated results of VSWR and gain of the optimized Ant 4 prototype is measured by using Rohde and Schwarz ZVA-40 vector network analyzer (VNA). The results appeared to be in the good agreement of measured VSWR-plots with simulated one. The Ant 4 offers wide impedance bandwidth of 17.33–40GHz that covers complete K- and K_a -bands and mm-wave spectrum of 30–40GHz.

Figure 4.18 depicts the simulated gain-plots of Ant 3 and Ant 4 on the right hand side of y-axis. The peak-gain of Ant 4 is enhanced by 1.12 dBi when compared to Ant 3 and its value is 9.08 dBi. Also, due to the reduction in copper losses and vertical component improvement in surface current, 3 dBi and 5 dBi gain-bandwidth is augmented to 14.01 GHz (22.45–36.46GHz) and 9.08 GHz (26.77–35.85GHz) respectively. With the huge augmentation in 3 dBi and 5 dBi gain-bandwidth the final Ant 4 can be used for indoor applications in K_a - band.

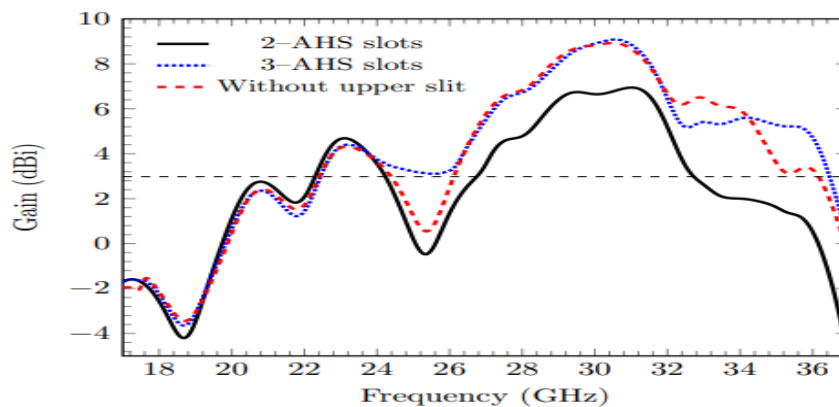


Figure 4.19: Simulated Gain-plots of Ant 4 as function of etched 2-AHSS, 3-AHSS and without upper slit.

Figure 4.19 provides the comparative analysis of the gain-plots of Ant 4 with etching of 2-AHSS, 3-AHS and without a thin rectangular strip of width W_3 . It is therefore observed that there is a huge augmentation in peak-gain and gain-bandwidth for etching of 3-AHSS in place of 2-AHSS for the final optimized design Ant 4. Thus, it can be concluded that the peak-gain and overall impedance bandwidth is much wider with etched 3-AHSS. Also, the 5 dBi gain-bandwidth is lowered at approximately 34 GHz without a thin rectangular strip of width W_3 of etched ITSS.

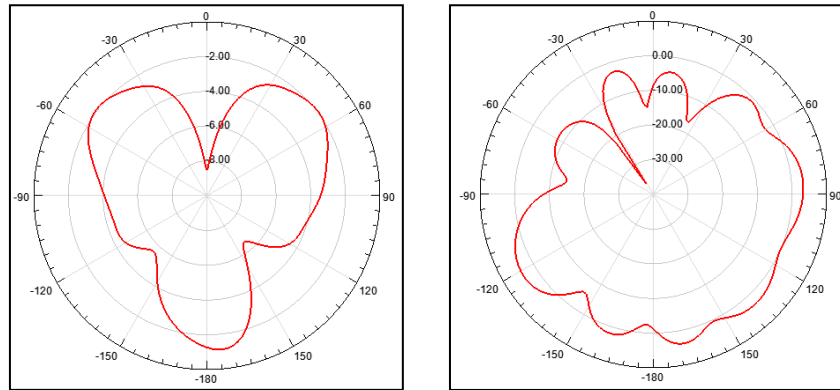


Figure 4.20: Simulated Radiation pattern (a) X-Z Direction (b) Y-Z Direction at 22.5 GHz

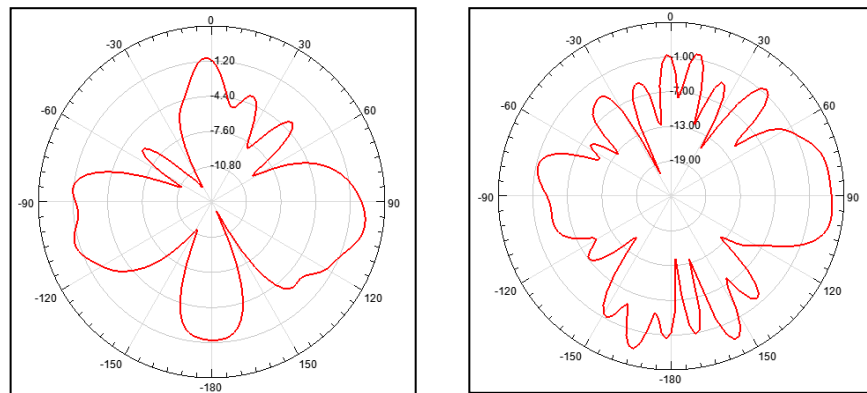


Figure 4.21: Simulated Radiation pattern (a) X-Z Direction (b) Y-Z Direction at 36 GHz

Figure 4.20 and 4.21 illustrates the radiation patterns both in X-Z and Y-Z directions at 22.5 and 36 GHz. The broadside patterns are observed in both the planes at such higher frequencies.

4.7 MIMO ANTENNA DESIGN

In order to enhance the performance of the designed antenna in terms of gain and the practical utilization for the 5G wireless applications without suffering any major signal losses for indoor applications, MIMO antenna array is designed. Initially the

proposed design of the MIMO antenna array is optimized for 2 elements as shown in figure 4.22.

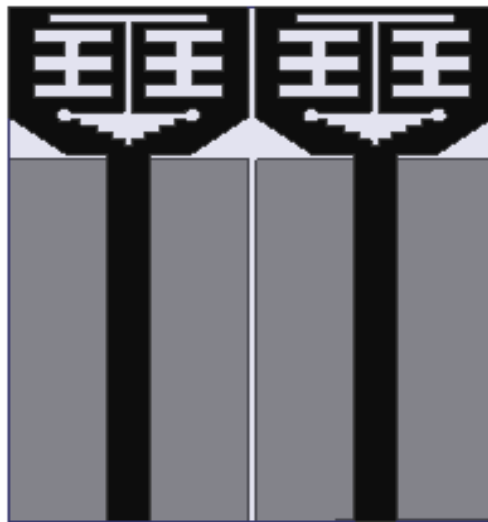


Figure 4.22: Two element MIMO antenna array

Figure 4.22 depicts the 1x 2 MIMO antenna array on the same substrate. The two antennas are therefore placed parallel to each other in order to increase the gain. However, the overall size is increased. The comparative performance of the various parameters such as VSWR, Gain and ECC are shown in figure 4.24, 4.25 and 4.26 respectively.

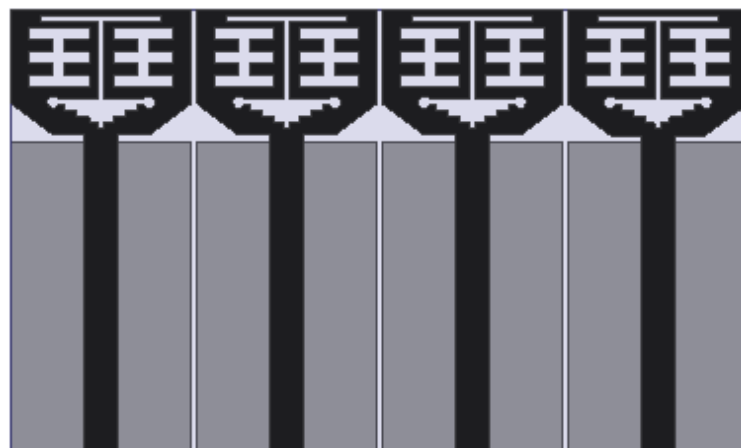


Figure 4.23: Four element MIMO antenna array

In order to compensate the indoor communication losses, the antenna with configuration of 4 elements (1 x4) is designed on the same substrate with overall increase in size. All antennas are placed at the distance of 0.5mm to avoid mutual coupling as shown in figure 4.23.

Figure 4.24 demonstrates the simulated VSWR of single, two and four elements of the antenna. It can be observed that the antenna for VSWR shows almost the identical behavior for all the elements. Single and MIMO antenna for both the configurations (2 and 4 elements) covers the impedance bandwidth of 17.33 – 40 GHz which confirms the low mutual coupling among all the elements and high isolation.

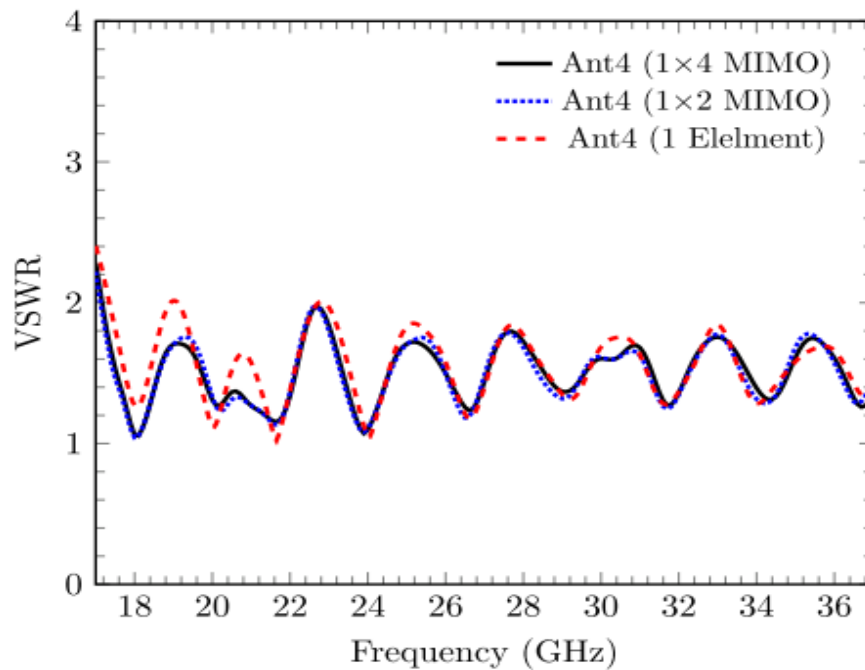


Figure 4.24: Simulated VSWR comparison of 1, 2 and 4 elements MIMO antenna

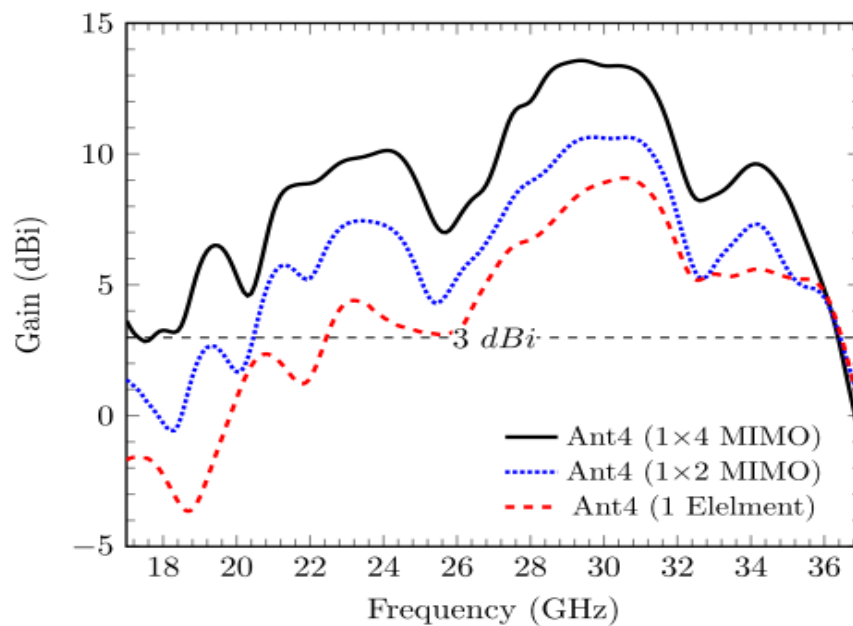


Figure 4.25: Simulated Gain comparison of 1, 2 and 4 elements MIMO antenna

Figure 4.25 illustrates the simulated gain for single, two (1 x 2) and four (1 x 4) elements of the antenna. Huge augmentation in peak gain for optimized 1 x 4 MIMO array is observed as compared to 1 x 2 and single element antenna. After optimization 1 x 4 MIMO antenna array provides peak gain of 13.69 dBi as compared to 1 x 2 (10.3 dBi) and 9.08dBi for single element antenna. It is also observed that for 1 x 4 element MIMO array provides 17 GHz (19 GHz – 36GHz) 5 dBi gain-bandwidth as compared to 9GHz (22 GHz -31 GHz) for 1 x 2 element MIMO array and 4 GHz (28GHz – 32 GHz). Thus, it can be concluded that with the implementation of 1 x 4 elements MIMO antenna array, huge augmentation is observed for both gain and gain-bandwidth.

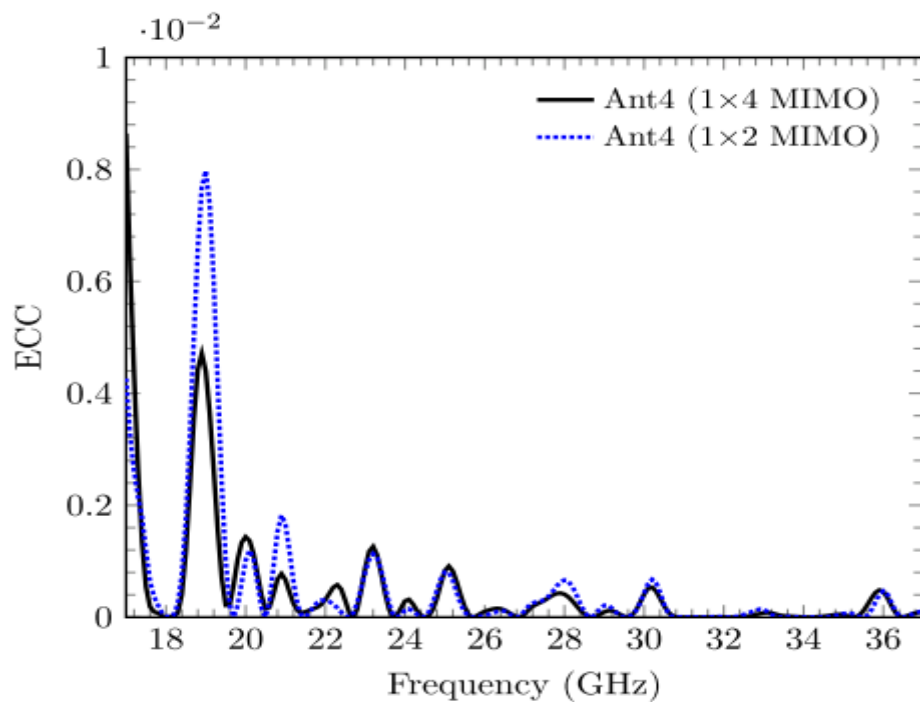


Figure 4.26: Simulated ECC of 2 and 4 elements MIMO antenna array

Figure 4.26 illustrates the simulated comparative analysis of envelope correlation coefficient (ECC) for the 2 and 4 elements of the MIMO antenna array in order to examine the individual port performance w.r.t. the frequency. It is calculated on the basis of several parameters such as VSWR, phase, polarization and far field radiation between two MIMO elements for diversity performance. It is preferred that the value of ECC should be < 0.5 .

Table 4.2: Comparison of mm-wave antennas with the proposed antenna

#	Dimensions (mm ²)	Configuration	Bandwidth (GHz)	Fractional BW (%)	Peak-Gain (dBi)	Gain bandwidth >3dBi	Substrate	Cost
124	20 x 20	Array [16 elements]	26–36	32.26	3.8	30–31.25 GHz	Copper	Moderate
133	20 x 20	Single Element	25–33	27.59	5.5	28–35 GHz	Copper	Moderate
134	20 x 20	Dielectric Resonator	23.9–24.75	---	6.3	23 – 24.75 GHz	Duroid	High
135	14.3 x 25	Dielectric Resonator	26.1–30.4	15.2	8.7	27.4–28.8 GHz	Rogers 3010 + Rogers 5880	High
136	30 x 30	Dual Feed	34 – 44	24.64	2.9	Nil	RO3003	High
137	25 x 12	MIMO	25 – 40	---	7.2	27.5 – 28 GHz	RT/Duroid –5880	High
138	26 x 11	MIMO	27 / 39	---	5/5.7	25–29, 37 – 41 GHz	Rogers 4003C	High
139	60 x 100	Array [2 x4]	26.8–28.4	5.80	3.86 / 9	----	RO3003	High
140	11 x 25.4	MIMO [1 x 2]	27.3–40	37.74	6.2	30–34 GHz	Polyethylene Terephthalate (PET)	High
141	23 x 7	Array [1 x4]	25–30	18.18	7	----	Rogers RO4350B	High
142	3.5 x 20	Array	28–33	16.39	6	----	Rogers 4350B	High
143	7 x 16	Array [32 Elements]	28 / 38	----	8.17	27–31 and 34 – 40 GHz	RT/Duroid –5880	High
This Work	37 x 15	Single Element	17.33–40	79.26	9.08	22-37 GHz	FR4	Low
	37 x 15	MIMO [1 x 4]	17.14 - 40	80.04	13.69	17.7 – 36.37 GHz	FR4	Low

4.8 SUMMARY

A compact printed antenna is proposed for K- and K_a-band applications with 3dBi gain- bandwidth > 14 GHz with peak gain > 9 dBi for single element antenna and >18GHz with peak gain > 13dBi for four element MIMO antenna array. Single element and four element antennas have also achieved critical 5dBi bandwidth > 9 dBi within the gain bandwidth of 30-30.96 GHz and 5dBi bandwidth > 13dBi within the gain bandwidth of 20.5 -35.9 GHz respectively. The improvement in 5dBi gain bandwidth is specially suited for mm-wave range applications. This improvement is achieved by etching of 3-AHSS and ITSS in the rectangular radiating patch with the uniform distribution of current on it. Also, the copper losses are minimized with these etched slots. Therefore, the proposed antenna is suitable for local multiple point distribution applications (LMDS, 5G cellular communication systems).

CHAPTER -5

mm-WAVE PATCH ANTENNA FOR HIGH DATA RATE COMMUNICATION APPLICATIONS

5.1 INTRODUCTION

With the constant increase in demand of such devices which can support and handle high data rate communication applications, millimeter wave (mm-wave) spectrum is greatly in demand in the current telecomm industry [3]. This requirement therefore leads to the foreword of compact mm-wave antennas which can support the latest 5G spectrum applications that had been suggested by the International Mobile Telecommunications Union's (IMT) in the World Radio-communication Conference WRC-19 [2]. However, in order to reduce the limitations of the bandwidth constraints of the current 4G network scenario and also to improve the performance in terms of data traffic and several other parameters, the upcoming 5G network infrastructure for the support of diversified data is greatly in demand to meet the network performance issues and also these type of global challenges. Several diverse techniques for the designing of antennas have been adopted to develop these prototypes such as array, Multi Input and Multi output (MIMO), Massive MIMO; defected ground structures (DGS) and beam forming to satisfy the above said mm-wave applications [76]. For applications such as commercial and defense which requires high data rate, the selection of low tangent loss suitable material is the most challenging task. Most of the antenna design researchers have selected to work on the suggested Ka-band spectrum and its applications as per the WRC-19 [2, 76, 88, and 98,130,131]. The high peak gain and spectral radiation efficiency requirement for Ka-band can be increased with MIMO / MU-MIMO antenna along with DGS configuration throughout the range [106].

Designs of antenna with diverse materials, printing techniques negotiates with low and high bandwidth for fifth generation based applications [99], [125]. From the previous contemplation, it has been learnt that several antennas which includes arrays [1, 76, 88, 98, and 99,106,125,130,131] have been developed and research is still going on to support the mm-wave spectrum heterogeneity. Many other techniques have been reported for the enhancement of gain bandwidth and depth of return loss [115,116,132]. In [98,125,130,131,144,145] the intended antennas for mm-wave were

bigger in size and also not covering the much wider impedance, gain and gain bandwidth.

With the day to day advancement in latest technology the communication devices are becoming handier and compact. Therefore, there is a need to miniaturize the overall size more compact and also improvement in impedance, gain bandwidth and radiation efficiency.

In this chapter, a compact broadband mm-wave antenna is designed to cover most of Ka-band and Partial Q-band applications. The inexpensive FR4 material is used to achieve impedance bandwidth and 3 dBi gain-bandwidth of 30.77–45.91GHz and peak gain of 7.9 dBi.

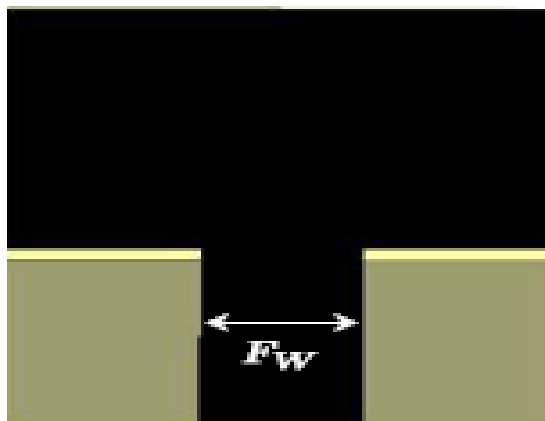
5.2 ANTENNA DESIGN METHODOLOGY

The proposed compact mm-wave antenna is designed on an inexpensive FR4 epoxy substrate having relative permittivity (ϵ_r) = 4.4, tangent loss (δ) = 0.02 and height (h) = 1.6 mm comprises of small symmetric patch and partial ground plane. The optimized parameters of the structured antenna are L_P , W_P , G_L , F_W , S_W , S_{L1} , S_{L2} , S_{L3} , S_{L4} , S_{W1} , S_{W2} , and S_{W3} discussed in Table 5.1. Initially, the structure of antenna is evolutionary from antenna (i.e. Ant1) having substrate dimensions of $10 \times 10 \text{ mm}^2$ and small rectangular patch of $5.7 \times 10 \text{ mm}^2$ and partial ground plane of $4 \times 10 \text{ mm}^2$. A reasonable gap of 0.3 mm is also initiated to achieve the mm-wave spectrum along with partial ground plane. The rectangular patch of Ant1 is fed with 50Ω microstrip feeding line of width F_W as shown in Figure 5.1(a). Therefore, in order to enhance the impedance bandwidth of Ant1, a horizontal E-formed slot is engraved at the centre of radiating patch as illustrated in Figure 5.1(b).

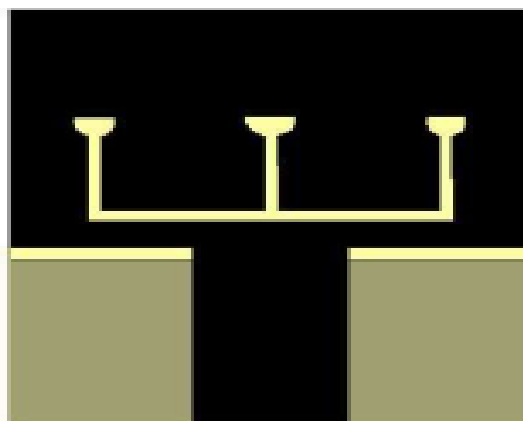
Further, the three semi-circular slots with small radius are etched at the finishing ends of each finger of horizontal E-shaped slot. Figure 5.2, illustrates the comparison of reflection co-efficient of Ant1 and Ant2 at $\theta = 90^\circ$ and $\phi = 90^\circ$. From figure, it can also be observed that Ant1 and Ant2 provide the impedance bandwidth of 32.8–38GHz and 30.4–37.75GHz respectively. Thus, it is evident that Ant2 provides 2.15 GHz additional impedance bandwidth than Ant1. Figure 5.3 illustrates the comparison of gain of Ant1 and Ant2. It can be noticed that the simulated peak-gain of these antennas are 5.36 dBi and 6.78 dBi respectively. The 3 dBi gain bandwidth of Ant1 are pragmatic in the two spectrums of 30.7–35.25GHz and 36.84–41.65GHz for designed frequency spectrum of 30.77–45.91GHz and similarly for Ant2 is 30.7–

40.8GHz. Thus, it is observed that the improvement in gain–bandwidth of Ant2 is in terms of distinct spectrum in place of two in Ant1. However, the peak–gain and impedance–bandwidth of Ant2 got improved by 0.6 dBi and 2.15 GHz over Ant1, even–though the 3 dBi gain–bandwidth of Ant2 is not covering the absolute preferred mm–wave spectrum of 30.77–45.91GHz.

Therefore, Ant2 is further modified to Ant3 as illustrated in Figure 5.4. For this the two slots which are of dumbbell shape are further etched at the center of the radiating patch and upper central segment of the radiating patch is also hyperbolically clipped in such a manner to reduce the copper losses. With this modification in Ant2 results in enhancement in the gain and gain–bandwidth manifold and therefore new modified antenna is considered to be Ant3. The utilization of partial ground plane has been done to achieve the wider spectrum for mm–wave applications. The final parameters of Ant3 are demonstrated in Table 5.2.



(a)



(b)

Figure 5.1: Antenna designs (a) Ant 1 (b) Ant 2

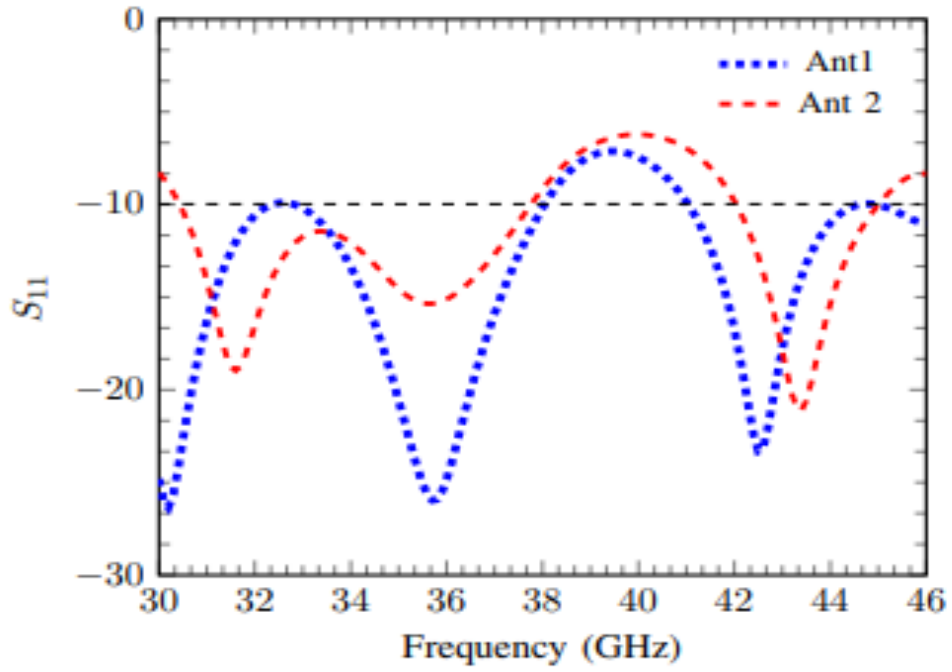


Figure 5.2: Simulated reflection co-efficient of Ant 1 and Ant 2 at $\theta = 90^\circ$ and $\varphi = 90^\circ$

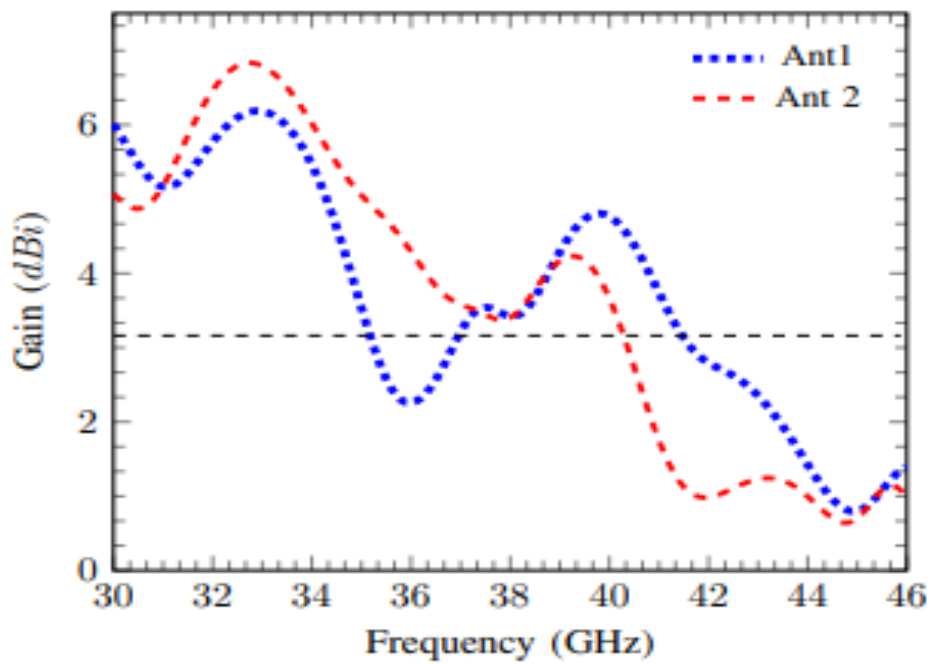


Figure 5.3: Simulated gain of Ant 1 and Ant 2 at $\theta = 90^\circ$ and $\varphi = 90^\circ$

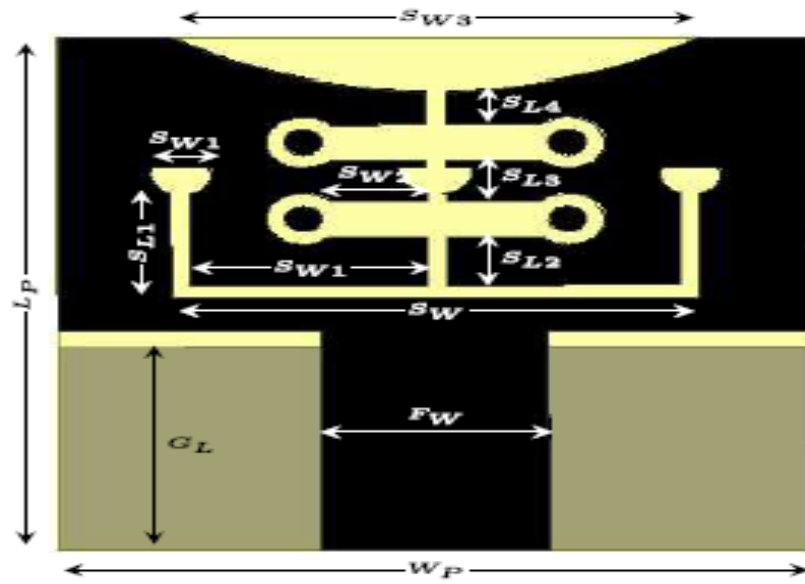
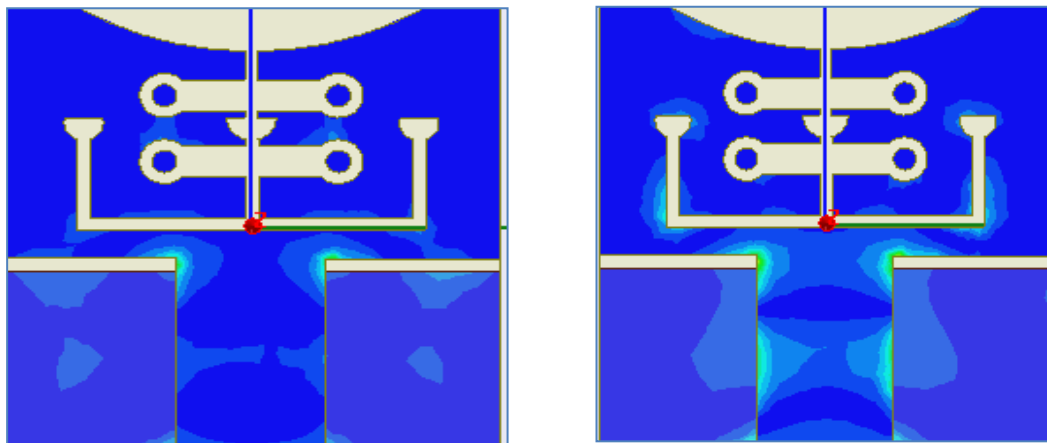


Figure 5.4: The antenna design Ant 3

Table 5.1: Dimensions of the proposed Patch Antenna (in mm)

L_P	10	S_W	7	W_P	10
G_L	4	S_{L2}	0.95	F_W	3
S_{L4}	0.65	S_{W1}	3.15	S_{W2}	1.24
S_{L1}	2.05	S_{L3}	0.9	S_{W3}	7

5.3 CURRENT DISTRIBUTION



(a)

(b)

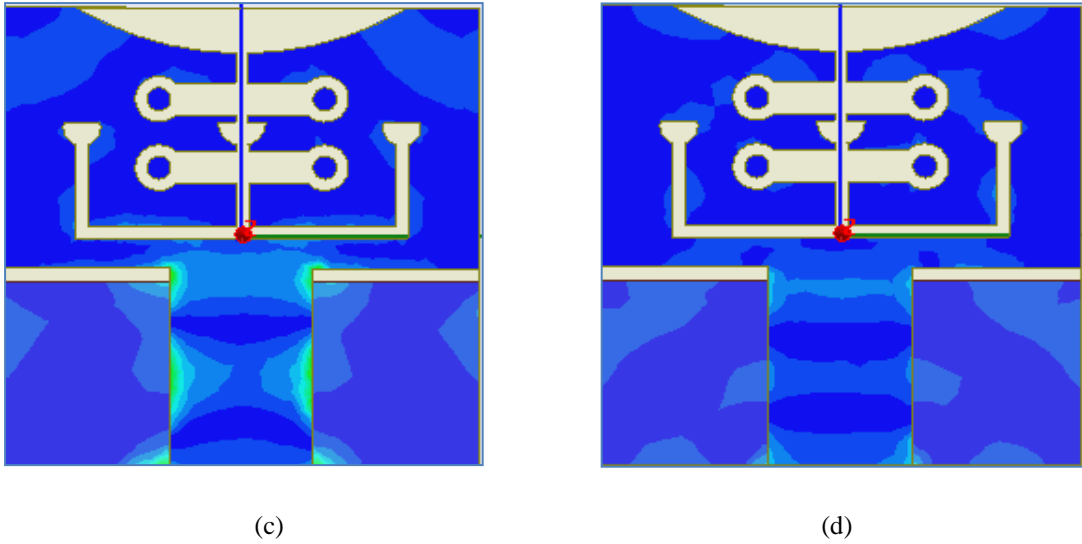


Figure 5.5: Simulated Current Distribution at (a) 30GHz (b) 34 GHz (c) 36 GHz (d) 40 GHz

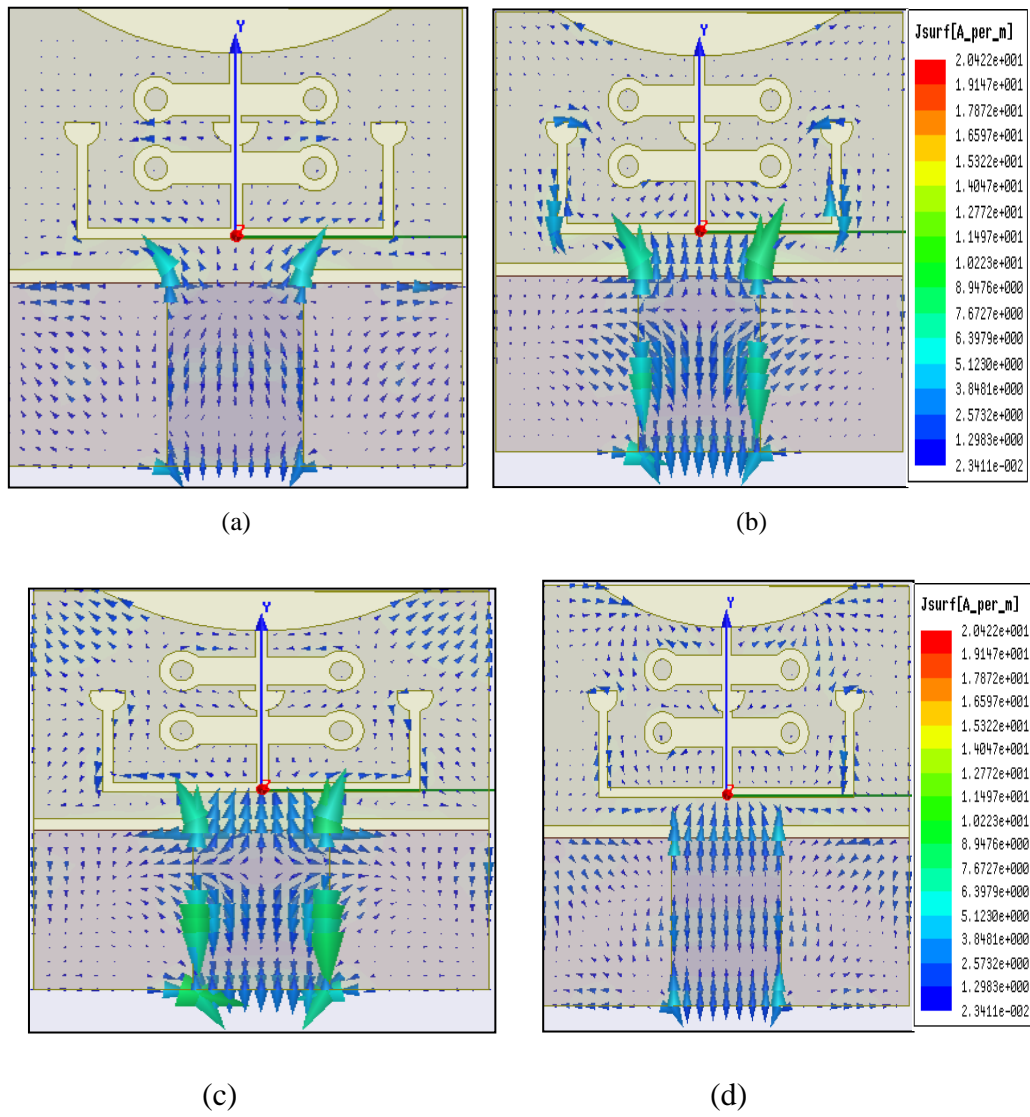


Figure 5.6: Simulated Vector Current Distribution (a) 30GHz (b) 34 GHz (c) 36 GHz (d) 40 GHz

Figure 5.5 and 5.6 depicts the distribution of the current in the magnitude and in vector manner. It can be observed from the figure 5.5 that the intensity of the current distribution at different frequencies both in magnitude and in vector manner.

5.4 PARAMETRIC ANALYSIS

The parametric analysis has been done by varying the parameters of slot lengths such as SL2, SL3, SL4 and radius of the inner circular slot.

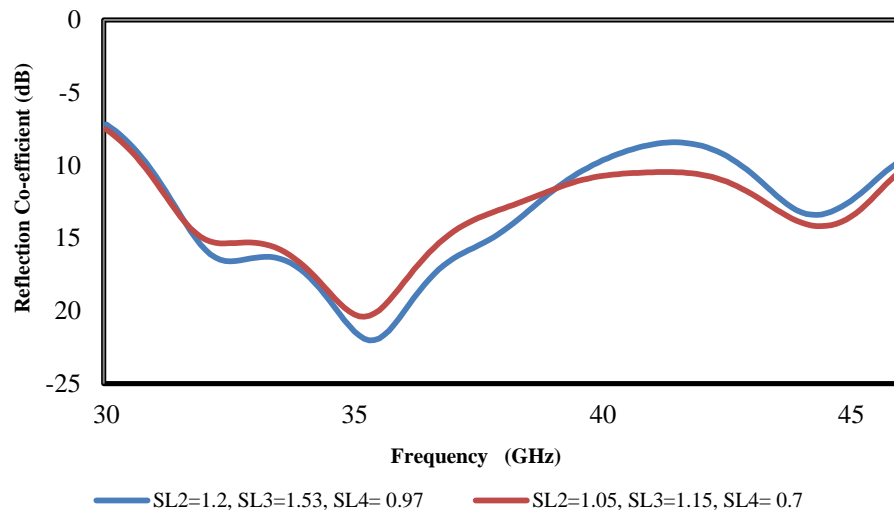


Figure 5.7: Simulated Parametric Analysis of reflection coefficient

Figure 5.7 depicts the impact on reflection coefficient by varying slot lengths (SL2, SL3 and SL4). It can be observed that slot length in blue line is greater than -10dB and slot lengths on red line have no impact on the reflection coefficient.

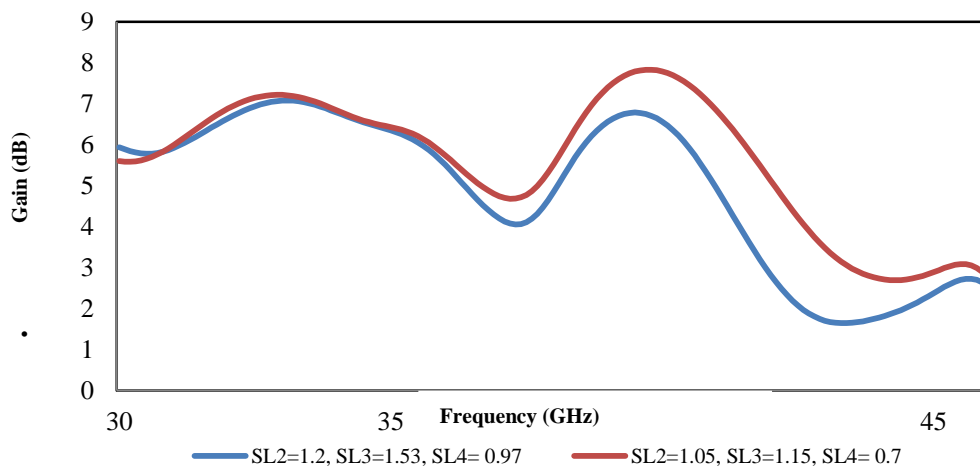


Figure 5.8: Simulated Parametric Analysis of Gain

Figure 5.8 depicts the impact on gain by varying slot lengths (SL2, SL3 and SL4). It can be observed that slot lengths in blue line is having peak gain of 6.2 dBi whereas variation in slot lengths in red line is having peak gain of 7.8 dBi

5.5 SIMULATED ANTENNA RESULTS

The Figure 5.9 illustrates the reflection coefficient of Ant2 and Ant3 at $\theta = 90^\circ$ and $\phi = 90^\circ$. It is depicted from the above said figure that Ant3 provides the impedance bandwidth spectrum of 15.14 GHz (30.77–45.91GHz) and it is 7.79 GHz supplementary than Ant2. It can be observed clearly that by integrating the two dumbbell slots on extended central E-shaped slit, the higher and additional resonant frequencies got excited; hence additional impedance bandwidth is achieved than that of Ant2. It is also observed that with the shifting of the lower cut off frequency of Ant3 is to higher value than Ant2 due to lengthen of electric current path at surface of patch.

Figure 5.10 compares the gain of an Ant2 and Ant3. From figure, it is evident that gain is enhanced due to removal effect of non-participant copper material at radiating patch in radiations, the copper losses are minimized. It is also depicted that the peak-gain of 7.91 dBi is achieved at 40 GHz for Ant 3. It is also observed that the 3 dBi gain-bandwidth in the range of 30.77–45.91GHz has been achieved successfully, which can cover a majority of mm-wave applications which are in the specific range.

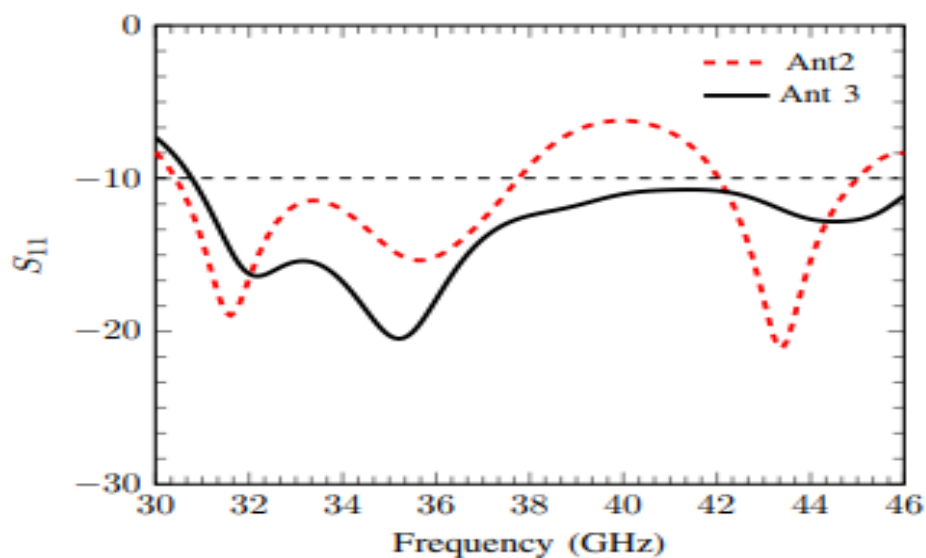


Figure 5.9: Simulated reflection co-efficient of Ant 2 and Ant 3 at $\theta = 90^\circ$ and $\phi = 90^\circ$.

The gain bandwidth of Ant3 is 5.11 GHz more than Ant2. It can also be observed that the values of gain at the particular frequency are improved for Ant3 in the desired spectrum, when it is compared with gain values of Ant2.

Figure 5.11 illustrates the enhancement in radiation efficiency of Ant3 as compared to Ant1 and Ant2. It is also observed that the radiation efficiency of Ant3 is reasonably enhanced for 30.7–45.91GHz spectrum and more enhancements are also observed beyond 36 GHz to 45.91 GHz. The average radiation efficiency of Ant3 is 82.83% compared to 78.8% of Ant2. Also, the improvement in radiation efficiency of Ant2 is observed over Ant1 beyond 37 GHz. From Figure 5.9 – 5.11 and Table 5.2, it is clearly observed that Ant3 is most appropriate for K_a -band and partial Q – band [1] applications like radar communication, satellite communication, cellular communication and mm-wave Integrated circuits 5G applications.

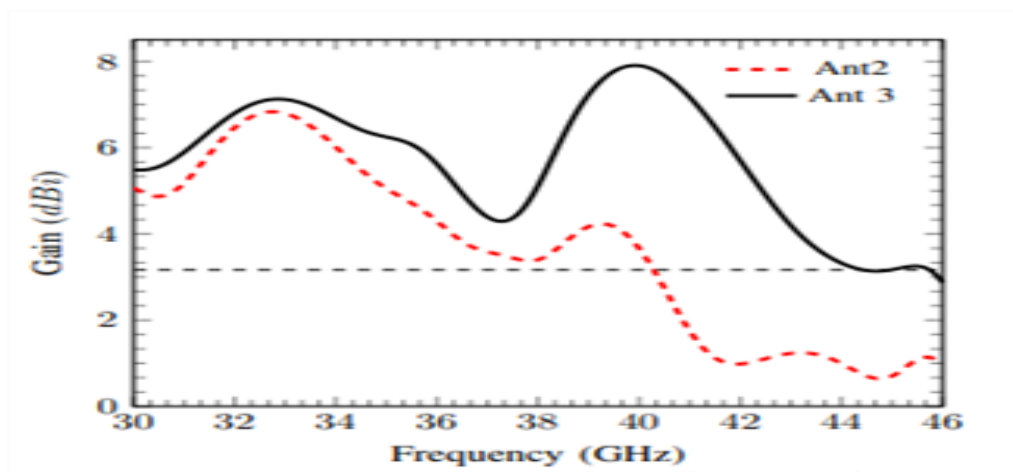


Figure 5.10: Simulated gain of Ant 2 and Ant 3 at $\theta = 90^\circ$ and $\phi = 90^\circ$.

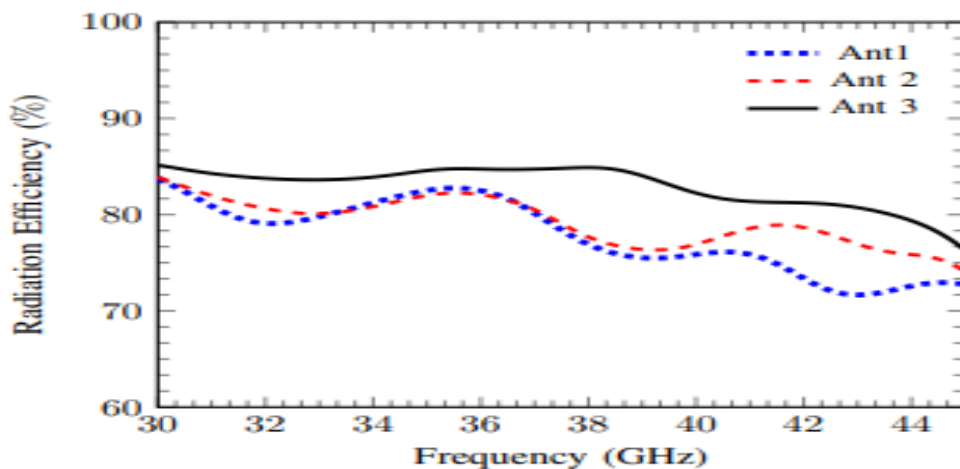


Figure 5.11: Simulated radiation efficiency of Ant 2 and Ant 3 at $\theta = 90^\circ$ and $\phi = 90^\circ$.

Figure 5.11 depicts the radiation efficiency of Ant 2 and Ant 3. The radiation efficiency of the antenna design throughout the whole band varies from 74 to 85%. In HFSS go to Results section, then go to create far field, then go to rectangular plot, then go to antenna parameters and finally in the radiation efficiency section with absolute parameter. Finally, export the result and calculate the average in .csv / excel file.

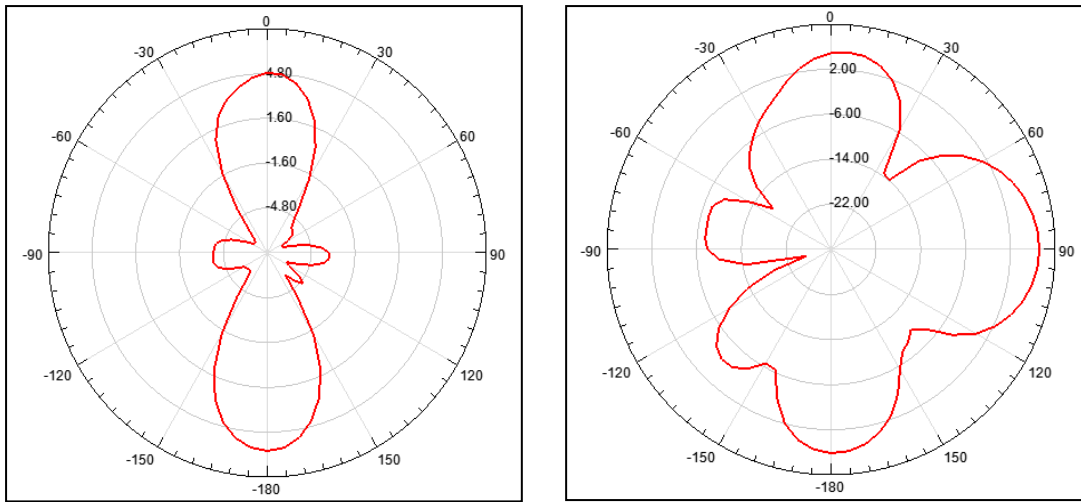


Figure 5.12: Simulated Radiation pattern (a) X-Z Direction (b) Y-Z Direction at 41 GHz

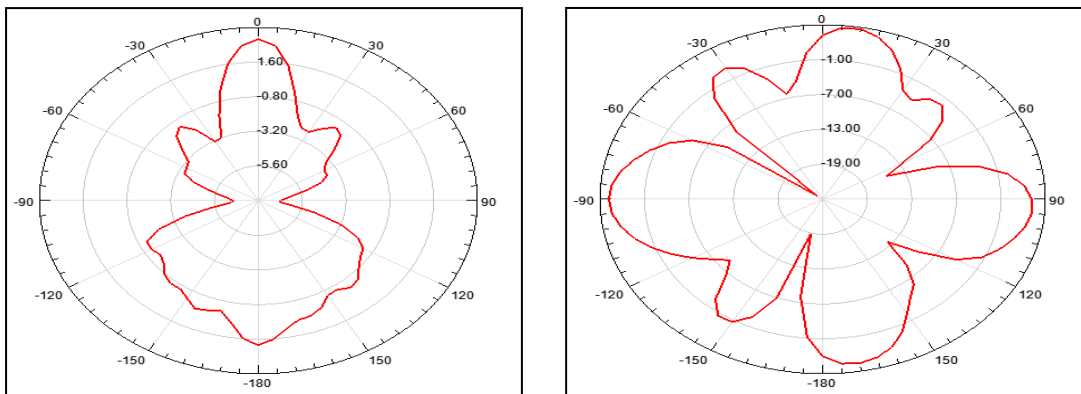


Figure 5.13: Simulated Radiation pattern (a) X-Z Direction (b) Y-Z Direction at 45 GHz

Figure 5.12 and 5.13 illustrates the radiation patterns both in X-Z and Y-Z directions at 41 and 45 GHz. The broadside patterns are observed in both the planes at such higher frequencies.

Table 5.2: The comparison of parameters of Ant1, Ant2 and Ant3

Designs	Bandwidth (GHz)	Peak Gain (dBi)	Gain Bandwidth (>3dBi)	Average Radiation Efficiency (%)
Ant 1	5.21	5.36	4.7	79.87
Ant 2	7.3	6.78	9.7	81.08
Ant 3	14.2	7.9	13.15	82.83

Table 5.3 compares the already designed prototypes with proposed prototype i.e. Ant3. It can be clearly observed that Ant3 is better than already available designed prototypes in terms of its size, impedance bandwidth, gain bandwidth, peak gain and also average radiation efficiency.

Table 5.3: The comparison of Previous Designs with Recent Antenna

#	Size (mm ²)	S ₁₁	Gain Bandwidth (GHz)	Peak Gain (dBi)	Radiation Efficiency Range (%)
98	--	26.5-33.0	7.5	6	--
125	11 x 12	26 – 40	14	8.7	63
130	20 x 11	26.9-30.6	3.7	7.9	--
131	7.5 x 12.8	22- 40	25	8.2	20 – 90
This Work	10 x 10	30.77- 46	15.1	7.9	83.6 - 85.12

5.6 SUMMARY

In this chapter, a low profile compact mm-wave rectangular antenna having 5G upper wide-bands for K_a- and partial Q-band applications has been attained and discussed in detail. From the results it can be observed that impedance bandwidth has been enhanced with etching of extended E-shaped slots on the radiating patch. It can also be observed that by etching two dumble shaped slots in the radiating patch, the high stable gain and average radiation efficiency above 83% is achieved. The proposed antenna with wide impedance and gain bandwidth of 16 GHz proved to be a potential candidate for the upcoming 5G applications.

CHAPTER -6

CONCLUSION AND FUTURE SCOPE

With the constant growth and evolution in wireless technology, wideband mm-wave microstrip antenna becomes the most emerging research topic of interest now days. Wideband mm-wave antenna fulfills the lower and upper fifth generation (5G) wireless communication application requirements ranging from above 30 GHz over differently specified frequency band of operation. Wideband mm-wave antennas with partial ground planes (PGP) microstrip patch antennas are designed for wide range of 5G wireless communication applications. Antennas are designed, simulated and optimized on high frequency structures (HFSS) simulator. Two antenna prototypes with different shapes and sizes are designed, optimized and tested based on partial ground planes to obtain wide impedance bandwidth characteristics. First antenna is designed with a partial ground plane with 3-point semi-circle arc for the smooth flow of current. The lower corners of the radiating patch are gradually clipped away so as to make the radiating patch shape close to elliptical. Further, in order to achieve the mm-wave range the two tilted slots at an angle $\alpha = 15^\circ$ are etched at the edges. These slots are responsible for the diversion of the peripheral current of the semi elliptical patch towards center portion of antenna by ensuring the participation in radiation of the central inner portion of radiating patch. Further to reduce the copper losses and smooth flow of current the upper corners of the radiating patch are also clipped away. A low-cost compact wideband mm-wave microstrip antenna is also proposed to cover the C-band to mm-wave applications. The massive impedance bandwidth of 5.86–40GHz (148.89 %) is achieved by diverting the radiating patch peripheral current with to the central portion of the radiating patch. With these techniques the current is uniformly distributed and hence augment the bandwidth in mm-wave range. The high gain is provided by the proposed structure in three bands K_a-bands i.e. 28 GHz (27.50–28.35GHz) n261-band and 37 GHz (37–38.6GHz) and 39 GHz (38.6–40GHz) n260-bands and have peak-gain of 8.76 dBi, 10.8 dBi and 9.92 dBi in their respective bands. The simulated and measured results show the good agreement in the values for entire range.

Second, a compact two-armed H- and inverted T- shaped slot antenna with the partial ground plane is simulated and fabricated on an inexpensive FR4 dielectric

substrate. Thus, compact antenna is proposed for K- and K_a-band applications. The Proposed structure shows good agreement between simulated and fabricated results in terms of S₁₁, VSWR. It covers zero dBi gain bandwidth of 20–36.5GHz and 3 dBi of 26.15–36.20GHz and provides high peak gain of 9.06 dBi at 30.6 GHz without array design. Further, design is also optimized for 1 x 4 MIMO antenna array with the achievement of 13.69 dBi gain and ECC < 0.5. The slots are optimized and etched in such a manner that the current is uniformly distributed over the radiating patch. The proposed antenna is suitable for indoor and 5G cellular communication system applications.

Third design of the antenna refers to the simulated and optimized one which can be practically utilized for high data rate communication applications. The proposed design covers K_a- band and partial Q-band applications. The improved wide impedance bandwidth gain bandwidth and radiation efficiency has been achieved successfully by properly etching of E- shaped and dumbbell shaped slots on the radiating patch. The proposed antenna with 16 GHz gain bandwidth is a potential and suitable candidate for the futuristic 5G applications.

6.1 FUTURE SCOPE

Wideband mm-wave microstrip patch antenna in various shapes and sizes with suitable techniques has gained much attention due to fulfilling the demands of wide range of wireless communication applications. Microstrip patch antenna also suffers from certain shortcomings like less peak gain, gain bandwidth, impedance bandwidth and its size. Therefore, in this thesis, research work is carried out to enhance peak gain, gain bandwidth >3dBi and 5dBi, and impedance bandwidth of the microstrip patch antenna using concept of different partial ground plane techniques in these structures to achieve high peak gain, impedance bandwidth, gain bandwidth and its compact size. This part explains the work that can be extended for future research work.

- ✚ In this thesis, research work is carried out on antenna gain, gain-bandwidth, impedance bandwidth, radiation efficiency with compact size using different partial ground plane geometries. In future, further gain can be enhanced using concept of Arrays for wireless applications.

- ✚ Antenna prototypes can be simulated, optimized and tested for frequencies up to and beyond 40 GHz with its performance which can be analyzed in terms of Radiation pattern and Gain.
- ✚ Proposed mm-wave antennas covers K- and Ka- bands and their frequencies and further these can be done for the future mobile handsets for the Specific Absorption Rate (SAR).

RESEARCH PUBLICATIONS

1. Malik, P. K., Wadhwa, D. S., and Khinda, J. S. (2020), “A survey of device to device and cooperative communication for the future cellular networks”, *International Journal of Wireless Information Networks, Springer*, 27 (3), 411–432.
2. Wadhwa, D. S., Malik, P. K., and Khinda, J. S. (2021), “mm–Wave Patch Antenna for High Data Rate Communication Applications”, *International Conference on Computing, Communication And Intelligent Systems (ICCCIS-2021)*, 778-781, DOI: [10.1109/ICCCIS51004.2021.9397221](https://doi.org/10.1109/ICCCIS51004.2021.9397221), *IEEE Xplore*.
3. Wadhwa, D. S., Malik, P. K., and Khinda, J. S. (2021), “High Gain Antenna for n260- and n261-bands and Augmentation in Bandwidth for mm-wave range by Patch Current Diversions”, *World Journal of Engineering, Emerald Insight*.
4. Wadhwa, D. S., Malik, P. K., and Khinda, J. S. (2021), “Improvement in 5 dBi gain-bandwidth of wide band antenna for indoor K-, Ka-band, millimeter-wave applications”, *International Journal of Infrared, Millimeter and Terahertz Waves, Springer. (Communicated)*.

Conference Certificate



Figure 6.1: Snapshot of IEEE Conference Certificate

APPENDIX A

A.1 CONNECTORS CONFIGURATION

To achieve the mm-wave frequency range, normal SMA connectors will not work for the designed antennas. Therefore, the female end launch coaxial connectors of 2.92mm have been used to achieve the mm-wave frequency range. The two connectors have been purchased and imported from the Mouser Electronics, USA. The details of the connectors are as shown in the table below:

Table A.1: Connectors configuration and Attributes

S.No	Attribute	Value
1	Company	Mouser Electronics, USA
2	Part Number	RF Connectors/coaxial connectors / 2.92 mm End Launch 0.062 in thick solder 530- 145-0701-841
3	Item Body	Brass / Gold / Nickel
4	Impedance	50 Ω
5	Frequency Range	0 – 40 GHz
6	VSWR	1.5
7	Operating Temperature	-40 to 85 ⁰ C
8	Cost per connector	2684.99/- (Without Taxes and shipping Charges)
9	Total Connectors Imported	02

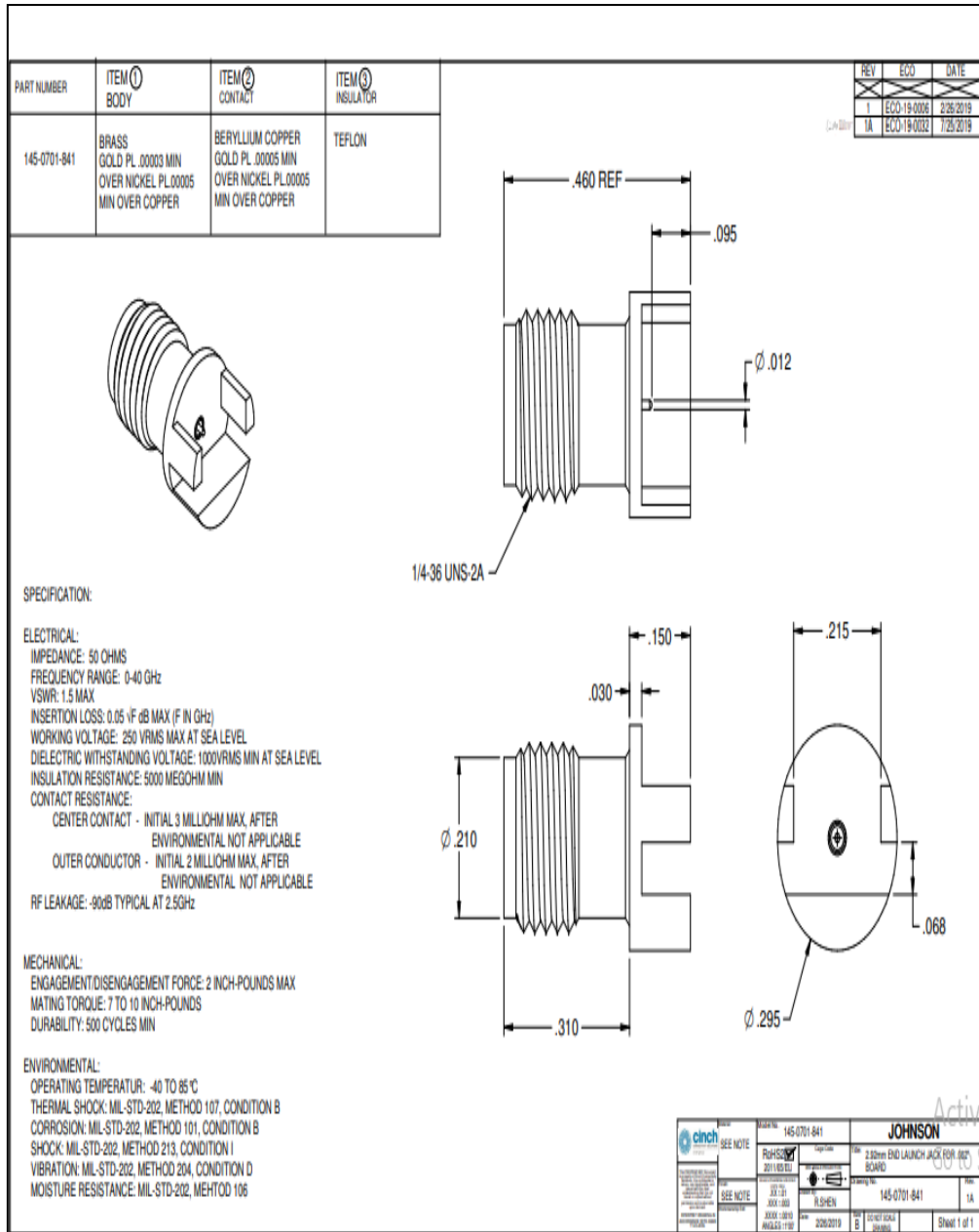


Figure A.1: Technical Datasheet of the Coaxial Connectors



1000 North Main Street, Mansfield, TX 76063
 Customer Service Rep: Internet Customer Service
 Customer Service: +91 80-4265-0000
 Credit: +91-80-42650003
 Federal ID# 61-1520598

Invoice - Credit Card Receipt

Invoice No.	Invoice Date	Page No.
578 65398	12-AUG-20	1 of 1

Purchase Order No.	Master Tracker No.
19604750	1387360376

Buyer Name	Ship Via	Customer No.	Terms	Order Date
DEEPIKAR SINGH MADHWA	DHL WORLDWIDE PRIORITY EX	602PC27	VE 3116	11-AUG-20

Bill To	Ship To
MADHWA, DEEPIKAR SINGH #516, PURANA HATHI KHANA, BEHIND NAHARAJA HIRA SINGH COMPLEX NABHA PUNJAB 147201 INDIA	DEEPIKAR SINGH MADHWA ATTN: DEEPIKAR SINGH MADH #516, PURANA HATHI KHANA, BEHIND NAHARAJA HIRA SINGH COMPLEX NABHA PUNJAB 147201 INDIA

Line No.	Mouser Part Number Customer/MFG Part No. Description	Quantity Ordered	Quantity Shipped	Quantity Pending	Unit Price (INR)	Extended Price (INR)
1	530-145-0701-841 MFG Part No: 145-0701-841 Johnson / Cinch Connectivity Solutions 2.92mm End Launch / RF Connectors / Coaxial Connectors US HTS:8536694010 ECCN:EAR99 COO:CN	2	2	0	2,684.99	5,369.98

Merchandise	Handling	Freight	TAX	Paid by credit card		INR 6,569.98
5,369.98	0.00	1,200.00	0.00			

Shipping Information						
Ship Date: Aug 12, 2020 These items are controlled by the U.S. Government and authorized for export only to the country of ultimate destination for use by the ultimate consignee or end-user(s) herein identified. They may not be resold, transferred, or otherwise disposed of, to any other country or to any person other than the authorized ultimate consignee or end-user(s), either in their original form or after being incorporated into other items, without first obtaining approval from the U.S. government or as otherwise authorized by U.S. law and regulations.						
Tracking Number(s) and Bill Weight(s)						
1387360376	0.23 lb					

This order is subject to all terms and conditions displayed at: <http://www.mouser.in/sale/terms/>

Figure A.2: Coaxial Connectors and part no description

**A.2 MoU BETWEEN LPU AND DEPARTMENT OF SPACE (DoS), SCL,
MOHALI**


 <p>LOVELY PROFESSIONAL UNIVERSITY <i>Transforming Education Transforming India</i></p>	Centre for Research Degree Programmes	
	LPU/CRDP/EC/070320/01	
	Date: 7 th March, 2020	
TO WHOM IT MAY CONCERN		
<p>This is to certify that Mr. Deepinder Singh Wadhwa (Registration number- 41400709) is pursuing Ph.D. (Electronics and Electrical Engineering) [Part Time] at Lovely Professional University under the guidance of Dr. Praveen Kumar Malik. He is working on topic "WIDE-BAND MICROSTRIP ANTENNA FOR FUTURISTIC COMMUNICATION SYSTEMS" and antenna has been fabricated. He wants to test the antenna parameters on VNA in your esteemed organization. Lovely Professional University has already signed an MOU dated on 18th April 2018 regarding same.</p>		
<p>You are requested to kindly allow him to carry out his research work at your organization. Your act of favorable consideration is sincerely solicited and shall be highly appreciated.</p>		
<p><i>Rau</i> Head</p>		
<p>Centre for Research Degree Programmes, Lovely Professional University, Phagwara, Punjab (India) – 144411</p>		
<p><i>Sharma</i> 25/3/20 Prepared by</p>	<p><i>Malik</i> 26/3/20 Checked by</p>	<p><i>Res</i> 26/3/20 Verified by</p>
<p>Jalandhar-Delhi G.T.Road, Phagwara, Punjab (India) - 144411 Ph : +91-1824-444594 E-mail : drp@lpu.co.in website : www.lpu.in</p>		

Figure A.3: Antenna Testing Permission Letter



**COLLABORATION ON RESEARCH AND DEVELOPMENT,
FACULTY AND STUDENT EXCHANGE
MEMORANDUM OF UNDERSTANDING**

In furtherance of their mutual interest in the fields of education and research and as a contribution towards increasing national cooperation, Semi-Conductor Laboratory, Department of Space, Government of India, having its registered address at Sector 72, S.A.S. Nagar - 160071, Punjab, India (hereinafter referred to as SCL) and Lovely Professional University, Jalandhar - Delhi G.T. Road, Phagwara - 144411, Punjab, India (hereinafter referred to as LPU) have entered into this Memorandum of Understanding (MOU) in the month of April..... 2018 as set forth below:

ARTICLE I

The MOU involves collaboration between SCL and LPU (both also referred to as institution) in related disciplines.

The two institutions shall seek to promote:

1. Exchange of Staff and Students (Faculty & Research Scholars, Under Graduate, Post Graduate & Doctoral Students and Research Project Employees) regarding Academics and Research for the mutual benefit of both institutions.
2. Exchange of Students for pursuing Courses of Study and Academic Programmes for mutual benefit of both institutions.
3. Collaboration in Teaching, Research & Development and Consultancy Activities.
4. Exchange of Academic & Research Material and Publications/IPs.
5. Cooperation in Projects and Research Activities of mutual interest.
6. Provision of Cultural and Intellectual enrichment opportunities for the Staff and Students of both institutions.
7. Collaboration in Research & Development in the areas of (i) Advanced VLSI Device Fabrication, (ii) MEMS Fabrication, (iii) VLSI Device / MEMS Characterization, (iv) VLSI/CMOS-RF Circuit Design and (v) VLSI Device Modeling at both LPU and SCL. This also includes collaboration in setting-up and upkeep of the relevant infrastructure in both the institutions.
8. Publication of Research Papers in International Scientific Journals and in the Conferences.
9. Exchange of Students for Summer/Winter Internships.

रवि शर्मा

Moussa
Gupta

of the appropriate authorities of each institution. To facilitate development of such plans, each institution shall nominate a member of its staff to coordinate activities arising under this MOU.

ARTICLE IV

Both institutions agree and undertake to keep confidential at all times information and /or data that may be exchanged, acquired and /or shared in connection with the area of cooperation, as mentioned above, unless otherwise the same information already exists in the public domain.

ARTICLE V

Ownership of findings of any joint research shall be vested in both institutions under this MOU and any publications regarding the same shall only be possible after prior approval from both institutions.

ARTICLE VI

The MOU shall remain in force for a period of 10 (TEN) years commencing from the date of signing and may be reviewed by mutual consent by serving 3 (Three) months written notice to the other institution. Upon renewal, both institutions shall select either to proceed with the existing or new terms of understanding.

ARTICLE VII

Both the SCL and LPU reserve the right to terminate this MOU by either institution giving 3 (Three) months written notice to the other. Where such termination occurs, the provisions of this MOU shall continue to apply to ongoing activities until their completion.

ARTICLE VIII

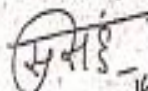
Participating staff and students involved in any activities under this MOU must adhere to the law of the country and the rules & regulations of the host institutions.

ARTICLE IX

SCL and LPU welcome establishment of this MOU for cooperation and jointly agree to provisions as set out above. There are two copies of this MOU equally valid, one for each institution, effective after its signing by authorized signatories.

Semi-Conductor Laboratory

Lovely Professional University

 14/04/18

Surinder Singh
Director

ਸੁਰਿੰਦਰ ਸਿੰਘ / Surinder Singh
ਨਿਰਦੇਸ਼ਕ / Director
ਸੇਮੀ-ਸੰਚਾਲਕ ਲੈਬੋਰੇਟਰੀ
Semi-Conductor Laboratory
ਭਾਰਤੀ ਸਪੇਸ, ਖਾਰਾ ਸਕੇਲਰ
Department of Space, Dept. of India
ਫਿਲੋ-72, ਸਾ.ਤ.ਸਿ. 144-100071, ਫਾਜ਼ਲ, ਖਾਰਾ
Sector-72, B.A.S. Nagar-160071, Punjab, INDIA

Witness

Date:

14/04/18

ਗੁਪ ਸਮੂਹ ਪ੍ਰੋਜੈਕਟ ਮੈਨਿੰਗ ਗਰੁੱਪ
Group Head-Project Manning Group
ਸੇਮੀ-ਸੰਚਾਲਕ ਲੈਬੋਰੇਟਰੀ
Semi-Conductor Laboratory
ਭਾਰਤੀ ਸਪੇਸ, ਖਾਰਾ ਸਕੇਲਰ
Department of Space, Government of India


Dr. Monica Gulati
Registrar
Lovely Professional University

Manish Gupta
Witness Dr. Manish Gupta,
Associate Registrar
Date: 14.04.2018

10. Publication of Intellectual Properties (IPs) developed jointly through Project / Research Collaboration. Such IPs would acknowledge joint inventor-ship of Personnel / Students belonging to both the institutions, as applicable.

11. Writing Books / Booklets jointly in the areas of mutual interest.

ARTICLE II

The activities under this MOU will include:

1. Staff Exchange

Staff Exchange activities cover visits to either institution for any of the following purposes:

- (i) Undertaking Joint Research
- (ii) Attachment of Staff for purposes of Curriculum Development & Review, Attendance in Courses and Upgrading of Teaching & Research Skills
- (iii) Participation in Seminars, Colloquia and other types of academic discussions
- (iv) Contributions to Teaching Programmes
- (v) Co-supervision of Post Graduate Students
- (vi) Conduct study tours, joint consultancy and research work
- (vii) Facilitation for pursuing Academic Courses (Post Graduate & Doctoral) for Department of Spots / SCL Employees at LPU.

2. Student Exchange:

Student Exchange activities (for Under Graduate, Post Graduate & Doctoral Students) cover visits to either institution for any of the following purposes:

- (i) Participation in Research
- (ii) Internships for LPU Students at SCL

3. Exchange of Academic Materials:

Exchange of relevant Academic Materials will be carried-out subject to mutual agreement of both institutions.

ARTICLE III

Implementation of cooperation based on this MOU shall be dealt with between the relevant Faculties and Divisions / Departments of both institutions. Wherever necessary, a specific plan shall be worked-out for each activity setting-forth detailed arrangements for collaboration. Such plans shall be subject to approval

०१/१५

Mansoor
Gulati

Figure A.4: MoU between LPU and DoS, Mohali

A.3 ANTENNA TEST PROCEDURE

A.3.1 MEASUREMENT OF RETURN LOSS USING VNA (ZVA-40)

A.3.1.1 ANTENNA FABRICATION

The process of antenna design is carried out in Antenna design and simulation software i.e. high frequency structured simulator (HFSS). After the simulated and optimized design, convert the corresponding antenna design HFSS file into gerber file and converting it into a film which is the initial step from where the antenna fabrication process starts. For Microstrip patch antenna, printed circuit board (PCB) fabrication technology is used. With the enhancement in fabrication demands of electronics components on boards as per the required application, there is a boost-up the need of PCB fabrication technology. PCB is a hard board that provides the relevant mechanical strength to components and provides connectivity between them through copper tracks for suitable communication. PCB can be single layer, but with double layer or multi-layer boards for antenna design it is known as substrate integrated waveguide (SIW). Major components of PCB for the antenna design for the suitable application are Substrate with required dielectric material. Specific dielectric material must be selected in order to achieve the desired characteristics of the antenna. Also, selection of dielectric constant material depends on applications and the methodology which is to be applied.

Dielectric materials with thick substrate and low dielectric constant provide high bandwidth and better antenna efficiency but leads to large size structures. On contrary, material with high dielectric constant give rise to more surface waves and less bandwidth is achieved due to this.

For the proposed antenna designs, an inexpensive FR4 dielectric substrate is selected with dielectric constant of 0.02 and thickness of 1.6mm with partial ground plane to enhanced bandwidth, high stable gain and good antenna efficiency. FR4 material is also available with other dielectric constant values also. As the most commonly used material is FR-4 Epoxy and it is a lossy material also but with the partial ground plane technique and other etched slots desired results have been achieved.

For PCB fabrication some steps and followed. Initially, design is prepared on HFSS software than Gerber files are created. Gerber files are created with the help of

software. It provides the complete information related to copper layers, solder mask and component notation etc. It creates a film of design also called photo negative. Next step is to print the PCB design using special printers called plotters. After preparing the blueprint of design, it is printed on the PCB and heated for some time. After some time wanted copper is kept and unwanted copper is removed. This process is called etching and in PCB designing Ferric chloride material is used for etching process. After removing the unwanted copper, PCB is washed with alkaline solution to further remove any leftover copper and dried. Figure A.1 shows the complete PCB designing process:

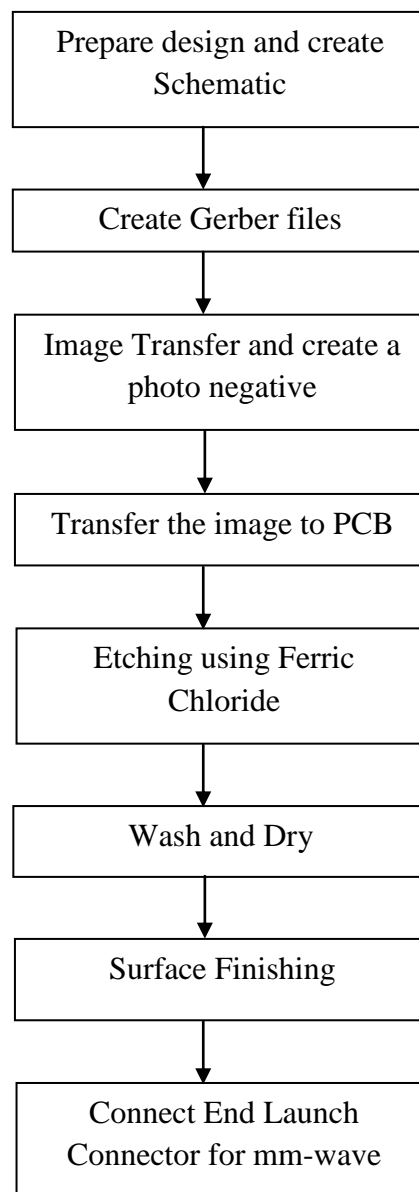


Figure A.5: PCB Fabrication process

A.3.2 ANTENNA TEST PROCEDURE

After the desired fabrication of the antenna using PCB, its performance is tested / analyzed on the vector network analyzer for impedance bandwidth, Impedance matching and voltage standing wave ratio (VSWR). Antenna Return loss and VSWR measurement can be done using VNA. For these measurements vector network is used and its model is specified in table A.2.

Table A.2: Apparatus used for Antenna parameter measurement

Antenna Parameters	Apparatus used	Model
Return loss (S_{11})	VNA	ZVA - 40
VSWR	VNA	ZVA - 40

For testing proposed antenna prototype, instruments used are given in following Table A.2 with specification.

Table A.3: Antenna testing devices used for proposed antenna Measurement

S. No.	Instrument Name	Company Name	Model No	Specification
1	Vector Network Analyzer	Rohde and Schwarz	ZVA- 40	10 MHz – 40 GHz

A.3.2.1 Return loss/VSWR measurement using VNA (ZVA-40)

VNA used for antenna return loss and VSWR measurement is of Rohde and Schwarz whose model is specified as ZVA- 40. It is high performance microwave network analyzer that covers frequency range of 10MHz to 40GHz. VNA can have two ports or four ports for connection of DUT (Device under test). Before antenna measurement, VNA should be calibrated properly using calibration kit. Following steps are taken to measure VSWR for proposed antenna.

A.3.2.1.1 Return loss Test procedure

1. Connect the test equipment.
2. Switch on the Vector Network Analyzer and set the desired band of frequency means set the start frequency i.e. 5GHz and Stop frequency that is 40GHz for Ant1 and 15GHz start and 40 GHz for Ant2.

3. Select S_{11} parameter for VSWR. Calibrate the Network Analyzer by connecting calibration module. Set the network analyzer for S_{11} / VSWR.
4. Connect the other end of the feeder cable to the Antenna under test (AUT)
5. Read the response in VNA over the band, which is the VSWR of the antenna
6. Note the Value of S_{11} /VSWR.

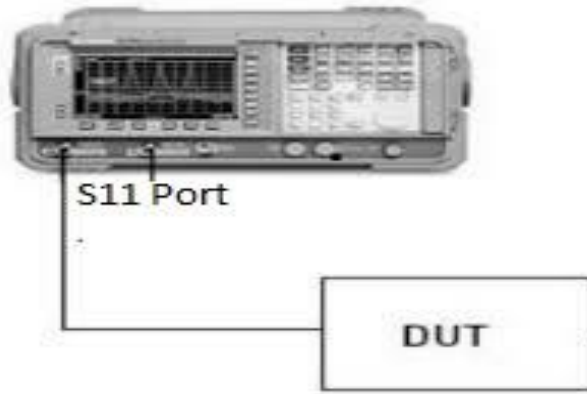


Figure A.6: Test setup for VSWR measurement

VNA port calibration can be done for frequency range between 5GHz to 40GHz using different methods like standard open, short and match load. Calibration means offset line after switching ON VNA should be aligned with Zero. After, this calibrated VNA has to connect with AUT (Antenna under Test) with cable on VNA S_{11} port. Fabricated antenna Return loss (S_{11}) characteristics can be obtained by making connection of antenna with any one port of calibrated network analyzer and operating VNA in S_{11} or S_{22} mode. The graph which is display on VNA display is observed and the frequency for which S_{11} value is lowest means a sharp dip is achieved on the S_{11} graph is called resonant frequency of cut of frequency. Return loss graph also provides information about antenna bandwidth of operation, range of frequencies for which return loss value is less than -10dB is mainly considered as antenna bandwidth. Antenna bandwidth is the range of high frequency cut off frequency and low cut off frequency below -10dB and calculated using following formula in percentage.

$$\text{Bandwidth (\%age)} = \frac{f_h - f_l}{f_c} \times 100 \quad (\text{A.1})$$

Where, f_h represents the higher -10dB point on graph, f_l denotes the lowest -10dB point on graph and f_c is the cut of frequency with minimum return loss value,

APPENDIX B

B.1 ANTENNA DESIGN EQUATIONS

1. To calculate effective length of the antenna:

$$L_{eff} = L + 2\Delta L$$

L is the length of the substrate

ΔL is the change in length of the substrate

2. To calculate Width of the antenna :

$$w = \frac{V_0}{2fr} \sqrt{\frac{2}{\epsilon_r + 1}}$$

Where w is the width of the substrate

f_r is the resonant frequency

ϵ_r is the dielectric constant of the substrate

V_0 is the velocity of light

3. Effective dielectric constant:

$$\epsilon_{\text{reff}} = \frac{\epsilon_r + 1}{2} + \frac{\epsilon_r - 1}{2} \left[1 + 12 \frac{h}{w} \right]^{-1/2} \quad \frac{w}{h} > 1$$

Where h is the height

ϵ_{reff} is the effective dielectric constant

4. Change in length (ΔL):

$$\frac{\Delta L}{h} = 0.412 \frac{(\epsilon_{\text{reff}} + 0.3) \left(\frac{w}{h} + 0.264 \right)}{(\epsilon_{\text{reff}} - 0.258) \left(\frac{w}{h} + 0.8 \right)}$$

5. Length of the antenna:

$$L = \frac{V_0}{2fr \sqrt{\epsilon_{\text{reff}}}} - 2\Delta L$$

BIBLIOGRAPHY

- [1] Ghosh, S., and Sen, D. (2019). An inclusive survey on array antenna design for millimeter-wave communications. *IEEE Access*, 7, 83137-83161.
- [2] Marcus, M. J. (2017). WRC-19 issues: A survey. *IEEE Wireless Communications*, 24(1), 2-3.
- [3] Malik, P. K., Wadhwa, D. S., and Khinda, J. S. (2020). A survey of device to device and cooperative communication for the future cellular networks. *International Journal of Wireless Information Networks*, 1-22.
- [4] Deschamps, G. A. (1953). Microstrip microwave antennas. In *Proceedings of the Third Symposium on the USAF Antenna Research and Development Program, Oct* (pp. 18-22).
- [5] Munson, R., and Krutsinger, J. (1973). *U.S. Patent No. 3,713,162*. Washington, DC: U.S. Patent and Trademark Office.
- [6] Howell, J. Q. (1975). Microstrip antennas. *IEEE Transactions on Antennas and Propagation*, 23, 90-93.
- [7] James, J., Hall, P., Wood, C., and Henderson, A. (1981). Some recent developments in microstrip antenna design. *IEEE Transactions on Antennas and Propagation*, 29(1), 124-128.
- [8] Fatthi Alsager, A. (2011). Design and analysis of microstrip patch antenna arrays.
- [9] Schaubert, D., and Pozar, D. M. (Eds.). (1995). *Microstrip Antennas: The Analysis and Design of Microstrip Antennas and Arrays*. IEEE.
- [10] Garg, R., Bhartia, P., Bahl, I. J., and Ittipiboon, A. (2001). *Microstrip antenna design handbook*. Artech house.
- [11] Carver, K., and Mink, J. (1981). Microstrip antenna technology. *IEEE transactions on antennas and propagation*, 29(1), 2-24.
- [12] Katehi, P., and Alexopoulos, N. (1984). On the modeling of electromagnetically coupled microstrip antennas--The printed strip dipole. *IEEE transactions on antennas and propagation*, 32(11), 1179-1186.
- [13] Kumar, G., and Ray, K. P. (2003). *Broadband microstrip antennas*. Artech house.
- [14] Balanis, C. A. (2015). *Antenna theory: analysis and design*. John wiley and sons.
- [15] Bailey, M., and Deshpande, M. (1982). Integral equation formulation of microstrip antennas. *IEEE Transactions on Antennas and Propagation*, 30(4), 651-656.
- [16] Richards, W. F. Y. T., Lo, Y., and Harrison, D. (1981). An improved theory for microstrip antennas and applications. *IEEE Transactions on antennas and propagation*, 29(1), 38-46.
- [17] Chen, W. L., Wang, G. M., and Zhang, C. X. (2009). Bandwidth enhancement of a microstrip-line-fed printed wide-slot antenna with a fractal-shaped slot. *IEEE Transactions on Antennas and Propagation*, 57(7), 2176-2179.
- [18] Lee, K. F., and Chen, W. (Eds.). (1997). *Advances in microstrip and printed antennas* (p. 21). New York: Wiley.
- [19] Cai, Y., Qian, Z. P., Zhang, Y. S., Jin, J., and Cao, W. Q. (2014). Bandwidth enhancement of SIW horn antenna loaded with air-via perforated dielectric slab. *IEEE antennas and wireless propagation letters*, 13, 571-574.

- [20] Li, D., and Mao, J. F. (2013). Coplanar waveguide-fed Koch-like sided Sierpinski hexagonal carpet multifractal monopole antenna. *IET Microwaves, Antennas and Propagation*, 8(5), 358-366.
- [21] Pan, C. Y., Horng, T. S., Chen, W. S., and Huang, C. H. (2007). Dual wideband printed monopole antenna for WLAN/WiMAX applications. *IEEE Antennas and Wireless Propagation Letters*, 6, 149-151.
- [22] Yao, J., Tchafa, F. M., Jain, A., Tjuatja, S., and Huang, H. (2016). Far-field interrogation of microstrip patch antenna for temperature sensing without electronics. *IEEE Sensors Journal*, 16(19), 7053-7060.
- [23] Richards, W. F., and Lo, Y. T. (1983). Theoretical and experimental investigation of a microstrip radiator with multiple lumped linear loads. *Electromagnetics*, 3(3-4), 371-385.
- [24] Schaubert, D., Farrar, F., Sindoris, A., and Hayes, S. (1981). Microstrip antennas with frequency agility and polarization diversity. *IEEE Transactions on Antennas and Propagation*, 29(1), 118-123.
- [25] Wang, C. J., and Hsu, D. F. (2004). Studies of the novel CPW-fed spiral slot antenna. *IEEE Antennas and Wireless Propagation Letters*, 3, 186-188.
- [26] Wu, J., Zhao, Z., Nie, Z., and Liu, Q. H. (2014). A printed UWB Vivaldi antenna using stepped connection structure between slotline and tapered patches. *IEEE Antennas and Wireless Propagation Letters*, 13, 698-701.
- [27] Azim, R., Islam, M. T., and Misran, N. (2013). Printed circular disc compact planar antenna for UWB applications. *Telecommunication Systems*, 52(2), 1171-1177.
- [28] Ray, K. P., and Ranga, Y. (2007). Ultrawideband printed elliptical monopole antennas. *IEEE transactions on antennas and propagation*, 55(4), 1189-1192.
- [29] Kishk, A. A. (1993). Analysis of spherical annular microstrip antennas. *IEEE transactions on antennas and propagation*, 41(3), 338-343.
- [30] Shakib, M. N., Islam, M. T., and Misran, N. (2010). Stacked patch antenna with folded patch feed for ultra-wideband application. *IET microwaves, antennas and propagation*, 4(10), 1456-1461.
- [31] Singhal, S., and Singh, A. K. (2015). Crescent- shaped dipole antenna for ultrawideband applications. *Microwave and Optical Technology Letters*, 57(8), 1773-1782.
- [32] Abdelhalim, C., and Farid, D. (2014). A compact planar UWB antenna with triple controllable band-notched characteristics. *International Journal of Antennas and Propagation*, 2014.
- [33] Kumar, R., Khokle, R. K., and Krishna, R. R. (2014). A horizontally polarized rectangular stepped slot antenna for ultra wide bandwidth with boresight radiation patterns. *IEEE Transactions on Antennas and Propagation*, 62(7), 3501-3510.
- [34] Wu, C. M. (2007). Wideband dual-frequency CPW-fed triangular monopole antenna for DCS/WLAN application. *AEU-International Journal of Electronics and Communications*, 61(9), 563-567.

- [35] Sarkar, D., Srivastava, K. V., and Saurav, K. (2014). A compact microstrip-fed triple band-notched UWB monopole antenna. *IEEE Antennas and Wireless Propagation Letters*, 13, 396-399.
- [36] Soltani, S., Azarmanesh, M., Lotfi, P., and Dadashzadeh, G. (2011). Two novel very small monopole antennas having frequency band notch function using DGS for UWB application. *AEU-International Journal of Electronics and Communications*, 65(1), 87-94.
- [37] Khinda, J. S., Tripathy, M. R., and Gambhir, D. (2017). Multi-edged wide-band rectangular microstrip fractal antenna array for C-and X-band wireless applications. *Journal of Circuits, Systems and Computers*, 26(04), 1750068.
- [38] Panda, D. C., Pattnaik, S. S., Khuntia, B., Neog, D. K., and Devi, S. (2003). Coupling of ANNN with GA for effective optimization of dimensions of rectangular patch antenna on thick substrate microstrip patch antenna on thick substrate. In *6th International Symposium on Antennas, Propagation and EM Theory, 2003. Proceedings. 2003* (pp. 720-725). IEEE.
- [39] Richards, W., Davidson, S., and Long, S. (1985). Dual-band reactively loaded microstrip antenna. *IEEE Transactions on Antennas and Propagation*, 33(5), 556-561.
- [40] Targonski, S. D., Waterhouse, R. B., and Pozar, D. M. (1998). Design of wide-band aperture-stacked patch microstrip antennas. *IEEE Transactions on Antennas and Propagation*, 46(9), 1245-1251.
- [41] Walker, G. J., and James, J. R. (1998). Fractal volume antennas. *Electronics Letters*, 34(16), 1536-1537.
- [42] Puente, C., Romeu, J., Pous, R., Garcia, X., and Benitez, F. (1996). Fractal multiband antenna based on the Sierpinski gasket. *Electronics Letters*, 32(1), 1-2.
- [43] Dhar, S., Ghatak, R., Gupta, B., and Poddar, D. R. (2013). A wideband Minkowski fractal dielectric resonator antenna. *IEEE transactions on antennas and propagation*, 61(6), 2895-2903.
- [44] Borja, C., Font, G., Blanch, S., and Romeu, J. (2000). High directivity fractal boundary microstrip patch antenna. *Electronics Letters*, 36(9), 778-779.
- [45] Guterman, J., Moreira, A. A., and Peixeiro, C. (2004). Microstrip fractal antennas for multistandard terminals. *IEEE Antennas and Wireless Propagation Letters*, 3(1), 351-354.
- [46] Manimegalai, B., Raju, S., and Abhaikumar, V. (2008). A multifractal cantor antenna for multiband wireless applications. *IEEE Antennas and Wireless Propagation Letters*, 8, 359-362.
- [47] Da Silva, M. R., Nóbrega, C. D. L., Silva, P. D. F., and D'Assunção, A. G. (2013). Dual-polarized band-stop FSS spatial filters using vicsek fractal geometry. *Microwave and Optical Technology Letters*, 55(1), 31-34.
- [48] Afrough, M., Fakharian, M. M., and Tavakol-Hamedani, F. (2015). Compact dual-band suspended microstrip slot antenna with an antipodal parasitic element for WLAN applications. *Wireless Personal Communications*, 83(1), 571-579.
- [49] Anguera, J., Martínez-Ortigosa, E., Puente, C., Borja, C., and Soler, J. (2006). Broadband triple-frequency microstrip patch radiator combining a dual-band modified Sierpinski fractal

- and a monoband antenna. *IEEE Transactions on Antennas and Propagation*, 54(11), 3367-3373.
- [50] Chang, D. C., Zeng, B. H., and Liu, J. C. (2008). CPW-fed circular fractal slot antenna design for dual-band applications. *IEEE Transactions on Antennas and Propagation*, 56(12), 3630-3636.
- [51] Hu, W., Wu, J. J., Zheng, S. F., and Ren, J. (2015). Compact ACS-fed printed antenna using dual edge resonators for tri-band operation. *IEEE Antennas and Wireless Propagation Letters*, 15, 207-210.
- [52] Hung, C., and Chiu, T. (2014). Dual-band reconfigurable antenna design using slot-line with branch edge. *IEEE Transactions on Antennas and Propagation*, 63(2), 508-516.
- [53] Kumar, Y., and Singh, S. (2015). A compact multiband hybrid fractal antenna for multistandard mobile wireless applications. *Wireless Personal Communications*, 84(1), 57-67.
- [54] Li, Y., and Yu, W. (2015). A miniaturized triple band monopole antenna for WLAN and WiMAX applications. *International Journal of Antennas and Propagation*, 2015.
- [55] Song, C. T. P., Hall, P. S., and Ghafouri-Shiraz, H. (2003). Perturbed Sierpinski multiband fractal antenna with improved feeding technique. *IEEE Transactions on Antennas and Propagation*, 51(5), 1011-1017.
- [56] Tsachtsiris, G. F., Soras, C. F., Karaboikis, M. P., and Makios, V. T. (2004). Analysis of a modified Sierpinski gasket monopole antenna printed on dual band wireless devices. *IEEE transactions on antennas and propagation*, 52(10), 2571-2579.
- [57] Tsachtsiris, G. F., Soras, C. F., Karaboikis, M. P., and Makios, V. T. (2004). Analysis of a modified Sierpinski gasket monopole antenna printed on dual band wireless devices. *IEEE transactions on antennas and propagation*, 52(10), 2571-2579.
- [58] Fu, S., Fang, S., Wang, Z., and Li, X. (2009). Broadband circularly polarized slot antenna array fed by asymmetric CPW for L-band applications. *IEEE Antennas and Wireless Propagation Letters*, 8, 1014-1016.
- [59] Chakrabarti, S. (2010). Development of shared aperture dual polarized microstrip antenna at L-band. *IEEE transactions on antennas and propagation*, 59(1), 294-297.
- [60] Rashmi, R., Prasan Ray, K., and Duttgupta, S. P. (2013). Bandwidth enhancement using gap-coupled hexagonal microstrip antennas in L band. *Microwave and Optical Technology Letters*, 55(11), 2703-2709.
- [61] Kamakshi, K., Singh, A., Aneesh, M., and Ansari, J. A. (2014). Novel design of microstrip antenna with improved bandwidth. *International Journal of Microwave Science and Technology*, 2014.
- [62] Salameh, S. F., and Abdelazeez, M. K. (2012). Multiband planar inverted-F dual-L antenna (PIFDLA) for WLAN applications. *Journal of King Saud University-Engineering Sciences*, 24(1), 61-69.
- [63] Cho, K., and Hong, S. (2011). Design of a VHF/UHF/L-band low-power active antenna for mobile handsets. *IEEE antennas and wireless propagation letters*, 11, 45-48.

- [64]Tae, H. S., Oh, K. S., Son, W. I., Lim, W. G., and Yu, J. W. (2012). Design of compact dual-band quadruple inverted-F/L antenna for GPS L1/L2 band. *IEEE transactions on antennas and propagation*, 61(4), 2276-2279.
- [65]Kumar, S., Kanaujia, B. K., Khandelwal, M. K., and Gautam, A. K. (2014). Stacked dual-band circularly polarized microstrip antenna with small frequency ratio. *Microwave and Optical Technology Letters*, 56(8), 1933-1937.
- [66]Cai, Y. M., Gao, S., Yin, Y., Li, W., and Luo, Q. (2016). Compact-size low-profile wideband circularly polarized omnidirectional patch antenna with reconfigurable polarizations. *IEEE transactions on antennas and propagation*, 64(5).
- [67]Khanna, A., Srivastava, D. K., and Saini, J. P. (2015). Bandwidth enhancement of modified square fractal microstrip patch antenna using gap-coupling. *Engineering Science and Technology, an International Journal*, 18(2), 286-293.
- [68]Li, Y., Zhao, F., Guo, J., and Zhang, L. (2012). Design of S-band circularly polarized double-layer microstrip antenna. *Transactions of Tianjin University*, 18(4), 248-252.
- [69]Nascetti, A., Pittella, E., Teofilatto, P., and Pisa, S. (2014). High-gain S-band patch antenna system for earth-observation CubeSat satellites. *IEEE antennas and wireless propagation letters*, 14, 434-437.
- [70]Nikfalazar, M., Kohler, C., Wiens, A., Mehmood, A., Sohrabi, M., Maune, H., ... and Jakoby, R. (2015). Beam steering phased array antenna with fully printed phase shifters based on low-temperature sintered BST-composite thick films. *IEEE Microwave and Wireless Components Letters*, 26(1), 70-72.
- [71]Qu, S. W., Li, J. L., Xue, Q., Chan, C. H., and Li, S. (2009). Wideband and unidirectional cavity-backed folded triangular bowtie antenna. *IEEE Transactions on antennas and propagation*, 57(4), 1259-1263.
- [72]Wang, Y., and Du, Z. (2015). Wideband monopole antenna with less nonground portion for octa-band WWAN/LTE mobile phones. *IEEE Transactions on Antennas and Propagation*, 64(1), 383-388.
- [73]Zhang, J., Lin, X. Q., Nie, L. Y., Yu, J. W., and Fan, Y. (2016). Wideband dual-polarization patch antenna array with parallel strip line balun feeding. *IEEE Antennas and Wireless Propagation Letters*, 15, 1499-1501.
- [74]Zhao, X. L., and Lin, Q. W. (2016). Dual-band patch antenna fed by meandering probe for low cross-polarization. *International Journal of Antennas and Propagation*, 2016.
- [75]Federal Communications Commission Revision of Part 15 of the Commissions Rules Regarding Ultra-Wideband Transmission Systems", *FIRST REPORT AND ORDER FCC*, pp. 02-48, April 2002
- [76]Emadian, S. R., and Ahmadi-Shokouh, J. (2015). Very small dual band-notched rectangular slot antenna with enhanced impedance bandwidth. *IEEE Transactions on Antennas and Propagation*, 63(10), 4529-4534.
- [77]Palandoken, M., Grede, A., and Henke, H. (2009). Broadband microstrip antenna with left-handed metamaterials. *IEEE Transactions on Antennas and Propagation*, 57(2), 331-338.

- [78] Chitra, R. J., and Nagarajan, V. (2013). Double L-slot microstrip patch antenna array for WiMAX and WLAN applications. *Computers and Electrical Engineering*, 39(3), 1026-1041.
- [79] Srivastava, G., and Mohan, A. (2015). Compact MIMO slot antenna for UWB applications. *IEEE Antennas and Wireless Propagation Letters*, 15, 1057-1060.
- [80] Rappaport, T. S., Sun, S., Mayzus, R., Zhao, H., Azar, Y., Wang, K., and Gutierrez, F. (2013). Millimeter wave mobile communications for 5G cellular: It will work!. *IEEE access*, 1, 335-349.
- [81] Marcus, M. J. (2017). WRC-19 issues: A survey. *IEEE Wireless Communications*, 24(1), 2-3.
- [82] Abdel-Wahab, W. M., and Safavi-Naeini, S. (2011). Wide-bandwidth 60-GHz aperture-coupled microstrip patch antennas (MPAs) fed by substrate integrated waveguide (SIW). *IEEE Antennas and Wireless Propagation Letters*, 10, 1003-1005.
- [83] Chin, K. S., Jiang, W., Che, W., Chang, C. C., and Jin, H. (2013). Wideband LTCC 60-GHz antenna array with a dual-resonant slot and patch structure. *IEEE Transactions on Antennas and Propagation*, 62(1), 174-182.
- [84] Deng, C., Xie, Y. J., and Li, P. (2009). CPW-fed planar printed monopole antenna with impedance bandwidth enhanced. *IEEE Antennas and Wireless Propagation Letters*, 8, 1394-1397.
- [85] Haraz, O. M. (2016). Broadband and 28/38-GHz dual-band printed monopole/elliptical slot ring antennas for the future 5G cellular communications. *Journal of Infrared, Millimeter, and Terahertz Waves*, 37(4), 308-317.
- [86] Lin, F., Jiao, Y. C., and Zhang, Z. (2013). Strip-fed tapered slot antenna with enhanced impedance bandwidth from 0.57 to 35 GHz. *Electronics letters*, 49(17), 1057-1058.
- [87] Mak, K. M., Lai, H. W., Luk, K. M., and Chan, C. H. (2014). Circularly polarized patch antenna for future 5G mobile phones. *IEEE Access*, 2, 1521-1529.
- [88] Park, J. S., Ko, J. B., Kwon, H. K., Kang, B. S., Park, B., and Kim, D. (2016). A tilted combined beam antenna for 5G communications using a 28-GHz band. *IEEE Antennas and Wireless Propagation Letters*, 15, 1685-1688.
- [89] Yang, W., Ma, K., Yeo, K. S., and Lim, W. M. (2015). A compact high-performance patch antenna array for 60-GHz applications. *IEEE Antennas and Wireless Propagation Letters*, 15, 313-316.
- [90] Qu, S. W., Ruan, C., and Wang, B. Z. (2006). Bandwidth enhancement of wide-slot antenna fed by CPW and microstrip line. *IEEE Antennas and Wireless Propagation Letters*, 5, 15-17.
- [91] Ge, L., Yang, X., Zhang, D., Li, M., and Wong, H. (2017). Polarization-reconfigurable magnetoelectric dipole antenna for 5G Wi-Fi. *IEEE Antennas and Wireless Propagation Letters*, 16, 1504-1507.
- [92] Ta, S. X., Choo, H., and Park, I. (2017). Broadband printed-dipole antenna and its arrays for 5G applications. *IEEE Antennas and Wireless Propagation Letters*, 16, 2183-2186.
- [93] Huang, H., Li, X., and Liu, Y. (2018). 5G MIMO antenna based on vector synthetic mechanism. *IEEE Antennas and Wireless Propagation Letters*, 17(6), 1052-1055.

- [94] Al-Saif, H., Usman, M., Chughtai, M. T., and Nasir, J. (2018). Compact ultra-wide band MIMO antenna system for lower 5G bands. *Wireless Communications and Mobile Computing, 2018*.
- [95] Jaiswal, A., Abegaonkar, M. P., and Koul, S. K. (2019). Highly efficient, wideband microstrip patch antenna with recessed ground at 60 GHz. *IEEE Transactions on Antennas and Propagation, 67(4)*, 2280-2288.
- [96] Khaleghi, S. S. M., Moradi, G., Shirazi, R. S., and Jafarholi, A. (2019). Microstrip line impedance matching using ENZ metamaterials, design, and application. *IEEE Transactions on Antennas and Propagation, 67(4)*, 2243-2251.
- [97] Jilani, S. F., Abbasi, Q. H., and Alomainy, A. (2018, August). Inkjet-printed millimetre-wave PET-based flexible antenna for 5G wireless applications. In *2018 IEEE MTT-S International Microwave Workshop Series on 5G Hardware and System Technologies (IMWS-5G)* (pp. 1-3). IEEE.
- [98] Kao, H. L., Yeh, C. S., Zhang, X. Y., Cho, C. L., Dai, X., Wei, B. H., ... and Chiu, H. C. (2014). Inkjet printed series-fed two-dipole antenna comprising a balun filter on liquid crystal polymer substrate. *IEEE Transactions on Components, Packaging and Manufacturing Technology, 4(7)*, 1228-1236.
- [99] Tighezza, M., Rahim, S. K. A., and Islam, M. T. (2018). Flexible wideband antenna for 5G applications. *Microwave and Optical Technology Letters, 60(1)*, 38-44.
- [100] Ojaroudiparchin, N., Shen, M., Zhang, S., and Pedersen, G. F. (2016). A switchable 3-D-coverage-phased array antenna package for 5G mobile terminals. *IEEE Antennas and Wireless Propagation Letters, 15*, 1747-1750.
- [101] Park, J. S., Ko, J. B., Kwon, H. K., Kang, B. S., Park, B., and Kim, D. (2016). A tilted combined beam antenna for 5G communications using a 28-GHz band. *IEEE Antennas and Wireless Propagation Letters, 15*, 1685-1688.
- [102] Ullah, H., and Tahir, F. A. (2020). A wide-band rhombus monopole antenna array for millimeter wave applications. *Microwave and Optical Technology Letters, 62(5)*, 2111-2117.
- [103] Khalily, M., Tafazolli, R., Rahman, T. A., and Kamarudin, M. R. (2015). Design of phased arrays of series-fed patch antennas with reduced number of the controllers for 28-GHz mm-wave applications. *IEEE Antennas and Wireless Propagation Letters, 15*, 1305-1308.
- [104] Naqvi, S. I., Naqvi, A. H., Arshad, F., Riaz, M. A., Azam, M. A., Khan, M. S., ... and Tenhunen, H. (2019). An integrated antenna system for 4G and millimeter-wave 5G future handheld devices. *IEEE Access, 7*, 116555-116566.
- [105] Ikram, M., Nguyen-Trong, N., and Abbosh, A. M. (2019). Realization of a tapered slot array as both decoupling and radiating structure for 4G/5G wireless devices. *IEEE Access, 7*, 159112-159118.
- [106] Jilani, S. F., and Alomainy, A. (2018). Millimetre-wave T-shaped MIMO antenna with defected ground structures for 5G cellular networks. *IET Microwaves, Antennas and Propagation, 12(5)*, 672-677.

- [107] Yang, Y. H., Sun, B. H., and Guo, J. L. (2019). A low-cost, single-layer, dual circularly polarized antenna for millimeter-wave applications. *IEEE Antennas and Wireless Propagation Letters*, 18(4), 651-655.
- [108] Zhang, Y., Deng, J. Y., Li, M. J., Sun, D., and Guo, L. X. (2019). A MIMO dielectric resonator antenna with improved isolation for 5G mm-wave applications. *IEEE Antennas and Wireless Propagation Letters*, 18(4), 747-751.
- [109] Ali, I., Jamaluddin, M. H., Kamarudin, M. R., Gaya, A., and Dahri, M. H. (2019). Gain enhancement of dielectric resonator antenna for millimeter wave applications. *TELKOMNIKA Telecommun. Comput. Electron. Control*, 17(4), 1670-1673.
- [110] Gong, K., Hu, X. H., Hu, P., Deng, B. J., and Tu, Y. C. (2018). A series-fed linear substrate-integrated dielectric resonator antenna array for millimeter-wave applications. *International Journal of Antennas and Propagation*, 2018.
- [111] Khandelwal, M. K., Kumar, S., and Kanaujia, B. K. (2018). Design, modeling and analysis of dual-feed defected ground microstrip patch antenna with wide axial ratio bandwidth. *Journal of Computational Electronics*, 17(3), 1019-1028.
- [112] Emadian, S. R., and Ahmadi-Shokouh, J. (2015). Very small dual band-notched rectangular slot antenna with enhanced impedance bandwidth. *IEEE Transactions on Antennas and Propagation*, 63(10), 4529-4534.
- [113] Kumar, G., and Ray, K. P. (2003). *Broadband microstrip antennas*. Artech house.
- [114] Balanis, C. A. (2005). Frequency independent antennas antenna miniaturization and fractal antennas. In *Antenna theory: analysis and design* (pp. 611-652). Wiley.
- [115] Khinda, J. S., Tripathy, M. R., and Gambhir, D. (2017). Multi-edged wide-band rectangular microstrip fractal antenna array for C-and X-band wireless applications. *Journal of Circuits, Systems and Computers*, 26(04), 1750068.
- [116] Khinda, J. S., Tripathy, M. R., and Gambhir, D. (2018). Improvement in depth of return loss of microstrip antenna for s-band applications. *Journal of Circuits, Systems and Computers*, 27(04), 1850058.
- [117] Eshtiaghi, R., Nourinia, J., and Ghobadi, C. (2010). Electromagnetically coupled band-notched elliptical monopole antenna for UWB applications. *IEEE Transactions on Antennas and Propagation*, 58(4), 1397-1402.
- [118] An, W., Li, Y., Fu, H., Ma, J., Chen, W., and Feng, B. (2018). Low-profile and wideband microstrip antenna with stable gain for 5G wireless applications. *IEEE Antennas and Wireless Propagation Letters*, 17(4), 621-624.
- [119] Khalily, M., Tafazolli, R., Rahman, T. A., and Kamarudin, M. R. (2015). Design of phased arrays of series-fed patch antennas with reduced number of the controllers for 28-GHz mm-wave applications. *IEEE Antennas and Wireless Propagation Letters*, 15, 1305-1308.
- [120] Qu, S. W., Li, J. L., Xue, Q., Chan, C. H., and Li, S. (2009). Wideband and unidirectional cavity-backed folded triangular bowtie antenna. *IEEE Transactions on antennas and propagation*, 57(4), 1259-1263.

- [121] Mruk, J., Hongyu, Z., Uhm, M., Saito, Y., and Filipovic, D. (2009, March). Wideband mm-wave log-periodic antennas. In *2009 3rd European Conference on Antennas and Propagation* (pp. 2584-2587). IEEE.
- [122] Bang, J., and Choi, J. (2018). A SAR reduced mm-wave beam-steerable array antenna with dual-mode operation for fully metal-covered 5G cellular handsets. *IEEE Antennas and Wireless Propagation Letters*, 17(6), 1118-1122.
- [123] Jilani, S. F., and Alomainy, A. (2018). Millimetre- wave T- shaped MIMO antenna with defected ground structures for 5G cellular networks. *IET Microwaves, Antennas and Propagation*, 12(5), 672-677.
- [124] Liu, D., Gu, X., Baks, C. W., and Valdes-Garcia, A. (2017). Antenna-in-package design considerations for Ka-band 5G communication applications. *IEEE Transactions on Antennas and Propagation*, 65(12), 6372-6379.
- [125] Jilani, S. F., Munoz, M. O., Abbasi, Q. H., and Alomainy, A. (2018). Millimeter-wave liquid crystal polymer based conformal antenna array for 5G applications. *IEEE Antennas and Wireless Propagation Letters*, 18(1), 84-88.
- [126] Saad, A. A. R., and Mohamed, H. A. (2019). Printed millimeter-wave MIMO-based slot antenna arrays for 5G networks. *AEU-International Journal of Electronics and Communications*, 99, 59-69.
- [127] Ojaroudi, N., and Ojaroudi, M. (2013). Novel design of dual band-notched monopole antenna with bandwidth enhancement for UWB applications. *IEEE Antennas and Wireless Propagation Letters*, 12, 698-701.
- [128] Eskandari, H., and Azarmanesh, M. N. (2009). Bandwidth enhancement of a printed wide-slot antenna with small slots. *AEU-International Journal of Electronics and Communications*, 63(10), 896-900.
- [129] Xiong, H., Hong, J. S., and Peng, Y. H. (2012). Impedance bandwidth and gain improvement for microstrip antenna using metamaterials. *Radioengineering*, 21(4), 993-998.
- [130] Alkaraki, S., Andy, A. S., Gao, Y., Tong, K. F., Ying, Z., Donnan, R., and Parini, C. (2018). Compact and low-cost 3-D printed antennas metalized using spray-coating technology for 5G mm-wave communication systems. *IEEE Antennas and Wireless Propagation Letters*, 17(11), 2051-2055.
- [131] Jilani, S. F., and Alomainy, A. (2016, April). Planar millimeter-wave antenna on low-cost flexible PET substrate for 5G applications. In *2016 10th European conference on antennas and propagation (EuCAP)* (pp. 1-3). IEEE.
- [132] Khinda, J. S., and Tripathy, M. R. (2015, December). Wideband triangular antenna design with enhanced gain bandwidth for wireless communication applications. In *2015 2nd International Conference on Recent Advances in Engineering and Computational Sciences (RAECS)* (pp. 1-5). IEEE.
- [133] Mantash, M., and Denidni, T. A. (2017). Finger- worn end- fire antenna for MM- wave applications. *Microwave and Optical Technology Letters*, 59(10), 2591-2593.

- [134] Pan, Y. M., Leung, K. W., and Luk, K. M. (2011). Design of the millimeter-wave rectangular dielectric resonator antenna using a higher-order mode. *IEEE transactions on antennas and propagation*, 59(8), 2780-2788.
- [135] Liu, Y., Jiao, Y. C., Weng, Z., Zhang, C., and Chen, G. (2019). A novel millimeter-wave dual-band circularly polarized dielectric resonator antenna. *International Journal of RF and Microwave Computer-Aided Engineering*, 29(10), e21871.
- [136] Li, S., Chi, T., Wang, Y., and Wang, H. (2017). A millimeter-wave dual-feed square loop antenna for 5G communications. *IEEE Transactions on Antennas and Propagation*, 65(12), 6317-6328.
- [137] Al Abbas, E., Ikram, M., Mobashsher, A. T., and Abbosh, A. (2019). MIMO antenna system for multi-band millimeter-wave 5G and wideband 4G mobile communications. *IEEE Access*, 7, 181916-181923.
- [138] Ali, W., Das, S., Medkour, H., and Lakrit, S. (2021). Planar dual-band 27/39 GHz millimeter-wave MIMO antenna for 5G applications. *Microsystem Technologies*, 27(1), 283-292.
- [139] Hussain, R., Alreshaid, A. T., Podilchak, S. K., and Sharawi, M. S. (2017). Compact 4G MIMO antenna integrated with a 5G array for current and future mobile handsets. *IET Microwaves, Antennas and Propagation*, 11(2), 271-279.
- [140] Jilani, S. F., Rahimian, A., Alfadhl, Y., and Alomainy, A. (2018). Low-profile flexible frequency-reconfigurable millimetre-wave antenna for 5G applications. *Flexible and Printed Electronics*, 3(3), 035003.
- [141] Kurvinen, J., Kähkönen, H., Lehtovuori, A., Ala-Laurinaho, J., and Viikari, V. (2018). Co-designed mm-wave and LTE handset antennas. *IEEE Transactions on antennas and propagation*, 67(3), 1545-1553.
- [142] Moreno, R. M., Kurvinen, J., Ala-Laurinaho, J., Khripkov, A., Ilvonen, J., van Wousterghem, J., and Viikari, V. (2020). Dual-polarized mm-Wave end-fire chain-slot antenna for mobile devices. *IEEE Transactions on Antennas and Propagation*.
- [143] Mahmoud, K. R., and Montaser, A. M. (2018). Synthesis of multi-polarised upside conical frustum array antenna for 5G mm-Wave base station at 28/38 GHz. *IET Microwaves, Antennas and Propagation*, 12(9), 1559-1569.
- [144] Przesmycki, R., Bugaj, M., & Nowosielski, L. (2021). Broadband microstrip antenna for 5g wireless systems operating at 28 GHz. *Electronics*, 10(1), 1.
- [145] Dwivedi, A. K., Sharma, A., Pandey, A. K., & Singh, V. (2021). Two Port Circularly Polarized MIMO Antenna Design and Investigation for 5G Communication Systems. *Wireless Personal Communications*, 1-15.